

RD-R167 878

A MORPHOFUNCTIONAL STUDY ON THE EFFECT OF CYTOCHALASIN

1/2

B ON INTESTINAL WATER TRANSPORT (U) GEORGE WASHINGTON

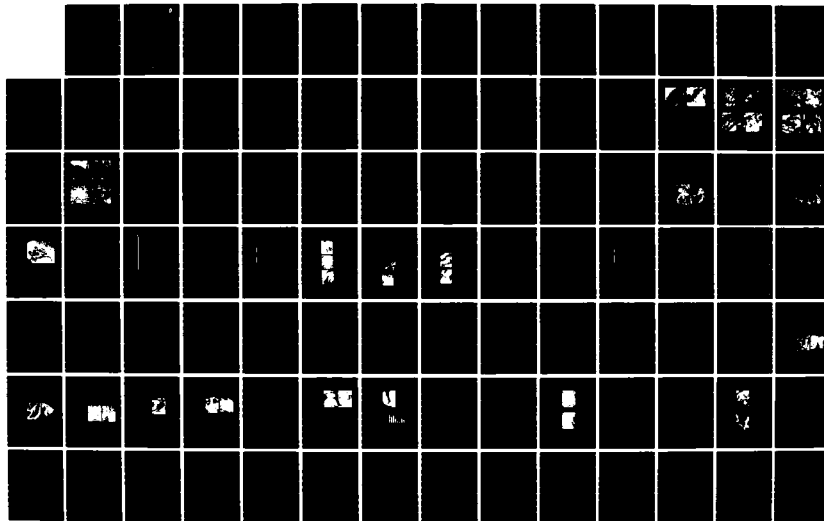
UNIV WASHINGTON DC M M CASSIDY 10 MAY 86

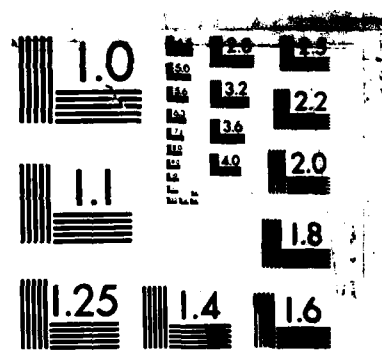
UNCLASSIFIED

N80014-79-C-0603

F/G 6/15

NL





MICROCOPY RESOLUTION TEST CHART  
NATIONAL BUREAU OF STANDARDS 1963 A

AD-A167 870

On DOD/Navy/UNR Contract

# N00014-79-C-0603

DTIC  
RECEIVED  
MAY 14 1986

D

D Final report

by *Maria M. Cassidy* 10 May 1986

The objective of this series of investigations was to explore and define the role of the cytoskeleton apparatus in the function and transport of solutes across the intestinal epithelium. Most epithelial cells, including the intestinal enterocyte and the mucin-secreting goblet cell are now known to possess a highly ordered cytoskeletal matrix comprised of microfilaments, intermediate filaments and microtubules. Macromolecular aggregates such as actin and a variety of related proteins are present in the amplification structures, i.e. microvilli of the mucosal surface. This component of the system was perturbed by the application of Cytochalasin B (CB), a macrolide antibiotic which interacts with mechanochemical proteins of microfilaments. Studies from a number of laboratories suggest that these cytokinins inhibit the rate of actin filament polymerisation and disrupt actin-based networks in a very dynamic manner. Work performed on this contract provides evidence that microfilaments and/or microtubules may be critical physicochemical transducers in the sequence of events leading to (1) transmural absorption of salts, organic solutes and osmotically-linked fluid flow; (2) mucin secretions by the goblet cells, which constitute approximately 20-30% of the surface cell population; (3) the expression of  $\beta$  receptors in HeLa cells by butyrate treatment is preceded by a dramatic reorganization of the intracellular cytoskeleton.

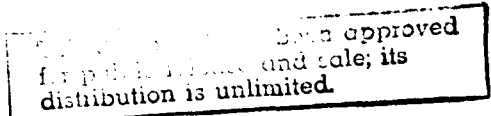
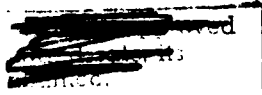
1. Serosal CB ( $1-5 \times 10^{-5} M$ ) evoked a significant rise in electrical resistance and a 25% decrease in hydrogen ion secretion by frog gastric mucosa. Resistive effects but not acid secretion modification was readily reversible. In vivo absorption of sodium, glucose and water by rat jejunum was inhibited by 50% during steady state transport periods during which luminal CB was present. The results can be suitably explained by an electrical model wherein the microfilament-disruptive action of CB is represented by changes in a cytoplasmic resistance. In a second study, similar alterations in electrical potential difference, resistance and  $H^+$  secretion rate were clearly a reflection of the structural state of the cell layer. A theoretical paper presented at a conference of investigators supported by ONR Biophysics Program at Virginia Polytechnic Institute in 1980 concluded that the range of absorption rates of isosmotic fluid across epithelia represents the need for energy-dependent

FILE COPY

AMIC

The George Washington University -  
Washington, DC

Title: A Morphofunctional Study on the Effect  
of Cytochalasin B on Intestinal Water  
Transport



transfer of fluid volume units as opposed to solute units per se. It may be appropriate to reconsider earlier models of a mechanical volume pump for transcellular relocation of fluid volume units, encompassing a cytoplasmic component. This model should permit a flexible specificity with respect to the actively transported solutes and obviously incorporate the presence or transport of  $\text{Na}^+$ ,  $\text{Cl}^-$ ,  $\text{HCO}_3^-$  ions. Morphological evidence utilizing scanning and transmission electron microscopy provides directional polarization and a structured pathway for the secretory transport system in the gastric parietal cell and the absorptive transport mechanism in the intestinal cell. Cytochalasin-treated epithelia revealed a significant widening of the junctional regions between contiguous cells, which are normally tightly opposed. Filamentous thread-like material was present on the apical cell surfaces and between cells and was of such morphometric dimensions as to permit the preliminary conclusion that it represented disarrayed or disgorged filaments.

Effects of Cytochalasin B in Epithelia / 361

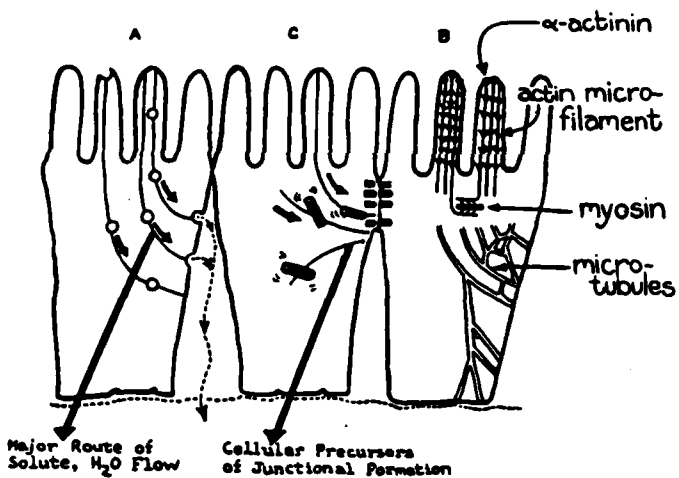


Fig. . This schematic diagram of intestinal epithelia illustrates 3 major concepts: A shows the major pathway for fluid absorption which is dependent on actively transported solutes. B represents our current understanding of the cytoskeletal scaffold present in these cells. It has not yet been demonstrated that the microfilaments present in the microvilli are architecturally contiguous with the intermediate filaments and the microtubules. C indicates that junctional formation and hence paracellular permeation characteristics may involve regulation by the cell in terms of microfilament assembly and transposition to the junctional region between individual cells.

Action For	
<input checked="" type="checkbox"/>	CRA&I
<input type="checkbox"/>	TAB
<input type="checkbox"/>	Announced
Classification	
Ltr. on file	
Availability Codes	
Dist	Avail and/or Special
A-1	



The foregoing figure summarizes a possible model (B) which incorporates our experimental findings. Other investigators have demonstrated the strong role of the parietal cell cytoskeleton in the tubulo-vesicular movement of acidic volume units to the secretory apical surface of the stomach. Hence, we conclude that the spectrum of effects observed in these two transporting epithelia is compatible with the concept of involvement of mechanochemical element(s) in the active secretion of  $[H^+]$  by frog gastric mucosa and isotonic transport of solutes and fluid by the in vivo rat intestine.

2. Structural-functional considerations with respect to epithelial transport mechanisms in organs exposed to external environments have rarely included a significant population of cells. Mucin synthesizing and secreting cells include most of the surface layer in the gastric and colonic loci and a fifth to a third of the mucosal barrier in the small intestine. The maintenance of a surface coat of mucus and its role in cell cytoprotection against acid or other noxious agents is now recognized to be a continuous rapid and dynamic mechanism. In an extensive investigative series aimed at defining the ultrastructural features of gastrointestinal mucosa subjected to cytoskeletal disruption, aspirin, prostaglandin or bile acid challenge morphometric findings clearly pointed to modifications of normal mucus secretory patterns.

These observations were followed by biochemical studies of mucus elaboration, in vivo, in a rat model. In almost all cases, the structural and biochemical methodologies yielded corroborative data. The ultrastructural techniques deployed were light microscopy, transmission and scanning electron microscopy. With these techniques in addition to blunt cryofracture of tissue specimens, correlative information concerning the detailed microarchitecture of the mucosal epithelial layers was derived.

Mucus-producing cells are clearly identifiable sub-populations of cells in many of the epithelial transport model systems studied; i.e. gastric, jejunal, and colonic epithelial of the rat. The distribution of these cells varies from a predominant location on the mucosal surface of the stomach to a regular degree of interspersion among the dominant columnar epithelial cell population in the small and large intestine. The functional state of these cells can be assessed by a variety of morphological techniques and their biochemical synthetic and secretory capacity estimated by isotopic tracer procedures. In the gastric or jejunal acute ulceration model, sulfo-

mucin production is decreased by aspirin and markedly enhanced by Prostaglandin E<sub>1</sub>, providing additional evidence for the cytoprotective role of the mucin blanket. With chronic feeding of the bile salt sequestrants which provoke colonic mucosal irritation and injury, there is also stimulated mucin output. Disruption of the cytoskeletal framework of the mucosal cells by Cytochalasin B or colchicine depresses mucin production and secretion. The implication of these studies is that the microfilament/microtubular sub-structure of the mucosal cell plays a role in the functional vectorial conveyance of materials across the mucosal layer whether the moieties involved be absorbed electrolytes and water or a secreted organic component, e.g. mucin.

3. In a final phase of this project, the role of the cellular microtubular array in the induction of  $\beta$ -adrenergic receptors of the cell membrane was probed in the HeLa cell line. Preliminary attempts to visualize the cytoskeleton in isolated enterocytes from the small intestine proved frustrating because of altered morphological integrity. Butyrate is a potent inducer of functional alterations in many cultured cells. These include induction of  $\beta$ -adrenergic and cholera Toxin receptors in HeLa cells, hormone and enzyme synthesis, metabolic modifications and shape changes. Using a HeLa cell line (ES-1), we report a three-fold functional induction of  $\beta$ -adrenergic receptors by 5 mM sodium butyrate and a five-fold increment in 1-isoproterenol-stimulated cAMP production following 24 hours of butyrate treatment. By indirect immunofluorescence microscopy using polyclonal and monoclonal antibodies untreated HeLa monolayers were observed to possess an extensive network of randomly arranged microtubules (MTN). In the presence of 5 mM butyrate for 24 hours, the previously reported elongate shape change was reflected in a reorganization of the MT system such that a majority were then oriented in the long axis of the cell, extending to the tips of the neurite-like processes or between them and few were seen in the vicinity of the nucleus. Essentially similar results were obtained with cells grown in chemically defined, serum-free medium. Colchicine ( $10^{-7}$  M) prevented the butyrate-induced shape and MT alterations. With colchicine alone a diffuse staining pattern, due perhaps to the presence of depolymerized tubulin, was evident. Cycloheximide (10  $\mu$ g/ml) was without effect per se but blocked the butyrate-induced alterations in shape and MT patterns. It is concluded that the induction of  $\beta$ -adrenergic receptors and shape alterations in HeLa cells by butyrate is associated with a dramatic reorientation of the cytoskeleton, which is perhaps related to membrane insertion of the known pool of intracellular receptors. Modification of protein synthesis and subsequent modification of cell function may then ensue.

Cytoskeletal reorganization is associated with the induction of  $\beta$ -adrenergic receptors in HeLa cells by butyrate

<sup>1</sup> Marie M. Cassidy, <sup>1,2</sup> Saleem Jahangeer\*, and Richard C. Henneberry <sup>2</sup>

1- Dept. of Physiology, George Washington University Medical Center  
Washington, D. C. 20037

and

2- Laboratory of Molecular Biology, NINCDS, NIH  
Bethesda, MD 20852

\* Present address: Max Planck Institut for Psychiatry *Department of Neurochemistry*,  
Martinsried, Munich, West Germany

Address reprint requests to: Dr. Marie M. Cassidy  
Dept. of Physiology  
George Washington University Medical Center  
2300 Eye St. NW  
Washington, D. C. 20037

Condensed title: Butyrate stimulates  $\beta$ -receptors, cAMP production and  
microtubular modification in HeLa cells

## ABSTRACT

Butyrate is a potent inducer of functional alterations in many cultured cells. These include induction of  $\beta$ -adrenergic receptors of HeLa cells, hormone and enzyme synthesis, metabolic modifications and shape changes. Using a HeLa cell (ES-1), we report a three-fold functional induction of  $\beta$ -adrenergic receptors by 5 mM sodium butyrate and a five-fold increment in l-isoproterenol-stimulated cAMP production following 24 hours of butyrate treatment. By indirect immunofluorescence microscopy using polyclonal and monoclonal antibodies untreated HeLa monolayers were observed to possess an extensive network of randomly arranged microtubules (MTN). In the presence of 5mM butyrate for 24 hours, the previously reported elongate shape change was reflected in a reorganization of the MT system such that a majority were then oriented in the long axis of the cell, extending to the tops of the neurite-like processes or between them and few were seen in the vicinity of the nucleus. Essentially similar results were obtained with cells grown in chemically defined, serum-free medium. Colchicine ( $10^{-7}$ M) prevented the butyrate-induced shape and MT alterations. With colchicine alone a diffuse staining pattern, due perhaps to the presence of depolymerized tubulin, was evident. Cycloheximide (10  $\mu$ g/ml) was without effect per se but blocked the butyrate-induced alterations in shape and MT pattern. It is concluded that the induction of  $\beta$ -adrenergic receptors and shape alterations in HeLa cells by butyrate is associated with a dramatic reorientation of the cytoskeleton, modification of protein synthesis and subsequent modification of cell function.

## INTRODUCTION

Butyrate is a potent inducer of differentiation in many cultured cell lines (1) and induces both morphological and biochemical changes in these systems. Treatment of HeLa cells with relatively low concentration of butyrate (1-10mM) leads to the following observable effects: (a) a change in the shape of the HeLa cells that involves extension of long, slender, filamentous protrusions or neurite-like processes (2); (b) inhibition of proliferation and blockade of cells in G<sub>1</sub> phase of the cell cycle (3); (c) increased production of <sup>FSH + α</sup> the  $\beta$  subunit of hCG (4, 5); (d) induction of various enzymes such as alkaline phosphatase (6), 5'-nucleotidase, (7) and sialyl-transferase (8); (e) the induction of  $\beta$ -adrenergic (9) and cholera toxin receptors (10); (f) histone hyperacetylation (11); (g) DNA hypomethylation (12). Perhaps #20 would be appropriate

A great deal of information about the biochemical characteristics of cytoskeletal elements has been accumulated over the last few years (13). However, analysis of the role of cytoskeleton in cellular physiology has begun relatively recently (14, 15, 16). The role of the cytoskeleton in cAMP production has been the subject of an excellent review by Zor (17).

This paper describes our initial studies on the role of microtubules in the modulation of  $\beta$ -adrenergic receptors in HeLa cells. HeLa cells contain low basal levels of  $\beta$ -adrenergic receptors which are increased more than 2-5 fold after treatment of HeLa cells with 5mM butyrate for 24 hours (18). This receptor induction can not be explained solely on the basis of histone hyperacetylation (19) or DNA hypomethylation (20). We have hypothesized that elements of the cytoskeleton may be involved, directly or indirectly, in butyrate induced  $\beta$ -adrenergic receptors up-regulation in HeLa cells. This was based on the observation that a minimum of 10-12 hours of exposure to 5mM butyrate is necessary before a significant increase in receptor number and morphological changes become overt. Thus, changes in the shape of the HeLa cells and  $\beta$ -adrenergic receptor induction appear to proceed in parallel. HeLa cells have been found to contain a large intracellular pool of latent  $\beta$ -adrenergic receptors. (Ref. --) (Lysko + Henneberry. Unpublished data)

Treatment with butyrate perhaps recruits these intracellular latent  $\beta$ -adrenergic receptors for expression on the plasma membrane. This exocytic traffic of macromolecules may involve cytoskeletal elements.

Methods

*used in this study originally*

Cell source and preparation: Original HeLa cells were obtained from Dr. Eric Stanbridge (Univ. of California, Irvine) in 1981. They have been continuously maintained at the NIH laboratory and are designated as the ES-1 line. Periodic examination precludes mycoplasmic contamination. The cells are grown in the Dulbecco's modified Eagle's minimal essential medium containing 2 mM glutamine and non-essential amino acids supplemented with 5% heat inactivated (56°C, 30 min) fetal calf serum (MA Bioproducts, Walkerville, MD)

Receptor and cAMP assays: Routine cell culture and subculturation were carried out as previously described. <sup>(R4 124)</sup>  $\beta$ -adrenergic receptor binding assays using whole cells in test tubes were performed according to the filtration procedures described by Tallman et al (9). The radioligand  $^3\text{H}$ -DHA and unlabeled ligand were freshly prepared prior to assay in ice-cold assay buffer. For routine binding assays, a single concentration of  $^3\text{H}$ -DHA (1 - 5nM final concentration) was used. Non-specific binding of  $^3\text{H}$ -DHA was determined by including 20  $\mu\text{M}$   $\alpha$ -propanolol. Both the total  $^3\text{H}$ -DHA binding (in the absence of propanolol) and the non-specific  $^3\text{H}$ -DHA binding (in the presence of propanolol) were determined in triplicate for all data points. Total binding minus the non-specific binding of radioligand (20) is, by definition, equal to the specific binding of radioligand (21).

For the measurement of catecholamine-stimulated cAMP production, the cells were harvested as described except that the cell pellet was suspended in the ice-cold assay buffer. cAMP was measured by the radioimmunoassay of Steiner et al (22) and was performed as recommended by New England Nuclear.

Fluorescence Microscopy: In the morphometric experiments described in this study, ES-1 cells were seeded at 2-5000 cells per sq.cm. in Lab-Tek 2 chamber tissues culture slides. Twentyfour hours after seeding cells were treated with 5.0 mM butyrate (Na salt) in fresh growth medium: untreated cells or cells with various concentrations of colchicine and/or cycloheximide (control) were exposed to fresh medium without butyrate. Both groups were then processed for immunofluorescence microscopy in order to visualize microtubules. Cells were washed in Dulbecco's phosphate buffered saline (PBS) to rinse of growth medium and lysed for 1-2 minutes in lysing buffer [0.5% Triton X-100 in PEM (80.0 mM Pipes buffer, 1.0 mM EDTA, 1.5 mM  $\text{MgCl}_2$  pH 6.9)]. This was followed by a 10-20 second rinse in stabilizing buffer (4% Polyethyleneglycol, average molecular weight 6000, in PEM). Cells were fixed in 3% formaldehyde (EM grade) in buffered saline for 1 hour and saline rinsed. The antibody sequence employed was the application of affinity-purified

polyclonal sheep anti-bovine brain tubulin antibody or mouse monoclonal antibodies (ascites fluid) against alpha and beta subunits of native chick brain microtubules. This step was followed by FITC-conjugated rabbit anti-sheep IgG <sup>or</sup> and sheep anti-mouse at 1:16 and 1:20 dilutions respectively (Miles Laboratories). The preparations were examined under a Zeiss microscope equipped with epifluorescence detection capabilities, using appropriate excitation and barrier filters. Negative controls were prepared by incubating cells with the second antibody only. Following incubation with the fluorescent label cells were extensively washed in buffered saline for 1 hour. After a final rinse in distilled water to each slide was added 2 drops of mounting medium containing 1 part PBS, 9 parts glycerol, pH 8.5. Each slide was then covered with clean glass coverslide (No. 1 $\frac{1}{2}$ ). All slides were sealed with acrylate and immediately examined under a Zeiss microscope equipped with epifluorescence using appropriate excitation and barrier filters for fluorescence.

All photographs were taken under oil immersion using Kodak Tri-X Pan black & white, 400 ASA film, processed at 800 ASA.

Antibodies were purchased from commercial sources as follows: (a) Affinity purified, polyclonal, sheep anti-bovine brain tubulin antibody from CABCO, Inc., Houston, and used at a concentration of 0.1 - 0.2 mg/ml; (b) mouse monoclonal anti- $\alpha$  tubulin and anti- $\beta$  tubulin (ascites fluid) against native chickbrain microtubules from Amersham, Illinois, and used at a concentration of 5-40  $\mu$ g/ml; (c) FITC-conjugated rabbit anti-sheep IgG either from Miles Laboratories, Inc., Indiana, or from CAPPEL Laboratories and used at 1/16 dilution; (d) FITC-conjugated sheep anti-mouse Ig (~~whole molecule~~) from Amersham and used at 1/20 dilution. All other chemicals were purchased from Sigma, Co.

#### RESULTS

Effect of butyrate on cell morphology: Untreated ES-1 cells have a typical HeLa cell structure. When treated with 5mM butyrate for 24 hours, a striking alteration in cell shape is induced. The shape changes induced by butyrate involved the extension of long, slender, neurite-like processes and were blocked by cycloheximide (10 $\mu$ g/ml). Exposure to butyrate also evoked a growth inhibitory effect on ES-1 cells. Removal of butyrate from ES-1 cell cultures was followed by reversal of shape change and resumption of normal growth rates. When analyzed by the trypan blue dye exclusion test, butyrate treated cells were found to be fully viable.

Induction of  $\beta$ -adrenergic receptors in ES-1 cells by butyrate: HeLa cells normally contain low levels of  $\beta$ -adrenergic receptors. As in HeLa R-73 cells, treatment of ES-1 cells with 5mM butyrate led to a 2-4 fold increase in  $\beta$ -adrenergic receptors and also caused a small increment in the amount of protein per cell. Concomitant with these effects, the isoproterenol-stimulated cAMP production in ES-1 cells was also increased (Table 1). At this concentration of butyrate, the induced receptors were fully coupled to the adenylate cyclase system and cAMP production was enhanced 10-fold by catecholamines.

Effects of butyrate on the microtubular network: Untreated HeLa cells were found to contain an extensive network of microtubules which appeared to be distributed randomly throughout the cell (Fig 1). There was a bright ring of microtubules around the nucleus where <sup>2</sup> in the peripheral parts of the cells, microtubules were found to be criss-crossing each other at various angles. The microtubular network appeared to originate from a single central, juxta-nuclear position and to radiate outwards to the margins of the cell. In HeLa cells treated with 5mM butyrate for 24 hours, a definite, more elongated, shape change which has previously been reported, was observed. The microtubular network in these cells appeared to be much more organized. Individual microtubules appeared to extend from the juxta-nuclear position to the tip of an extended neurite-like process or from the tip of one neurite-like process to the tip of another neurite-like process. A majority of the microtubules appeared to be lying along the long axis of a given cell with fewer criss-cross orientations being obvious (Fig 2). There also appeared to be fewer microtubules in the immediate vicinity of the nucleus. There was no significant difference in the amount of tubulin/cell as determined by  $^3\text{H}$ -colchicine binding between untreated and butyrate-treated HeLa cells. <sup>(HENNEBERRY, UNPUBLISHED OBSERVATIONS)</sup> Fig 3a demonstrates the microtubular distribution in cells exposed to butyrate and visualized with the polyclonal anti-tubulin antibody and Figure 3b was prepared using the monoclonal anti- $\alpha$  and anti- $\beta$  antibodies together.

HeLa cells grown as monolayers using conventional serum-supplemented medium and the newer hormone-supplemented, serum free medium gave essentially identical results in all cases. Colchicine prevents the butyrate-induced shape change in HeLa cells. At  $10^{-7}\text{M}$  and higher concentration, a 24 hour treatment of HeLa cells with colchicine was cytotoxic and only a small number of cells remained attached to the culture vessel. All these cells had a rounded appearance with no discernible microtubules being visible. However, a diffuse staining pattern was obtained

which may be attributed to the presence of depolymerized tubulin dimers. Occasionally, short segments of microtubules perhaps composed of tubulin paracrystals, <sup>or POLYMERIZA</sup> ~~ARRESTED~~ <sup>MICROTUBULE</sup> were seen in colchicine-treated cells.

Cells treated with  $10^{-7}$  M and higher concentrations of colchicine together with 5 mM butyrate did not show butyrate-induced shape changes and were <sup>morphologically</sup> ~~in fact~~ <sup>similar to</sup> just like HeLa cells treated with comparable concentrations of colchicine alone. Many of these cells also contained surface blebs which showed diffuse staining but no individual microtubules. At  $10^{-8}$  and  $10^{-9}$  M, colchicine alone had no apparent toxic effect on HeLa cells and the <sup>dr</sup> microtubules distribution pattern in these cells was similar to untreated HeLa cells (Fig 4a, 4b). 5 mM butyrate in the presence of  $10^{-8}$  M colchicine was able to induce a shape change in most cells but very few cells contained long strands of microtubules (Fig 5). Instead, most cells contained short, broken segments of microtubules. At  $10^{-9}$  M colchicine plus 5 mM butyrate, cells with altered morphology also displayed a change in microtubule distribution pattern comparable to cells treated with butyrate alone. However, many rounded cells were also present (Fig 6).

Cycloheximide also inhibits the butyrate-induced shape change in these cells. At 10  $\mu$ g/ml, cycloheximide alone had no effect on the microtubules distribution pattern which was <sup>identical to that in</sup> ~~exactly like~~ untreated cells (Fig 7). With monoclonal antibodies, extremely low background <sup>was</sup> obtained. In addition, with both anti- $\alpha$  and anti- $\beta$  tubulin monoclonal antibodies, many microtubules gave a segmented appearance indicating the position of alpha and beta subunits of a tubulin dimer in a given microtubule.

In Table II is summarized the alterations in HeLa cell conformation and microtubular patterns observed following 24 hour of exposure to butyrate, colchicine and cycloheximide, either separately or in various combinations. Low doses of colchicine or cycloheximide do not evoke a change in cell shape and the microtubular array is similar to control cells. At higher concentrations, or in combination, there was disorganization and disintegration of the microtubular network. Only butyrate (5mM) alone promoted a triangular cell architecture in which the microtubules exhibited a polar orientation aligned with the long axis of the cell. Colchicine and cycloheximide blocked the shape change and caused extensive damage to the microtubular network with multiple surface blebs or vesicles which reacted intensely with tubulin antibodies.

## DISCUSSION

An extensive intricate cytoskeletal network is found in mammalian cells, consisting of three major filamentous systems; microfilaments, intermediate filaments and microtubules (23). The microtubules are cytoplasmic organelles composed of tubulin aggregates. The protofilaments of the tubulin protein consist of two very similar molecules,  $\alpha$  and  $\beta$  tubulin, each having a molecular weight of about 55,000. In stable form, the tubulin is an  $\alpha$ - $\beta$  heterodimer with a molecular weight of 110,000. The structure of the microtubules vary in length from a fraction of a micrometer to several micrometers and have a rather constant diameter of about 25 nm (16). Significant progress with respect to structural-functional aspects of this system has been made recently with the availability of specific immunofluorescent techniques for the visualization of tubulin and its sub-units. The actual mechanisms whereby butyrate causes the multitude of effects described in the Introduction Section is not yet understood. Based on past experimental evidence correlating histone hyperacetylation with gene expression, it had been proposed that most of the effects of butyrate could result from histone hyperacetylation and subsequent changes in chromatin structure as measured by accessibility to DNA (1). Others have argued that "... the consequences of butyrate treatment are far more complex than an inhibition of histone deacetylase activity would suggest. Therefore, it is premature to conclude that histone hyperacetylation per se, is the major triggering mechanism responsible for the alterations of phenotype and G<sub>1</sub>-arrest of butyrate-treated cells." (11).

Butyrate treatment has also been shown to cause DNA hypomethylation and it has, therefore, been argued that induction of differentiation by butyrate is mediated by hypomethylation of DNA (23). Our own studies lead us to conclude that the induction of  $\beta$ -adrenergic receptors in HeLa cells could not be explained solely on the basis of either DNA hypomethylation or hypermethylation.

Changes in the cytoskeletal elements of the cell, especially the microtubular apparatus, have long been implicated in butyrate-induced morphological alterations in HeLa cells (2). However, this aspect of the effect of butyrate on HeLa cells ~~has~~ not been pursued in any detail. In a single published study so far, it was found that the exposure of transformed NRK cells to butyrate results in the appearance of cytoplasmic actin fibers in a distribution which closely resembles the actin distribution patterns of untransformed NRK cells and is distinctly different from the actin distribution pattern of transformed but untreated NRK cells (25).

Strong evidence has been adduced that during the intracellular transport of membrane components, the final transport step from the Golgi apparatus to the cell surface occurs by specific vesicles that migrate to the plasma membrane (26). We have investigated the effect of butyrate on microtubular distribution patterns in HeLa cells utilizing both polyclonal and monoclonal antibodies and report a considerable effect of butyrate on the microtubular distribution in HeLa cells. Of profound interest is whether the membrane mobilization of latent  $\beta$ -adrenergic receptors in HeLa cells by butyrate could be directed by elements of the cytoskeleton.

The original hypothesis has been challenged recently. Rogalski et al (27, 28) have shown that intracellular processing of an integral surface protein is independent of the assembly status of cytoplasmic microtubules. In a detailed study on the intracellular transport of the G. glycoprotein of vesicular stomatitis virus in cells infected with the virus, it was concluded that disruption of the microtubules did not inhibit the rate or extent of surface expression of the G protein (27). These investigations however, are predominantly dependent on poisoning of the microtubular polymerization by colchicine or other disruptive agents and the evidence is hence, indirect.

It has been shown, at least in some systems studied so far, that  $\beta$ -adrenergic receptors are normally constrained in the plasma membrane by a mechanism which involves microtubules or microfilaments (29). A reorganization of the microtubular network in HeLa cells induced by butyrate may be responsible for removing or lessening such a constraint so that receptor mobility is increased leading to efficient coupling of the  $\beta$ -adrenergic receptor with the adenylate cyclase. This reorientation of microtubules may also enhance or facilitate movement of  $\beta$ -adrenergic receptors from an intracellular pool to the cell surface.

However, changes in the distribution pattern of microtubules are not implied as being the sole mechanism for increased  $\beta$ -adrenergic receptor numbers in HeLa cells after butyrate treatment. Concomitant alterations in genome expression and membrane physiology undoubtedly occur. Cycloheximide prevents  $\beta$ -adrenergic receptor induction by butyrate in HeLa cells but does not have any effect, *per se*, on the microtubules (Table I). Thus, additional protein(s) are perhaps necessary for  $\beta$ -adrenergic receptor induction or insertion to take place. Paradoxically, colchicine at  $10^{-8} M$ , while it does not promote butyrate-treated HeLa cells and depolymerizes the microtubules in this study appears not to block receptor induction by butyrate (11) as measured by biochemical techniques.

Thus, the role of the cytoskeleton in butyrate-mediated receptor induction is far from clear. It remains likely, however, that the many membrane events in cultured cells, associated with butyrate-induction, involving genome to membrane signal transfer may be associated or, in fact, preceded by a dramatic reorganization of cytoplasmic structure and metabolism. The cytoskeletal network offers one possible route of transduction from the nucleus or cytosol to the plasma membrane and the very recent availability of highly specific antibodies renders this concept a hypothesis worthy of pursuit.

TABLE I

Effect of sodium butyrate on specific binding of  $^3\text{H}$ -DHA and l-isoproterenol stimulated cAMP production in HeLa - ES-1 cells.

Condition	Specific $^3\text{H}$ -DHA binding (f.mol/mg protein)	cAMP production p.moles/mg protein/min
Control	181	2.0
Treated (5mM butyrate)	562	10.3
Control	165	
Treated (10 $\mu\text{g}/\text{ml}$ cycloheximide)	190	
Treated (5mM butyrate)	490	
Treated (5mM butyrate + 10 $\mu\text{g}/\text{ml}$ cycloheximide	145	

Cell monolayers were treated with or without either 5 mM butyrate 10  $\mu\text{g}/\text{ml}$  cycloheximide or both together in fresh growth medium for 24  $\pm$  1 hour. Monolayers were harvested and used for the assay of  $\beta$ -adrenergic receptor binding utilizing 5 nM  $^3\text{H}$ -DHA and l-isoproterenol (10  $\mu\text{M}$ ) stimulated cAMP production. All experiments were performed in triplicate and were uniformly reproducible with different batches of cells  $^3\text{H}$ -DHA.

TABLE II

Summary of the structural alterations in HeLa ES-1 cells with and without exposure to butyrate, colchicine and cycloheximide

Condition	Cell Shape	Microtubular Network (MTN)
Control	Oval, circular conformation	Random organization of microtubules
5mM butyrate	Elongate shape change	Microtubules are oriented parallel to the long axis of the cells
Colchicine ( $10^{-8}$ , $10^{-9}$ M)	No shape change	MTN is similar to control
Colchicine ( $10^{-8}$ M) + 5mM butyrate	No shape change	Many cells contain short or broken microtubules
Colchicine ( $10^{-9}$ M) + 5 mM butyrate	No shape change	Cells appear normal
Cycloheximide (10 $\mu$ g/ml)	No shape change	Cells appear normal
Cycloheximide (50 $\mu$ g/ml) + colchicine ( $10^{-8}$ M)	No shape change	There is extensive disorganization and destruction of the MTN
5mM butyrate + colchicine ( $10^{-8}$ M) + 50 $\mu$ g/ml cycloheximide	No shape change	Diffuse disorganization of the microtubules. Many of the surface bleb structures stain for the antibody

#### LEGENDS TO FIGURES

Figure 1. The microtubular network (MTN) in an untreated HeLa cell. The MTN was visualised by using monoclonal anti- $\alpha$  tubulin (ascites fluid diluted 1:1000). A bright concentric ring of microtubules is located around the nucleus. In the peripheral region of the cell microtubules are observed to criss-cross each other at multiple angles. X =

Figure 2. The MTN in a HeLa ES-1 cell treated with 5.0 mM butyrate for 24 hr. The MTN was visualized by using monoclonal anti- $\alpha$  tubulin (ascites fluid 1:500). Relatively few microtubules are seen in the vicinity of the nucleus. Most of them are seen lying parallel to the long axis of the cell or extending from the tip of one cell to the other. X =

Figure 3a. MTN appearance in ES-1 cells treated with 5.0 mM butyrate. The antibody is polyclonal anti-tubulin. X =

Figure 3b. MTN as visualized by monoclonal anti- $\alpha$  tubulin together with monoclonal anti- $\beta$  tubulin (1:500) in ES-1 cells treated with 5.0 mM butyrate. X =

Figure 4a. HeLa ES-1 cells treated with  $10^{-8}$  M colchicine for 24 hr. (Monoclonal anti- $\beta$  tubulin, diluted 1:500). Note the lack of effect of colchicine on the MTN at this concentration. X =

Figure 4b. HeLa ES-1 cells treated with  $10^{-9}$  M colchicine for 24 hr. (Monoclonal anti- $\beta$  tubulin, diluted 1:500) the microtubular network is intact. X =

Figure 5. HeLa ES-1 cells treated with 5.0 mM butyrate plus  $10^{-8}$  M colchicine for 24 hr. (Monoclonal anti- $\beta$  tubulin diluted 1:500). Many of the cells contain short or broken microtubules. X =

Figure 6. HeLa ES-1 cells exposed to 5.0 mM butyrate plus  $10^{-9}$  M colchicine for 24 hr. (Monoclonal anti- $\beta$  tubulin, diluted 1:500). Note that the shape changes evoked by butyrate are not blocked by colchicine at this concentration. X =

Figure 7. HeLa ES-1 cells treated with 10.0  $\mu$ g/ml cycloheximide for 24 hr. (Monoclonal anti- $\beta$  tubulin, diluted 1:500). The microtubular network presents a distribution pattern essentially similar to that of control cells. X =

Figure 8. HeLa ES-1 cells treated with 5.0 mM butyrate and 10  $\mu$ g/ml cycloheximide (monoclonal anti- $\beta$  tubulin, diluted 1:500). The microtubules appear to be attached to the nucleus and radiate outwards to the cell border. X =

Figure 9. ES-1 cells exposed to  $10^{-8}$  M  $\mu$ g/ml colchicine + 50  $\mu$ g/ml cycloheximide for 24 hr (polyclonal anti-tubulin). This treatment results in extensive destruction of the MTN. X =

Figure 10. ES-1 cells treated with 5.0 mM butyrate,  $10^{-8}$  M colchicine and 50  $\mu$ g/ml cycloheximide (polyclonal anti-tubulin). The butyrate shape change is blocked and many of the surface bleb structures stain for the antibody. X =

#### REFERENCES

1. Kruh J: (1982) Effects of sodium butyrate, a new pharmacological agent, on cells in culture. *Mol. Cell. Biochem* 42: 65-82.
2. Henneberry RC, Fishman PH, Freese E: (1975). Morphological changes in cultured mammalian cells: prevention by the calcium ionophore A23187. *Cell* 5 1-9.
3. Henneberry RC and Fishman PH: (1976). Morphological and biochemical differentiation in HeLa cells. *Exp. Cell. Res.* 103:55-62.
4. Ghosh NK and Cox RP: (1976). Production of human chorionic gonadotropin in HeLa cell cultures. *Nature* 259: 416-417.
5. Ghosh, NK and Cox RP: (1977). Induction of human follicle-stimulating hormone in HeLa cells by sodium butyrate. *Nature* 267:435-437.
6. Cox GS: (1980). Synthesis of the glycoprotein  $\alpha$ -subunit and placental alkaline phosphatase by HeLa cells: Effects of timoca, ucom, 2-deoxyglucose and sodium butyrate. *Biochemistry* 20:4893-4900.
7. Deutsch SI, Silvers DN, Cox RP, Griffin MJ and Ghosh NK: (1976). Ultrastructural and enzymic modulation of HeLa cells induced by sodium butyrate and the effects of cytochalasin B and colcemid. *J. Cell. Sci* 21:391-406.
8. Fishman PH, Bradley RM and Henneberry RC: (1976). Butyrate-induced glycolipid biosynthesis: properties of the induced sialyltransferase. *Arch. Biochem. Biophys.* 172:618-626.
9. Tallman JF, Smith CC and Henneberry, RC: (1977). Induction of functional  $\beta$ -adrenergic receptors in HeLa cells. *Proc. Natl. Acad. Sci. USA* 74:873-877.
10. Fishman PH, and Henneberry RC: (1980). Induction of ganglioside biosynthesis in cultured cells by butyric acid. In: *Cell Surface Glycolipids* (ed. CC Sweeley). ACS Symp. Ser# 128, 223-239.
11. Riggs MG, Whittaker RG, Neumann DR and Ingram VM: (1977) N-butyrate causes histone modification in HeLa and Friend erythroleukemia cells. *Nature* 268:462-464.
12. Jahangeer S, Elliott RM and Henneberry RC: (1982).  $\beta$ -adrenergic receptor induction in HeLa cells: synergistic effect of 5-Azacytidine and Butyrate. *Biochem. Biophys. Comm.* 108:1434-40.
13. Alberts B, et al.: (1983). *Molecular Biology of the Cell*. pp. 598-671. Garland Pub. Co. New York.
14. Murti KG and Goorha R: (1983). Interaction of frog virus 3 with the cytoskeleton: altered organization of microtubules, intermediate filaments and microfilaments. *J. Cell Biology* 96:1248-1257.

15. Meza J, Sabanero M, Stefani E and Cerejido M: (1982). Occluding junctions in MDCK cells: modulation of transepithelial permeability by the cytoskeleton. *J. Cell Biochem.* 18:407-421.
16. Jacobson BS: (1983). Interaction of plasma membrane with the cytoskeleton: an overview. *Tissue and Cell* 15:829-852.
17. Zor V: (1983). Role of cytoskeletal organization in the regulation of adenylate cyclase-cyclic adenosine monophosphate by hormones. *Endocrine Reviews* 4:1-21.
18. Henneberry RC, Smith CC and Tallman JF: (1977). Relationship between  $\beta$ -adrenergic receptors and adenylate cyclase in HeLa cells. *Nature* 268:252-254.
19. Boffa LC, Gruss RJ and Allfrey VG: (1981). Manifold effects of sodium butyrate on nuclear function. Selective and reversible inhibition of phosphorylation of histone H<sub>1</sub> and H<sub>2</sub>A and impaired methylation of lysine and arginine residues in nuclear protein fractions. *J. Biol. Chem.* 256:9612-9621.
20. Christman JK, Weich N, Schoenbrunn N, Schneiderman N and Acs G: (1980). Hypomethylation of DNA during differentiation of Friend erythroleukemia cells. *J. Cell. Biol.* 86:366-370. FRIEND
21. Bylund DB: (1980). Analysis of receptor binding data. In: *Receptor Binding Techniques*. Soc. for Neurosciences. Cincinnati, Ohio pp.70-99.
22. Steiner AL, Parker CW and Kipnis DM: (1972). Radioimmunoassay for cyclic nucleotides I: Preparation of antibodies and iodinated cyclic nucleotides. *J. Biol. Chem.* 247:1106-1113.
23. Schliwa M and van Blerkom J: (1981). Structural interaction of cytoskeletal components. *J. Cell. Biol.* 90: 222-235.
24. Jahangeer S: (1983). Induction of  $\beta$ -adrenergic receptors in cultured mammalian cells. Ph.D. Thesis. The George Washington University, Washington, D.C.
25. Alenburg BC, Via DP and Steiner SH: (1976). Modification of the phenotype of murine sarcoma-virus-transformed cells by sodium butyrate. *Exp. Cell. Res.* 102:223-241.
26. Farquhar M and Palade GE: (1981). The Golgi apparatus (complex) - (1954-1981) - from artifact to center stage. *J. Cell. Biol.* 91:773-1035.
27. Rogalski A, Bergmann JE and Singer SJ: (1984). Effect of microtubule assembly status on the intracellular processing and surface expression of an integral protein of the plasma membrane. *J. Cell. Biol.* 99:1101-1109.
28. Boyd AE III, Bolton WE, and Brinkley BR: (1982). Microtubules and beta cell function: Effect of colchicine on microtubules and insulin secretion in vitro by mouse beta cell. *J. Cell Biol.* 92:425-434.

29. Cherksey BD and Zadunaiskey JA: (1981). Membrane  $\beta$ -receptors: interaction with the cytoskeleton in chloride secretory systems. Ann. N.Y. Acad. Sci. 372:309-331.

# **Effect of Bile Salt-Binding Resins on the Morphology of Rat Jejunum and Colon A Scanning Electron Microscopy Study**

**MARIE M. CASSIDY, FRED G. LIGHTFOOT, LAURETTA E. GRAU, TIMOTHY ROY,  
JON A. STORY, DAVID KRITCHEVSKY, and GEORGE V. VAHOUNY**

Reprinted from  
**DIGESTIVE DISEASES AND SCIENCES**  
New Series Vol. 25, No. 7, July 1980  
© 1980, Published by Plenum Publishing Corporation  
Printed in U.S.A.

# Effect of Bile Salt-Binding Resins on the Morphology of Rat Jejunum and Colon

## A Scanning Electron Microscopy Study

MARIE M. CASSIDY, FRED G. LIGHTFOOT, LAURETTA E. GRAU, TIMOTHY ROY,  
JON A. STORY, DAVID KRITCHEVSKY, and GEORGE V. VAHOUNY

*One mechanism suggested to account for the hypocholesterolemic effect of dietary fibers is their ability to sequester bile salts. Since bile salts have been found to alter intestinal structure, the morphological effects of several commonly used, xenobiotic, bile salt-binding agents was investigated. Wistar rats were fed a purified stock diet, ad libitum, for 6 weeks containing either 2% cholestyramine, 2% colestipol, or 2% DEAE-Sephadex. The bile salt-binding capacity of these substances was tested in vitro using taurocholate and glycocholate. The effect of in vivo feeding of the resins was to evoke ultrastructural topographical deviations from control appearance in both jejunal and colonic mucosae. Colonic cell injury was more severe than that observed in the jejunum of both colestipol- and DEAE-Sephadex-fed animals while the reverse was true for the rats fed cholestyramine. The degree of distortion in each condition was positively correlated with the extent of bile salt-binding capability in vitro. The rank order of both effects in terms of increasing severity was DEAE-Sephadex < colestipol < cholestyramine.*

Cholestyramine, colestipol, and DEAE-Sephadex are synthetic, nonabsorbable anion-exchange resins which effectively bind bile acids *in vitro* (1, 2) and *in vivo* (3-5). This binding reduces the effective micellar concentration of bile acids in the upper intestinal tract, thereby decreasing the solubilization of cholesterol and of the monoglycerides and fatty acids derived from lipolysis (6). This, in turn, leads to hypolipidemia and increased fecal elimination of certain lipids (7, 8). In addition to the possible direct effects of cholestyramine on cholesterol absorption, there is also a tenfold increase in fecal excretion of the bound bile acids (9), resulting in reduced feed-

Manuscript received August 6, 1979; revised manuscript received February 11, 1980; accepted February 11, 1980.

From the Departments of Physiology and Biochemistry, The George Washington University, School of Medicine and Health Sciences, Washington, D.C.; and The Wistar Institute of Anatomy and Biology, Philadelphia, Pennsylvania.

Address for reprint requests: Dr. M.M. Cassidy, The George Washington University, School of Medicine and Health Sciences, 2300 I Street, N.W., Washington, D.C. 20037.

back control of hepatic bile acid production. The increased conversion of cholesterol to bile acids in the liver and the decreased absorption of endogenous and exogenous cholesterol in the intestine result in sustained reduction in plasma cholesterol levels and total body cholesterol (6). Since cholestyramine is not absorbed in the gastrointestinal tract, its major side effects are considered to be limited to the gut. Our primary interest was in determining whether the hypolipidemic properties of these materials could be associated with morphological modifications of the epithelial layer.

The purpose of the present study was to assess the relative bile salt-binding capacities of cholestyramine, colestipol, and DEAE-Sephadex and to compare their specific effects on the morphology of jejunal and colonic mucosa. The present report describes the marked effects of these resins on the morphology of the jejunum and colon as assessed by light and scanning electron microscopy (SEM).

## BILE SALT-BINDING RESINS

TABLE 1. EFFECT OF ANION-EXCHANGE RESINS ON BILE SALT-BINDING IN VITRO AND ON INTESTINAL MORPHOLOGY IN VIVO\*

Resin addition†	Bile salt-binding in vitro (%)		Percentage of intestinal villi or colonic ridges with abnormal structure‡		Extent of deviation from normal (1.0-4.0)	
	Taurocholate	Glycocholate	Jejunum	Colon	Jejunum	Colon
DEAE-Sephadex	35.08	35.28	13.0 ± 3.6	40.6 ± 9.1	1.6 ± 0.7	2.5 ± 0.6
Colestipol	57.0 ± 0.5§	56.0§	35.9 ± 12.6*	55.0 ± 10.1	1.5 ± 0.4	2.9 ± 0.4
Cholestyramine	81.5 ± 0.2¶	69.3 ± 0.3	64.2 ± 4.7*	39.5 ± 10.5	3.7 ± 0.2*	3.2 ± 0.6

\*A minimum of 300 intestinal villi and 300 colonic folds from 3 animals per condition was examined. The criteria for morphological damage were twofold: the percentage of abnormal villi or colonic ridges observed to be abnormal; and the extent of deviation from normal as assessed by assigning a number from 1 to 4 to each villus or ridge examined.

†The purified diets were fed *ad libitum* for 6 weeks and contained in g/100 g: dextrose 53; casein, 25; corn oil, 14; salt mix, USP XIV, 5; vitamin mix, 1; resin, 2.

‡Means ± SEM of 4 analyses.

§The figures for bile salt binding *in vitro* represent the percentages of 100 μmol of the particular bile salt bound by 40 mg of the specific resin in 5 ml of saline at 37°C during 1-hr incubation period.

¶Means of 2 analyses.

\* = Significantly different from DEAE-Sephadex ( $P < 0.05$ ).

¶ = Significantly different from DEAE-Sephadex ( $P < 0.001$ ).

## MATERIALS AND METHODS

**Animals and Diets.** Male albino rats of the Wistar strain (Carsworth Farms), weighing 150-200 g, were maintained in individual cages and provided the diet and drinking water *ad libitum* for six weeks. They were housed in quarters maintained at 23°C and with a 12-h dark-light cycle. The isocaloric, isoglycemic diets administered in these studies were comparable to those used earlier (2) and consisted of the following ingredients in g/100 g diet: dextrose, 55; casein, 25; corn oil, 14; salt mix, USP XIV, 5; vitamin mix, 1; in the resin-fed groups cholestyramine, colestipol, or DEAE-Sephadex was added as 2% of the diet at the expense of dextrose in the control group. Food consumption and final body weights were similar in control and treated groups.

**Bile Acid and Cholesterol Binding by Cholestyramine.** *In vitro* studies on the binding of bile acids were carried out essentially as described earlier (2). Forty milligrams of resin were mixed with 100 μmol of the appropriate radioactive bile salt in 5 ml physiological saline (pH 7.0). These were incubated in sealed tubes for 1 hr at 37°C under constant gentle agitation. After incubation, the tubes were centrifuged at 32,000 g for 15 min. Aliquots (0.15 ml) of the supernatant were added to 10 ml of scintillation mixture and radioactivity was determined in a Beckman LS-250 liquid scintillation spectrometer.

**Morphological Methods.** Three rats in each dietary group and three in the control group were prepared for both light and scanning electron microscopic examination. At the end of the 6-week feeding period the rats were anesthetized with sodium pentobarbital and subjected to laparotomy. The alimentary tract from the pyloric sphincter to the terminal colon was removed and the jejunum was identified as the middle fifth of the small intestine. Colon samples were derived from the middle 5-cm segment of that organ. Rectangular segments of both regions were pinned flat and fixed in 3% phosphate-buffered glutaraldehyde. Efforts were made to keep the degree of tissue stretch during fixation as reproducible as possible.

During fixation the mucosal surface was brushed gently with a sable brush to remove loose debris (10). For scanning electron microscopy 1-cm<sup>2</sup> tissue samples were dehydrated and critical-point dried (Samdri PVT-3) using CO<sub>2</sub>. The samples were mounted on aluminum stubs with mucosal surface uppermost and coated with approximately 10 nm of gold/palladium using a Hummer I sputtering device. They were coded and observed in either an AMR 1000 or a JSM-35 scanning electron microscope using 20-25 kV accelerating voltage. The microscopists were unaware of the identity of the coded samples. A preliminary assessment was made by a single viewer. Two other microscopists reassessed those samples and then analyzed the results of a repeated experiment. All of the numerical values recorded for the previously agreed upon criteria (number of villi, severity of damage) were pooled and examined statistically (cf Table 1). A minimum of 300 jejunal villi and 300 colonic ridges from three animals per condition was examined, and the number of villi or ridges with abnormal structure was recorded. The degree of deviation from normal was graded on the following scale: 1 = apical swelling of cells, disordered microvillar array; 2 = dimpling of swollen cell surface, partial denudation of microvilli; 3 = loss of most microvilli, rents or tears in apical membrane; 4 = extrusion of cell contents and loss of cells from the epithelial layer.

Light microscopy preparations were obtained by post-fixation of glutaraldehyde-fixed samples in phosphate-buffered 2% OsO<sub>4</sub>, followed by dehydration and embedding in Epon resin. Sections approximately 0.5 μm thick were cut on a Sorvall MT2-B ultramicrotome, stained with toluidine blue, and examined in a Zeiss phase contrast microscope equipped with a Reichert automatic camera for photographic recording.

## RESULTS

The jejunal villi of control animals, fed the control diet which did not contain the resin material,



Fig 1. Individual villus of control jejunum. SEM reveals smooth and rounded contours and mucus strands are evident (arrow). The columnar epithelial cells tightly abut the basement membrane in LM insert. ( $\times 450$ , insert  $\times 325$ .)

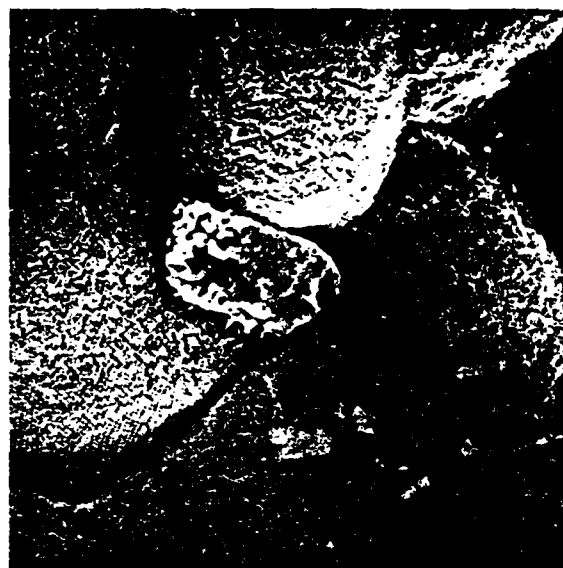


Fig 2. High-magnification SEM in control jejunum displaying epithelial cells with tightly packed microvilli surrounding a goblet cell with fewer microvilli. ( $\times 5000$ .)

are leaf-shaped and smooth in contour with intertwined mucin strands (Figure 1). Villar tips display an occasional protruding intact cell. At higher magnification (Figure 2) individual cell outlines are faintly demarcated, and the goblet cells appear as indentations or with mucus extrusions surrounded by the tightly packed microvilli of neighboring enterocytes. In Figure 2 a goblet cell is shown in the process of being shed into the lumen. The SEM appearance of goblet cells has been previously cross-correlated by transmission electron microscopy studies (14). Figure 3 shows the appearance of control colonic mucosa in SEM and light microscopy. The colon exhibits a smooth, regularly indented topography with the goblet cells interspersed among the more dominant absorptive epithelial cells. The microvilli of the latter are fairly dense and essentially similar to those in the small intestine (Figure 4).

**Cholestyramine Feeding.** In the cholestyramine-fed rats there was evidence of cell disruption and damage, primarily at the apices of the jejunal villi (Figure 5). Enlargement of a portion of Figure 5 clearly demonstrates apical cell swelling, microvillar denudation, partial or total disruption of the apical surface, and breaks or tears in the cell membrane. Expulsion of cell contents was frequently observed (Figure 6). The colons of the cholestyramine-fed rats show a whorled configuration with vi-

sual evidence that a large number of goblet cells are engaged in the process of secretion (Figure 7). In addition, sheets of mucus are present, overlying the mucosal surface. Many of the surface cells are damaged, exhibiting some hemorrhagic material, uneven swelling of microvilli (blebbing), loss of microvilli, and varying degrees of apical erosion (Figure 8).

**Colestipol Feeding.** The jejunum of colestipol-fed animals showed fairly normal structural features with mild disruption of microvillar morphology in a limited number of cells. In some samples, fibrin, erythrocytes, and other hemorrhagic debris were present on the surface of the tissue (Figure 9). Swollen, partially denuded cells surrounded by normal cells are shown at high magnification in Figure 10. The colonic samples were less smooth in topography than controls and showed evidence of cell necrosis with several of the surface cells being devoid of microvilli. Individual cell boundaries were clearly defined and cells appeared swollen at the apices (Figure 11). At higher magnification, microvillar denudation and cell loss could be seen (Figure 12).

**DEAE-Sephadex Feeding.** Chronic ingestion of 2% DEAE-Sephadex by rats appeared to be associated with more convoluted jejunal villi than those characteristic of control animals (Figure 13), but this point has not been evaluated quantitatively. Denudation of the brush border and erosion of a



Fig. 3. Control colonic mucosa with a smooth and corrugated appearance. LM displays a histologically intact pattern reflecting that observed by the SEM mode. ( $\times 85$ , insert  $\times 150$ .)



Fig. 4. High magnification of control colon shows several goblet cells (arrows), mucus (M) from a goblet cell, and an empty goblet cell orifice (O) being extruded. Note surrounding microvilli are densely packed. ( $\times 4200$ .)



Fig. 5. Individual villus of cholestyramine-treated jejunum. A line of cell damage traverses the apex of the villus. Insert: The uppermost cells show swelling and separation from the contiguous normal cells, whereas cells along the side of the villus are undamaged. ( $\times 785$ , insert  $\times 155$ .)



Fig. 6. At higher magnifications of cholestyramine-treated jejunum cellular damage is seen as cell disruption and extrusion of cytoplasmic components (arrow). ( $\times 3600$ .)

limited number of cells at the villus tips was frequently observed, as exemplified by Figure 14. The colonic surface in this condition was distinctly abnormal. Instead of the smooth ridges seen in control

tissues (cf Figure 3), the cells were arranged in deep whorls with a large amount of mucin present (Figure 15). Some cells were distorted in shape, with tears in the apical membrane (Figure 16).

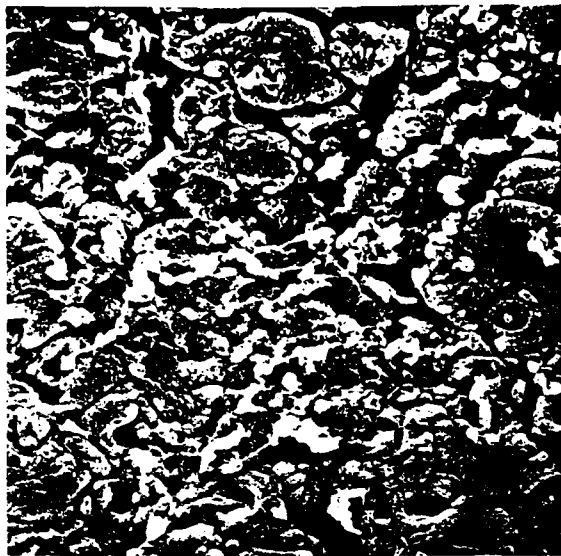


Fig. 7. Colonic mucosa of cholestyramine-treated animals shows a whorled pattern with considerable mucus present. ( $\times 300$ .)



Fig. 8. High magnification of cholestyramine colon. Cell outlines are visible and totally denuded cells are interspersed throughout (arrows). ( $\times 1200$ .)



Fig. 9. In colestipol-treated jejunum erythrocytes are enmeshed in fibrin clots. The villi appear otherwise unaffected. ( $\times 400$ .)



Fig. 10. Colestipol-treated jejunum at high magnification displays occasional denudation and cellular damage. ( $\times 3850$ .)

Table 1 summarizes the ability of the various resins to bind the more common bile salts *in vitro* and the effect of chronic feeding of these resins on the morphology of the jejunum and colon. There ap-

pears to be at least a qualitative correlation between these two parameters. Cholestyramine-feeding was associated with significantly greater ultrastructural damage when compared to Sephadex feeding. With



Fig. 11. Colonic mucosa of colestipol-treated animal reveals a moderate degree of whorling and cellular disruption. ( $\times 150$ .)

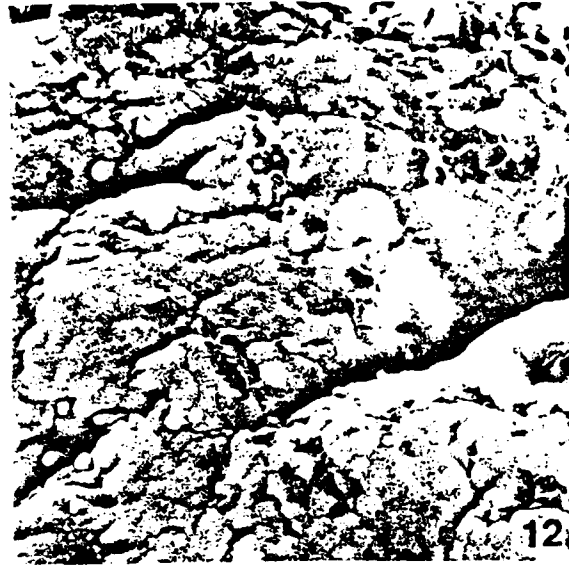


Fig. 12. High magnification of colestipol-treated colon. Individual cells are clearly demarcated with a prevalence of microvillar denudation and cell extrusion. ( $\times 100$ .)

the exception of cholestyramine, the specific structural alterations noted here were more severe and more extensive in the colon than in the jejunum.

#### DISCUSSION

Epithelial cell renewal plays an important role in the maintenance of mucosal integrity in the gastrointestinal tract. Recent SEM studies on the release of senescent mucosal cells indicate that these cells appear to be exfoliated from the surface of the stomach and the tips of the villi as intact cells (15, 16). For rat jejunum and colon we have confirmed this finding with this study (Figures 1, 2, & 3), and also by means of an extensive survey of nine other control animals.

The functional significance of the erosive damage at the villar tips seen with all three bile salt-binding resins is unclear. It is certainly a phenomenon which appears to be distinct from normal epithelial replacement modes. Damage to the mucosa of the small intestine and occasionally to the colonic mucosa has been found to occur with oral administration of several agents such as aspirin (13-16), alcohol (20), laxatives (12, 18, 19), cholera enterotoxin (23), and bile salts (21, 22).

It has been postulated that nonspecific mucosal injury appears to be a potent cocarcinogenic factor (29). More recently a strong association has been

suggested between high levels of fecal bile acids and the incidence of human colon cancer (30) and that secondary bile acids resulting from bacterial metabolism may be particularly important in this regard. Oral administration of bile acids or of cholestyramine (26) significantly enhances the carcinogenesis caused by chemical tumorigenic agents, and this stimulation is independent on the presence of intestinal bacteria (25). In similar experiments, it has been reported (27) that the majority of the bile acid components remained bound to cholestyramine while in transit through the alimentary tract. These results were originally interpreted as being contrary to the suggested role of bile acids as cocarcinogens (26, 27). However, neither of these studies considered that the resin itself, or the resin-bound bile acids might, *per se*, enhance the carcinogenic effect of 1,2-dimethylhydrazine (26, 27).

Light and transmission electron microscopy studies by several workers (14, 15) clearly show that the type of *in situ* cell degeneration observed in the present study causes breaks in the continuity of the mucosal barrier, allowing penetration of luminal materials to subepithelial layers. In the normal mature rat, 1.7% of intact antigenic protein is absorbed by the small intestine and 0.13% by the colon (26, 28). Several of the injury-provoking agents, such as bile salts and laxatives, significantly enhance the permeability of the intestine (23) and the colon (25).



Fig 13. Individual villus of DEAE-Sephadex-treated jejunum. Cell boundaries are pronounced and occasional microvilli disarray and partial denudation (arrow) is seen. ( $\times 600$ .)



Fig 14. High magnification of jejunal tissue treated with DEAE-Sephadex reveals apically eroded and partially denuded cells. ( $\times 5000$ .)



Fig 15. DEAE-Sephadex-treated colonic mucosa displays a moderately whorled pattern. ( $\times 320$ .)



Fig 16. High magnification of a whorled region of DEAE-Sephadex-treated colon shows loosely packed microvilli and tears in the epithelial membrane (arrows). ( $\times 6250$ .)

to macromolecules. With the mucosal irritation and disruption evoked by the feeding of the resin materials, significant quantities of antigenic or toxicogenic material could reach the bloodstream.

In the leaf-shaped villi of the resin-treated rats, lines of cell injury traversing the villar apices are

clearly seen. Therefore, it would appear that the epithelial cells most affected by these agents are the senescent enterocytes which occupy the tips of the intestinal and colonic folds. Whether or not these ultrastructural perturbations are directly linked to the enhanced incidence of tumor growth with cho-

## BILE SALT-BINDING RESINS

lestyramine which has been documented cannot be established at this time. A semiquantitative correlation has been found in the present study between the bile acid sequestration capability of a particular resin *in vitro* and the morphological damage to the jejunal mucosa induced by all three resins *in vivo*. This fact would seem to implicate the resin-bile salt complex as the primary etiologic factor in causing mucosal damage. The morphologic aberrations caused by either colestipol or DEAE-Sephadex feeding were quantitatively more pronounced in the colon than in the small intestine. Cholestyramine feeding appeared to damage less of the colonic surface area, but individual cells were more severely affected (Table 1). A compelling reason to account for the fact that cholestyramine alters a smaller number of the colonic ridges than do the other two bile sequestrants cannot be offered at this time. However, one possible explanation may be that the bile salts remain more tightly bound to cholestyramine in the colonic locus than do those attached to the other two sequestration agents.

Many factors associated with this type of cell degeneration are known to stimulate cytokinetic proliferation in both the small and large intestine by a postulated villus-to-crypt feedback mechanism (29). It remains to be determined whether the resin itself, free bile acids, or the resin-bile acid complex is the ultimate provocative agent causing epithelial disruption, either directly or indirectly. However, it could be suggested that long-term feeding of bile salt-binding materials may be linked to altered rates of cell repair and renewal in both intestinal and colonic loci within the alimentary tract.

### ACKNOWLEDGMENTS

This research was supported in part by U.S.P.H.S. grants HL-02033, HL-03299, Career Research Award (D.K.) HL-00734, and the I.T.T. Continental Baking Co. Research and Development Fund of the Biochemistry Department, George Washington University.

The authors gratefully acknowledge the generous gift of cholestyramine from Dr. H. Sarett of the Mead Johnson Research Center, Evansville, Indiana.

### REFERENCES

1. Kritchevsky D, Story J: *In vitro* binding of bile acids and bile salts. *Am J Clin Nutr* 28:305-306, 1975
2. Vahouny GV, Roy T, Gallo L, Story JA, Kritchevsky D, Cassidy MM, Grund B, Treadwell C: Dietary fiber and lymphatic absorption of cholesterol in the rat. *Am J Clin Nutr* 31:S208-S210, 1978
3. Heaton KW, Heaton ST, Barry RE: Comparison of two bile acid-binding agents, cholestyramine and lignin. *Clin Sci* 38:25P, 1970
4. Parkinson TM, Gunderson K, Nelson NA: Effects of colestipol (U-26, 597A), a new bile acid sequestrant on serum lipids in experimental animals and man. *Atherosclerosis* 11:531-537, 1970
5. Goodwin D, Noble RP, Dell RB: Effect of colestipol resin and colestipol plus clofibrate on turnover of plasma cholesterol in man. *J Clin Invest* 52:2646-2655, 1973
6. Yeshurn D, Gotto AM Jr: Drug treatment of hyperlipidemia. *Am J Med* 60:379-396, 1976
7. Glueck CJ, Ford SJ, Scheel D, Steiner P: Colestipol and cholestyramine resin. Comparative effects in familial type II hyperlipoproteinemia. *J Am Med Assoc* 222:676-681, 1972
8. Weizel A, Estrich DL, Splitter SD, Pomeroy V, Kinsell LW: Cholestyramine effect on plasma triglycerides in normolipidemic patients. *Proc Soc Exp Biol Med* 130:149-150, 1969
9. Danhof IE: The effect of cholestyramine on fecal excretion of ingested radioiodinated lipids. *Am J Clin Nutr* 18:343-349, 1966
10. Lightfoot FG, Cassidy MM: The effect of aspirin and prostaglandin E<sub>1</sub> intestinal mucus secretory pattern. *Scanning Electron Microsc* 2:719-726, 1978
11. Harding RK, Morris GP: Cell loss from normal and stressed gastric mucosae of the rat. An ultrastructural analysis. *Gastroenterology* 72:857-863, 1977
12. Gaginella TS, Lewis JC, Phillips SF: Rabbit ileal mucosa exposed to fatty acids, bile acids and other secretagogues. *Am J Dig Dis* 22:781-789, 1977
13. Cassidy MM, Lightfoot F: Electron microscopic study of gastrointestinal acetylsalicylic acid. *J Submicrosc Cytol* 11:449-462, 1979
14. Hingson DJ, Ito S: Effect of aspirin and related compounds on the fine structure of mouse gastric mucosa. *Gastroenterology* 61:156-177, 1971
15. Ivey KJ, Baskin WM, Krause WJ, Terry B: Effect of aspirin and acid on human jejunal mucosa: An ultrastructural study. *Gastroenterology* 76:50-75, 1978
16. Morris GP, Harding RK: Topography and fine structure of acute fundic mucosal erosions in the rat. *Lab Invest* 30:639-646, 1974
17. Fox JE, McElligott TF, Beck IT: Effect of ethanol on the morphology of hamster jejunum. *Am J Dig Dis* 23:201-209, 1978
18. Saunders DR, Sillery J, Rachmilewitz D: Effect of dioctyl sodium sulfosuccinate on structure and function of rodent and human intestine. *Gastroenterology* 69:380-386, 1975
19. Gaginella TS, Phillips SF: Ricinoleic acid (Castor oil) alters intestinal surface structure. A scanning electron microscopic study. *Mayo Clin Proc* 51:5-12, 1976
20. Asakura H, Tsuchiya M, Watanabe Y, Enomoto Y, Morita A, Morishita T, Fukumi H, Ohashi M, Castro A, Uylanog C: Electron microscopic study on the jejunal mucosa in human cholera. *Gut* 15:531-544, 1974
21. Low-Bear TS, Schneider RE, Dobbins WO III: Morphological changes of the small intestinal mucosa of guinea pig and hamster following incubation *in vitro* and perfusion *in vivo* with unconjugated bile salts. *Gut* 11:486-492, 1970
22. Saunders DR, Hedges JR, Sillery J, Esther L, Matsumura K, Rubin CE: Morphological and functional effects of bile salts on rat colon. *Gastroenterology* 68:1236-1245, 1975
23. Pozharisski KM: The significance of nonspecific injury for colon carcinogenesis in rats. *Cancer Res* 35:3824-3830, 1975

24. Reddy BS, Wynder EL: Large-bowel carcinogenesis: Fecal constituents of populations with diverse incidence rates of colon cancer. *J Natl Cancer Inst* 50:1437-1442, 1973
25. Reddy BS, Weisburger JH, Wynder EL: Colon cancer: Bile salts as tumor promoters. In *Carcinogenesis*, Vol 2, Mechanisms of Tumor Promotion and Carcinogenesis. TJ Slaga, A Swak, RK Boutwell (eds). New York, Raven Press, 1978, pp 452-464
26. Nigro ND, Bhadrachari N, Chomachi C: A rat model for studying colonic cancer: effect of cholestyramine on induced tumors. *Dis Colon Rectum* 16:438-443, 1973
27. Asano T, Pollard M, Madsen D: Effects of cholestyramine on 1,2-dimethylhydrazine induced enteric carcinoma in germfree rats. *Proc Soc Exp Biol Med* 150:780-785, 1975
28. Warshaw AL, Bellini GA, Walker WA: The intestinal mucosal barrier to intact antigenic protein. Differences between colon and small intestine. *Am J Surg* 133:55-58, 1977
29. Sprinz H: Factors influencing intestinal cell renewal. *Cancer* 28:71-74, 1971

A ROLE FOR THE CYTOSKELETON IN VECTORIAL EPITHELIAL  
TRANSPORT IN STOMACH AND SMALL INTESTINE?

Marie M. Cassidy, and Mumtaz A. Dinno\*

Department of Physiology, The George Washington  
University Medical Center, Washington, D.C., and

\*The Department of Physics and Astronomy, The  
University of Mississippi, Oxford, MS 38677

INTRODUCTION

Cytochalasin B (CB) is a macrolide antibiotic which interacts with the mechanochemical proteins present in microfilaments in a manner similar to the effect of colchicine on microtubules. Work from a number of laboratories suggest that the cytokinins inhibit the rate of actin filament polymerization and disrupt actin-based networks in a very dynamic manner (Lin, et al, 1980, McLean, Fletcher and Pollard, 1980). Most epithelial cells are now known to possess a highly ordered cytoskeletal matrix comprised of microfilaments, intermediate filaments and microtubules (Osborn et al, 1978). Macromolecular aggregates such as actin and actinin are present in the amplification structures of the small intestinal mucosal surface (Tilney and Mooseker, 1971, Mukherjee and Staehelin, 1971) and in frog skin (Pratley and McQuillen, 1973). It has been suggested that microfilaments may be critical physicochemical transducers in the chain of events leading to the interaction of hydro-osmotic forces with vasopressin, which evokes altered fluid flow across epithelia (Taylor, 1977). Microfilaments are closely associated with ouabain-resistant water transport in liver slices (Van Rossum and Russo, 1981). It has been proposed that cytokinin effects on membrane constituents, cell shape, electrophysiological parameters and ion transport are mediated by cAMP concentrations within the cells and associated with modification of junctional permeability (Bentzel and Hainau, 1979). More recent studies with an epithelial cultured cell preparation (MDCK cells)

indicate that the sealing of intercellular junctions involves the cellular assembly of microfilaments and microtubules and that Cytochalasin B disorganizes actin filaments, evokes functional opening and a decrement in the electrical resistance across the tissue layer (Cereijido et al, 1981).  $\text{Ca}^{++}$  ions, both extracellular and intracellular, play a role in these processes.

It is clearly recognized that for effective vectorial conveyance of solutes and water across epithelia segregated ions pumps and leaks exist in apical and basolateral membranes (Finn et al, 1981, Lewis and Wills, 1981). More importantly, such a design is only functional if mechanism(s) exist for apical to basolateral communication (Schultz, 1981). Rapid transmission of information between these discrete barriers is probably exerted by several signals including ion fluxes, alterations in conductance channels,  $\text{Ca}^{++}$  translocation and other intracellular messengers, e.g. the cyclic nucleotides. It is also possible that the structured cytomatrix of the epithelial cell is an organized medium for this purpose and, in addition, regulates the balance between transcellular and paracellular flow pathways (Bentzel and Hainau, 1979).

Electromechanical alterations in the cytoskeleton may manifest themselves as alterations in passive or active ionic conductance,  $\text{Ca}^{++}$  availability and cellular metabolism.

Using Cytochalasin B to disrupt microfilament assembly and organization we have been studying two epithelial models of transport with respect to this hypothesis. The first is the classic *in vitro* secretory preparation of frog gastric mucosa with which  $\text{H}^{+}$  secretion rates, electrical potential difference and resistance can easily be measured. The second is the intact *in vivo*, perfused rat jejunum in which steady-state absorption of major electrolyte and other solutes and fluid can be assessed. We have also examined morphological features of these transporting tissues by transmission and scanning electron microscopy. Ultrastructural examination is necessary to discern any possible cytoarchitectural deviations brought about by Cytochalasin treatment which would indicate possible links between perturbation of the cytoskeleton and functional transport status.

## METHODS

Frog Gastric Mucosa Preparation In Vitro

Stripped gastric mucosa from *Rana pipiens* were mounted in a modified Ussing chamber at 22°. The serosal fluid compartment contained a bicarbonate buffered NaCl Ringer's solution and a NaCl secretory solution was present in the mucosal compartment. The pH in the mucosal fluid was maintained at 5.0. Histamine ( $10^{-4}$ M) was placed in the serosal compartment to stimulate acid secretion. Two identical calomel electrodes were used to measure the transmural potential difference (PD). The electrical resistance across the mucosa was measured as the change in PD per microamps of current passed for 0.5 sec. in both directions sequentially. Serosal bathing solution contained in mM;  $\text{Na}^+$ : 101,  $\text{K}^+$ : 6.0,  $\text{Ca}^{++}$ : 1.0,  $\text{Mg}^{++}$ : 0.8,  $\text{Cl}^-$ : 81,  $\text{HCO}_3^-$ : 2.5,  $\text{PO}_4^{3-}$ : 1.0, glucose: 10. The mucosal bathing solution contained in mM;  $\text{Na}^+$ : 102,  $\text{K}^+$ : 4,  $\text{Cl}^-$ : 106. Both solutions were aerated with 95%  $\text{O}_2$ , 5%  $\text{CO}_2$ . In the experiments with CB, it was pre-dissolved in 0.1 ml DMSO and added to the serosal medium to a final concentration of  $10^{-5}$  M in the bathing medium.

Perfused Rat Jejunum, In Vivo

Male Wistar rats were anesthetized with Nembutal (40 mg/kg) and a tracheotomy performed. The abdomen was opened and the jejunum (middle 25 cm) of the small intestine was cannulated. The segment was rinsed gently with perfusate, returned to the abdominal cavity and the incision sutured. The perfusate was pumped at 0.5 ml/min (Holter microinfusion pump) through the proximal cannula and returned to the reservoir via the distal cannula. The perfusate contained a bicarbonate/phosphate-buffered Krebs Ringer solution. In the glucose perfusates, glucose was present at 36 mM and substituted for sodium.

Isotopically labelled polyethylene glycol (MW = 4000) was used as a tracer for net fluid transport. Recovery of infused PEG was  $98.2 \pm 2.6\%$ . Labelled  $^3\text{H}$ glucose and  $^3\text{H}$ erythritol (5 mM) were included in the appropriate perfusate to monitor net solute transport of these sugars. Sodium content of the perfusate solutions was determined by flame photometry. Net water and solute transport was

METHODS

Frog Gastric Mucosa Preparation In Vitro

Stripped gastric mucosa from Rana pipiens were mounted in a modified Ussing chamber at 22°. The serosal fluid compartment contained a bicarbonate buffered NaCl Ringer's solution and a NaCl secretory solution was present in the mucosal compartment. The pH in the mucosal fluid was maintained at 5.0. Histamine ( $10^{-4}$ M) was placed in the serosal compartment to stimulate acid secretion. Two identical calomel electrodes were used to measure the transmural potential difference (PD). The electrical resistance across the mucosa was measured as the change in PD per microamps of current passed for 0.5 sec. in both directions sequentially. Serosal bathing solution contained in mM; Na<sup>+</sup>: 101, K<sup>+</sup>: 6.0, Ca<sup>++</sup>: 1.0, Mg<sup>++</sup>: 0.8, Cl<sup>-</sup>: 81, HCO<sub>3</sub><sup>-</sup>: 2.5, PO<sub>4</sub><sup>3-</sup>: 1.0, glucose: 10. The mucosal bathing solution contained in mM; Na<sup>+</sup>: 102, K<sup>+</sup>: 4, Cl<sup>-</sup>: 106. Both solutions were aerated with 95% O<sub>2</sub>, 5% CO<sub>2</sub>. In the experiments with CB, it was pre-dissolved in 0.1 ml DMSO and added to the serosal medium to a final concentration of  $10^{-5}$  M in the bathing medium.

Perfused Rat Jejunum, In Vivo

Male Wistar rats were anesthetized with Nembutal (40 mg/kg) and a tracheotomy performed. The abdomen was opened and the jejunum (middle 25 cm) of the small intestine was cannulated. The segment was rinsed gently with perfusate, returned to the abdominal cavity and the incision sutured. The perfusate was pumped at 0.5 ml/min (Holter microinfusion pump) through the proximal cannula and returned to the reservoir via the distal cannula. The perfusate contained a bicarbonate/phosphate-buffered Krebs Ringer solution. In the glucose perfusates, glucose was present at 36 mM and substituted for sodium.

Isotopically labelled polyethylene glycol (MW = 4000) was used as a tracer for net fluid transport. Recovery of infused PEG was  $98.2 \pm 2.6\%$ . Labelled <sup>3</sup>Hglucose and <sup>3</sup>Herythritol (5 mM) were included in the appropriate perfusate to monitor net solute transport of these sugars. Sodium content of the perfusate solutions was determined by flame photometry. Net water and solute transport was

calculated from differences in the above parameters and changes in PEG concentration as follows:

1. net  $H_2O$  transport =  $P_R (1 - PEG_{in} / PEG_{out})$  dry wt.  
(ul/kg dry wt/min)
2. net solute transport =  $P_R (Solute_{in} - Solute_{out})$   
 $PEG_{in}/PEG_{out}$   
(uEq or u mols/kg dry wt/min)

$P_R$  = perfusion rate

The jejunum was perfused at 0.5 ml/min for two to three 30-minute transport periods to establish steady-state absorption. Cytochalasin B ( $1 \times 10^{-4}$  uM), dissolved in 0.1% dimethylsulfoxide, was then added to a fresh reservoir of perfusate and the experiment continued for an additional 2-3 hours.

#### Morphological Methods

Three tissues in each experimental group were prepared for light, transmission and scanning microscopy. Samples from the perfused jejunal loop and gastric mucosa sheets were fixed *in situ*, and at that time post-CB exposure produced an effect in the measured transport parameters that was discernable. Efforts were made to keep the degree of tissue stretch during fixation as reproducible as possible during primary fixation in 3% phosphate-buffered glutaraldehyde. For scanning electron microscopy 1  $cm^2$  tissue samples were dehydrated and critical-point dried (Samdri PVT-3) using  $CO_2$ . Samples were mounted on aluminum stubs, mucosal surface uppermost, and coated with 10 nm of gold/palladium. They were examined in a JSB-35 scanning electron microscope at 20-25 kV accelerating voltage.

Transmission microscopy preparations were obtained by post-fixation in phosphate-buffered 2% OsO<sub>4</sub> followed by dehydration and embedment in Epon resin. Thin sections (60nm) stained *en bloc* with uranyl acetate and lead citrate were observed in a JEOL 100 B transmission electron microscope. A minimum of 200 discrete villi (jejunal mucosa) and 100 oxyntic cells (gastric mucosa) per condition were studied.

## RESULTS AND DISCUSSIONS (GASTRIC MUCOSA)

The frog gastric mucosa is usually described as a relatively 'tight' epithelium. In these experiments, discrete populations of preparations could be distinguished on the basis of indigenous resistance (those with less than  $150 \text{ ohm.cm}^2$  and those with resistance greater than  $170 \text{ ohm.cm}^2$ ). This fact was utilized to enable us to differentiate possible effects of cytochalasin B (CB) on predominantly low conductance pathways and those of high conductivity. The CB vehicle, DMSO had no effect on the measured parameters, per se.

The Effect of CB in  $\text{Cl}^-$  Media

The addition of CB to the serosal medium bathing the mucosa consistently caused a decline in the titrated amount of NaOH in the mucosal fluid. This decrease in  $\text{H}^+$  secretory rate continued even after several washes in CB-free Ringers

TABLE 1 THE EFFECT OF CYTOCHALASIN B ON ELECTROPHYSIOLOGICAL PARAMETERS IN FROG GASTRIC MUCOSA FOR MEMBRANES WITH RESISTANCE LESS THAN  $150 \text{ }\Omega\text{.cm}^2$  IN  $\text{Cl}^-$  MEDIA

	PD (mV)	R ( $\Omega\text{.cm}^2$ )	$I_H$ ( $\mu\text{.eq.hr}^{-1}\text{cm}^{-2}$ )
CONTROL	$16.1 \pm 2.5 (6)^*$	$120 \pm 15$	$2.20 \pm 0.45$
CYTOCHALASIN B $5 \times 10^{-5} \text{ M}$	$19.3 \pm 1.4$ ( $P < 0.05$ )	$139 \pm 12$ ( $P < 0.05$ )	$1.64 \pm 0.41$ ( $P < 0.05$ )
CB-FREE WASH	$16.9 \pm 0.96$ ( $P > 0.20$ )	$122 \pm 18^{**}$ ( $P > 0.20$ )	$1.04 \pm 0.37$ ( $P < 0.05$ )

\*Mean  $\pm$  SD (No. of exp.) P values w.r.t. control.

\*\*Also not significantly different from value in the presence of CB.

solution. In all of these studies CB was added to the bathing solution after the membrane had reached a steady-state behavior, i.e., constant (PD), (R), and  $I_H$ . In general the addition of CB caused an increase in both (PD) and (R), while decreasing the  $H^+$  secretory rate. When CB was removed from the serosal bathing medium by repeated washing, the membrane potential and resistance showed a return to control levels. If CB was present for more than ten minutes, a continuous decline in (PD) occurred while the (R) remained constant. Table 1 provides a statistical analysis for the data obtained with membranes for which (R) is less than  $150 \text{ cm}^2$ , (PD) and (R) both increased with CB and reverted to control values following a CB-free wash. The  $H^+$  secretory rate decreased with the application of CB and continued to fall after the CB was removed. In Table 2 is shown the response of high resistance membranes in  $Cl^-$  media to CB.

TABLE 2 THE EFFECT OF CYTOCHALASIN B ON ELECTROPHYSIOLOGICAL PARAMETERS IN FROG GASTRIC MUCOSA FOR MEMBRANES WITH RESISTANCE GREATER THAN  $170 \Omega \cdot \text{cm}^2$  IN  $Cl^-$  MEDIA

CONDITION	PD (mV)	R ( $\Omega \cdot \text{cm}^2$ )	$I_H$ ( $\Omega \cdot \text{eq} \cdot \text{hr}^{-1} \cdot \text{cm}^{-2}$ )
CONTROL	$19.0 \pm 1.8 (5)^*$	$251 \pm 65$	$1.00 \pm 0.15$
CYTOCHALASIN B $5 \times 10^{-5} \text{M}$	$18.4 \pm 3.3$ ( $P > 0.20$ )	$275 \pm 49$ ( $P > 0.20$ )	$0.52 \pm 0.20$ ( $P < 0.05$ )
CB-FREE WASH	$12.5 \pm 2.1$ ( $P < 0.05$ )	$242 \pm 46$ ( $P > 0.20$ )	$0.22 \pm 0.09$ ( $P < 0.05$ )

\*Mean  $\pm$  SD (No. of exp.) P values w.r.t. control.

This agent had little detectable effect on (PD) or (R), but the  $H^+$  secretion was significantly reduced even during CB-free wash period when the (PD) also falls significantly. Cytochalasin B therefore exhibits different and distinct

effects on gastric mucosa depending on initial ionic conductance status of the preparation. It should be pointed out here that these two distinct groups of low vs. high resistance membranes could also be distinguished as high and low secretors, as one would expect. Accordingly, Cytochalasin B has a more pronounced effect on preparations with lower  $H^+$ -rate than on those with higher initial rates. This effect would be expected in view of the findings of other investigators in which the integrity of cytoskeletal structure affects significantly cellular function. Such findings are also confirmed in this study as will be presented in our morphological studies.

#### Morphological Effects of CB on Frog Gastric Musosa

Figure 1 demonstrates the ultrastructural characteristics of gastric mucosal parietal cells in the control

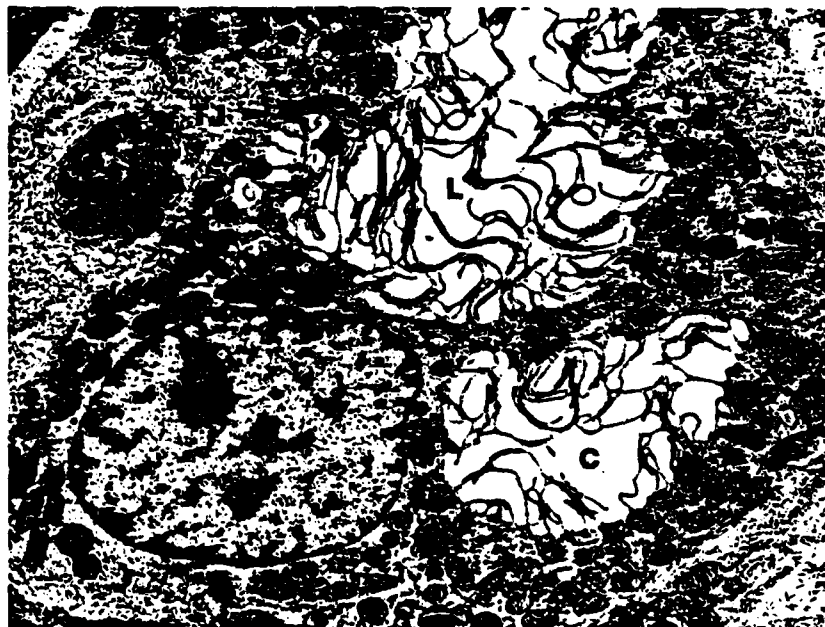


Fig. 1. Transmission electron micrograph of secretory parietal cells of frog gastric mucosa (control) L = lumen: TJ = tight junctions: C = secretory canalculus X = 7,200

$H^+$  secretory mode. The lumen of the gland (L) is visible with surface amplification structures, i.e., the microvilli. The oxytic cell canalici with microvillar processes were mostly patent. Several parietal cells surround the lumen, each cell demarcated by the cell to cell junctional nexus (TJ). The microvilli are long and irregular in shape but are few in number, compared to the density of microvilli in the small and large intestine (Fig. 2). Microfilaments can



Fig. 2. Transmission electron micrograph of apical luminal surface of gastric parietal cells in the secretory state (control). Microvilli are slender tortuous and sparse compared to intestinal microvilli and project into the lumen (L)  $\times 15,500$ .

be observed within the microvilli but they do not appear to penetrate to any great degree into the apical cytoplasm. Treatment of the tissue with  $1 \times 10^{-5}M$  (CB) sufficient to decrease the  $H^+$  secretory rate by 50% was associated with

several morphological effects. The secretory canaliculi appeared collapsed, with exposed surface and fewer microvilli. Many vacuolated structures containing electron-dense material which may be derived from tubulovesicles were present in the cytoplasm (Figs. 3 and 4). The luminal microvilli were pleomorphic in character and considerable membranous debris was found in the luminal space itself. Lysosomal-like organelles were also significantly more prominent in parietal cell cytoplasm. These *in vitro* preparations showed a greater than normal aridity for the heavy metal stains leading to osmophilic depositions which were not removable by extensive washing.

Microfilaments have been identified in the microvilli of parietal cells from several species both amphibian and mammalian (Black et al 1982). Several lines of evidence

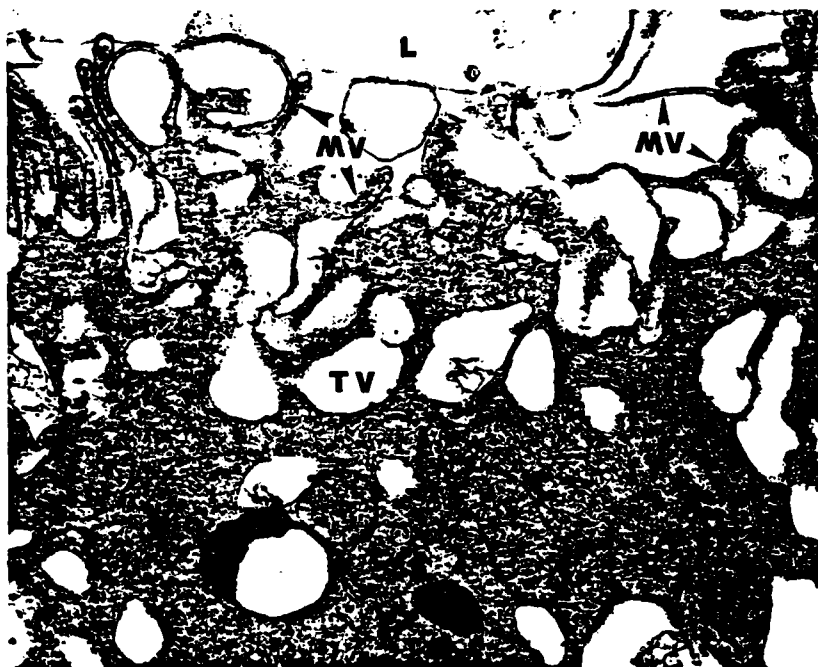


Fig. 3. TEM of frog gastric mucosa treated with  $1 \times 10^{-5}M$  (CB). Secretory canaliculus (C) is narrow with few microvilli. Extensive tubulovesicular structures (TV) are present in the cytoplasm X = 8,500.

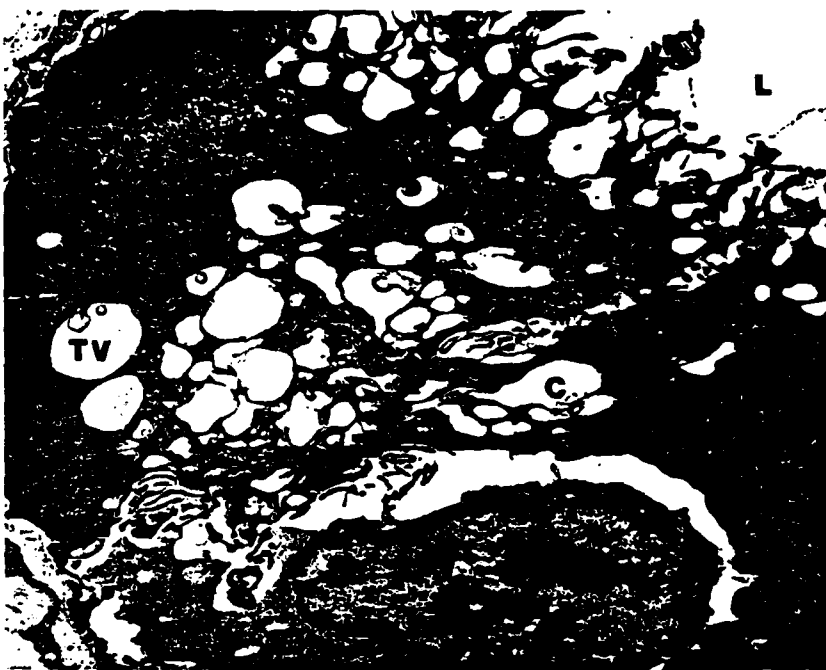


Fig. 4. TEM of gastric mucosa treated with  $1 \times 10^{-5}M$  (CB). The microvilli (MV) in the luminal surface are distended and distorted.  $\times 10,000$

have suggested that when  $H^+$  secretion begins, tubulovesicles move towards and fuse with the apical membranes of the cells. This migration of the tubulovesicular machinery and consequent maturation of the microvilli is a relatively rapid and dynamic process. As with many other secretory systems, e.g. the thyroid (Williams and Wolff, 1971), the pancreas (Orci et al. 1972) and mucin cells (Cassidy, et al. 1981) the microfilaments and/or the cytoskeleton may provide directional polarization and a structured pathway for the transport system. Our findings parallel those of Black et al. (1982) in that (CB) inhibits stimulated  $H^+$  secretion and causes distinct morphological alterations. The Forte group have also identified the presence of both actin and myosin in cytoplasmic fractions from rabbit and piglet gastric mucosa (Forte et al. 1981).

It is interesting to point out that, in a number of experiments where CB was left in the bathing media for more than 40 minutes, titration of NaOH came to a complete halt, and the pH on the luminal side actually showed a significant increase with time. Such an increase in the pH could best be interpreted as a leak of the serosal solution (pH = 7.4) to the luminal surface (pH = 5.0).

It is therefore obvious that the effect of CB is primarily related to changes in the cytoskeletal structure of the parietal cell and secondarily related to perturbations of transmural pathways which eventually caused the increase in the luminal pH. This later effect is not necessarily a localized effect to either the intracellular or the paracellular pathways. A disruption to the cytoskeletal structure could extend its effects to cause changes in the shunt pathways.

#### RESULTS AND DISCUSSION (RAT JEJUNUM)

##### Effect of Cytochalasin B on Rat Jejunum

Fluid absorption by the *in vivo* rat jejunum is believed to be isotonic and can generally be demonstrated to be related to the presence of both sodium and glucose in the mucosal fluid. The addition of glucose to the perfusate medium is associated with higher steady-state rates of water absorption compared to glucose-free perfusate (Powell and Malawer, 1968) and this observation is reiterated in the experiments shown in Fig. 5. In the absence of glucose in the luminal fluid  $H_2O$  absorption declined somewhat after 90 minutes. However, the addition of  $1 \times 10^{-4}M$  (CB) to the perfusate reservoir was associated with a rapid fall in fluid absorption from control rates in both the glucose-free and glucose media. The inhibition was in the range of 50-60%. When glucose was present, some recovery of transport was evident within 60 minutes, even though (CB) was still present in the luminal perfusate. The initial 1 hour relative depression of net fluid transport by Cytochalasin B was not influenced significantly by the availability of luminal glucose. The reversibility of the (CB) effect was not tested in these experiments since the inherent viability of the preparation is questionable after 4-5 hours.

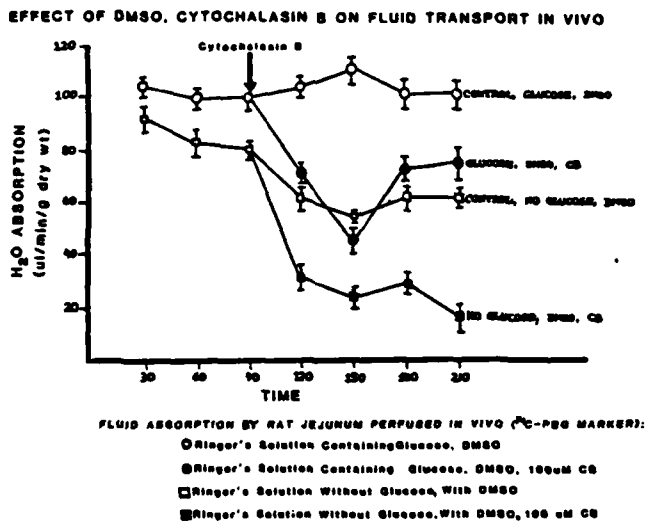


Fig. 5. Effect of DMSO, and Cytochalasin B on jejunal fluid transport, in vivo.

The absorption of sodium from the luminal perfusate was examined by flame photometry. In eight rats, 3 steady-state control and 3 steady-state (CB) treated periods were statistically analyzed and the results are shown in Fig. 6. 0.1% Dimethylsulfoxide, used as the solvent for (CB), did have an inhibiting effect on these absorption rates in contradistinction to its lack of effect on measured transport parameters in the in vitro gastric mucosal preparation. Nonetheless,  $1 \times 10^{-4}\text{M}$  (CB) in the mucosal fluid evoked a significant inhibition of luminal sodium uptake both in the presence and absence of glucose. The effect of DMSO, *per se*, on sodium and fluid transport in rat small intestine may be a direct lipolytic effect of the solvent on the membranes since the osmolarity of the perfusate introduced into the lumen did not alter with 0.1% DMSO addition.

In an attempt to characterize phenomenologic effects of Cytochalasin B and hence microfilament involvement in organic solute transport processes in the small intestine, we have

investigated the influence of (CB) on the absorption of labelled glucose (an actively transported solute) and labelled erythritol (a passively transported solute) in this system. Steady-state glucose absorption was depressed

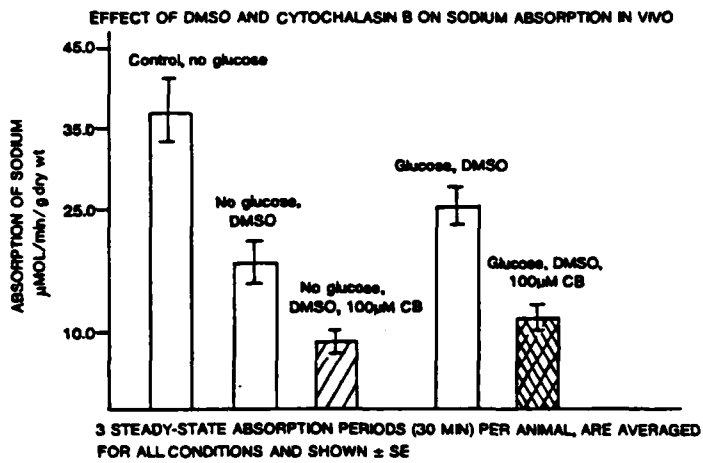


Fig. 6. Effect of DMSO and Cytochalasin B on Sodium Absorption In Vivo.

by the addition of  $1 \times 10^{-4}\text{M}$  (CB) but only after a one hour lag period (Fig. 7). Thereafter glucose uptake from the perfusate fell off very rapidly. The only cell membrane effect currently attributed to Cytochalasin B is its documented effect on the passive glucose carrier system (Mizel and Wilson, 1972). Kimmich and Randles (1979) have shown that in isolated intestinal cells, (CB) causes inhibition of glucose exit from the cells allowing intensive intracellular accumulation of the sugar. The time-lag of the (CB) inhibition of hexose transport observed here (Fig. 7) may be related to an effect of this agent on the serosal transport of glucose in the in vivo perfused jejunum. Cytochalasin B also affected the uptake of erythritol from the perfusate, but in the case of this sugar the depression was induced by the first 30 minute measurement period following the addition of (CB) to the perfusate. Clearly, both passive and active transport in these organic solutes are impaired by (CB) treatment of the intestinal mucosal epithelium (Fig. 8).

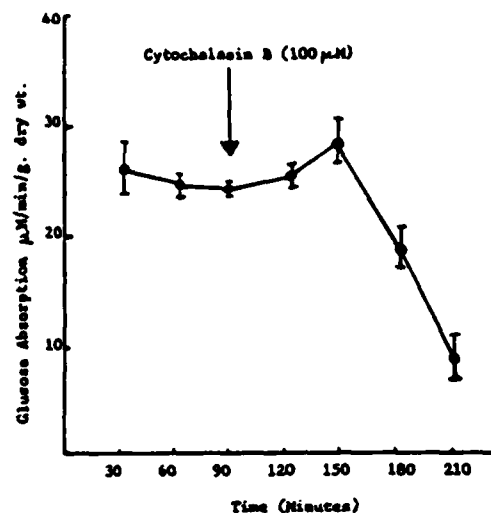


Fig. 7. The Effect of (CB) Addition on the Steady-State Absorption of Glucose in the Rat.

IN VIVO STEADY STATE TRANSPORT OF FLUID ( $^3\text{H}$ -PEG MARKER) AND A PASSIVE SOLUTE ( $^{14}\text{C}$ -ERYTHRITOL) IN THE ABSENCE AND PRESENCE OF CB ( $1 \times 10^{-6}\text{M}$ )

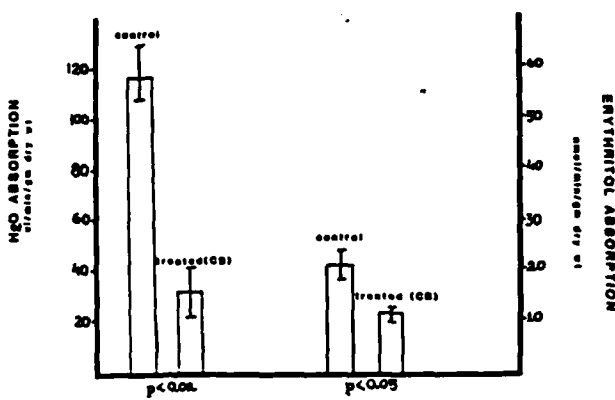


Fig. 8. Fluid Absorption and That of  $^{14}\text{C}$  Labelled Erythritol in the Rat Jejunum in the Presence and Absence of Cytochalasin B.

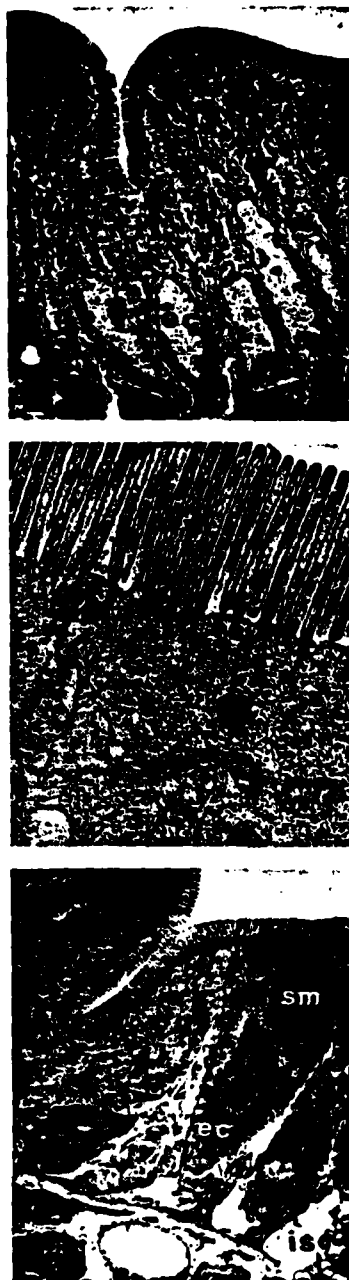


Fig. 9a. Transmission electron micrograph of jejunal mucosa in steady-state absorptive conditions. Epithelial cells (EC) are regular, columnar with no large intercellular spaces evident.  $\times = 1,920$

Fig. 9b. Apical surface of rat jejunum (transmission electron micrograph) in control absorptive conditions. The microvilli (MV) are tall and their cytoskeletal matrix projects vertically into the apical cytoplasm (arrow).  $\times = 8,000$

Fig. 9c. Transmission electron micrograph of CB-treated jejunal mucosa. Epithelial cells (EC) are distorted compared to normal columnar configuration and an expansion of the lateral intercellular space (IS) is noted. SM = surface mucin goblet cells  $\times = 1,920$

### Morphological Effects of (CB) Exposure on Rat Jejunal Ultrastructure

Transmission electron microscopy of normal transporting rat jejunum *in vivo* reveals columnar epithelial cells (Fig. 9a) with few apparent intercellular spaces. The microvilli show central microfilaments which project longitudinally into the terminal web area (Fig. 9b). At this level of morphology, the most obvious effect noted was a contraction of the basal portions of the epithelial enterocytes and/or an expansion of the intercellular spaces (Fig. 9c). The apical portions of the epithelial cells, following treatment for one hour with luminal Cytochalasin B ( $1 \times 10^{-4}M$ ), showed several distinct abnormalities. The microvilliar membranes bulged outwards, their internal structure appeared to collapse and the proximal portions of the cells contained many vacuoles (Fig. 10a, 10b). The



Fig. 10a. Apical surface of CB-treated rat jejunum. Blebbing and distortion of microvilli (MV) are evident as are abnormal and numerous vacuoles (V) in the apical cytoplasm of the epithelial cells.  $\times = 8,000$



Fig. 10b. Apical surface of rat jejunum treated with Cytochalasin B to inhibit absorption. The microvilli are shorter, the outer microvillus membrane is collapsed and the inner microvilliar matrix is less rigidly vertical (arrows).  $\times = 8,400$

microvilli became pleomorphic in character (Knutton et al. 1976). Scanning electron microscopy of transporting perfused jejunum demonstrates the densely-packed microvilli on the epithelial cells. Each surface mucin (ie. goblet cell) is surrounded by enterocytes, and cell to cell junctional regions are not perceptible from the surface view (Fig. 11a). In the Cytochalasin-treated intestines approximately 30% of the epithelial cells were clearly demarcated from the contiguous cells by an electron-dense gap (arrows, Fig. 11b) and filamentous thread-like material was present on the surface.

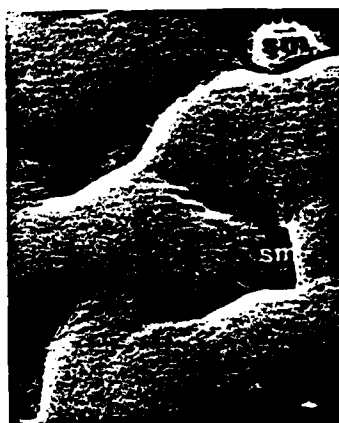


Fig. 11a. Scanning electron micrograph of jejunal mucosa in control steady-state absorption. SM = surface mucin cells, ie. goblet cells. X = 7,000



Fig. 11b. Scanning electron micrograph of CB-treated jejunum when steady-state absorption is depressed. EC = epithelial cells. Note the separation of cell to cell junctional regions and the presence of filamentous material on the surface (arrows). X = 7,800

## GENERAL DISCUSSION

In the interpretation of the *in vivo* intestinal data, the question arises as to whether the inhibition of absorption observed could be due to a nonspecific cytotoxic effect of this agent. While this conclusion remains a possibility, there are several factors which render it unlikely. In these studies, the absorption of sodium fluid and organic solutes was not abolished by exposure to (CB): the degree of inhibition varied from 30-60% with one hour of treatment. Secondly, the morphological deviations found are subtle and only obvious at an ultrastructural level. In routine light microscopy, tissue sections presented a non-pathological appearance with the documented presence of microfilaments in the apical and brush-border regions of the enterocytes, and the known effects of (CB) on these filaments (CB) accentuates the elongation of embryonic intestinal microvilli and alters the spatial distribution of the microvilli and the structure of the terminal web (Burgess and Grey, 1974). These findings have been interpreted to suggest a role for the terminal web as a platform for the growing cone filaments to push against. Binding of [<sup>3</sup>H] Cytochalasin B to isolated actin preparations demonstrates one binding site per F-actin filament, indicating that (CB) probably has a specific action on the ends of actin filaments (Brown and Spudich, 1979, Lin et al. 1980). Thus it is possible that the primary mechanism of action of (CB) is disruption of the continuous assembly and maintenance of the filamentous cones of the microvilli.

The concept that leaky 'tight' junctions, eg. intestine, may be regulated by the ability of the epithelial cells to modulate molecular flow through the junction is illustrated in C, Fig. 12. Bentzel et al., using *Necturus* gall-bladder (1980), found Cytochalasin B to induce rapid, reversible increments in transepithelial resistance, and (PD) with no change in the ratio of relative cell membrane resistances. These effects were accompanied by morphological changes in the microvillar filaments similar to those reported here and with enhanced disorder of the intestinal meshwork structure of the junction itself. In cultured MDCK cells, (CB) reversibly disrupts the cytoplasmic microfilaments and abolishes the electrical resistance of the monolayer (Meza et al. 1980). In these studies, it is interesting to note that removal of extracellular  $Ca^{++}$  causes the junctions to open, while (CB) inhibits resealing of the junction by promoting filament disorganization. These authors conclude

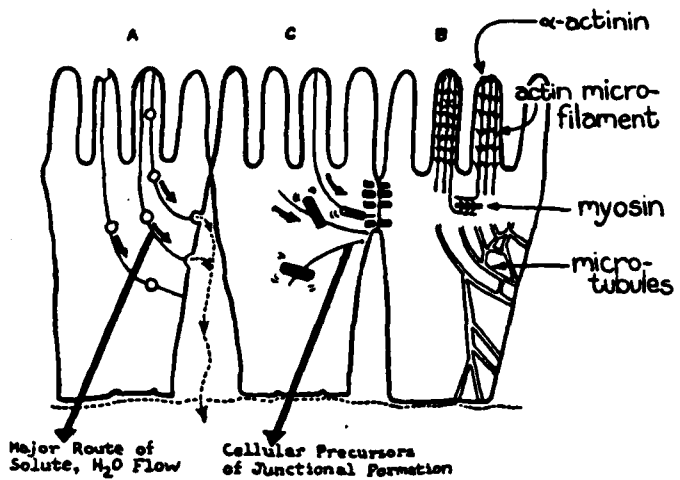


Fig. 12. This schematic diagram of intestinal epithelia illustrates 3 major concepts: A shows the major pathway for fluid absorption which is dependent on actively transported solutes. B represents our current understanding of the cytoskeletal scaffold present in these cells. It has not yet been demonstrated that the microfilaments present in the microvilli are architecturally contiguous with the intermediate filaments and the microtubules. C indicates that junctional formation and hence paracellular permeation characteristics may involve regulation by the cell in terms of microfilament assembly and transposition to the junctional region between individual cells.

that in this MDCK preparation, available evidence concerned with cell shape, cytoskeletal patterns and electrical resistance suggests that the microfilaments, through their association with plasma membrane components, exert a role in the architecture of the junctional strands and hence influence the degree of sealing of the occluding junctions. One piece of evidence from our work implies a partially similar effect in the rat intestine, in that scanning electron microscopy shows abnormal junctional fenestration between the adjacent enterocytes and excluded filamentous material. (Compare Figs. 11a and 11b.)

In an extensive series of studies some years ago Mak et al. (1974) could detect little or no effect of (CB) on the transport and synthetic functions of adult hamster or rabbit intestine. This finding may reflect significant species differences, but we have noted that the demonstration of (CB) effects in both preparations tested here is dependent on the freshness of the reagent used, and that the inhibitory effects are consistent within one batch of the material but vary from lot to lot.

Finally, although Cytochalasin B may have been found to impact plasma membrane transport mechanisms directly, rather than cytoplasmic processes, the only such effect proven to date of which we are aware is an effect on passive sugar carrier fluxes in simple cells and epithelia (Kimmich and Randles, 1979, Mizel and Wilson, 1972). Hence we conclude that the spectrum of effects induced in these two transporting epithelial preparations is compatible with the concept of the involvement of mechanochemical element(s) in the active secretion of  $[H^+]$  by frog gastric mucosa and isotonic transport of solutes and fluid by the in vivo rat intestine.

#### ACKNOWLEDGEMENTS

These studies were supported by contracts N00014-79-C-0971, N00014-81-K-0063, and N0014-79-C-603 from the Office of Naval Research. The authors wish also to extend their appreciation to Ms. Beth Dillinger (Blacksburg, VA) for her expert technical assistance and Ms. Susan Tarvin and Ms. Janet Conley (Oxford, MS) for their patient assistance in preparing this manuscript.

#### REFERENCES

Bentzel CJ, Hainau B (1970). Cellular regulation of tight-junction in a resorptive epithelium. In Binder HJ (ed): "Mechanisms of Intestinal Secretion", New York: Alan R. Liss, pp 275-286.

Bentzel CJ, Hainau B, Ho S, Hui SW, Edelman A, Anagnostopoulos T and Benedetti EL (1980). Cytoplasmic regulation of tight-junction permeability: effect of plant cytokinins. Am J Physiol 239:C75-C89.

in a cultured transporting epithelium. *J Cell Biol* 87: 756-754.

Mizel SB, Wilson L (1972). Inhibition of the transport of several hexoses in mammalian cells by Cytochalasin B. *J Biol Chem* 247:4102-4105.

Mukherjee TM, Staehelin LA (1971). The fine-structural organization of the brush of intestinal epithelial cells. *J Cell Sci* 8:573-599.

Orci LK, Gabbay H, Malaisse WJ (1972). Pancreatic beta-cell webb: its possible role in insulin secretion. *Science* 175:1128-1130.

Osborn M, Born T, Koitzsch HJ, Weber K (1978). Stereo immunofluorescence microscopy. 1. 3-dimensional arrangement of microfilaments, microtubules and tonofilaments. *Cell* 14:477-488.

Pratley JN, McQuillen NK (1973). The role of microfilaments in frog skin ion transport. *J Cell Biol* 56:850-857.

Schultz SG (1981). Homocellular regulatory mechanisms in sodium transporting epithelia: avoidance of extinction by "flush-through". *Am J Physiol* 241:579-580.

Taylor A (1977). Role of microtubules and microfilaments in the action of vasopressin. In Androli T, Grantham J, Rector F (eds): "Disturbances in Body Fluid Osmolarity." *Am Physiol Soc* 397.

Tilney LG, Mooseker M (1971). Actin in the brush-border of epithelial cells of the chicken intestine. *Proc Natl Acad Sci US* 68:2611.

Van Rossum GDV, Russo MA (1981). Ouabain-resistant mechanism of volume control and the ultrastructural organization of liver slices recovering from swelling in vitro. *J Mem Biol* 59:191-209.

Williams JA, Wolff J (1971). Cytochalasin B inhibits thyroid secretion. *Biochem Biophys Res Comm* 44:422-425.

SOME REFLECTIONS ON THREE COMPARTMENT MODELS  
FOR TRANSEPITHELIAL TRANSPORT

Dr. Marie M. Cassidy, Ph.D.

Department of Physiology  
George Washington University Medical Center  
Washington, D.C. 20037

The demonstrated capacity of epithelial membranes to absorb and secrete a variety of salt and water solutions is a subject of major physiological importance. Although the detailed mechanisms involved are not understood, the dominant theoretical and experimental paradigm has revolved around the acceptance of:

- (a) active sodium transport as the primary driving force for the movement of water, organic solutes, and other nutrients, and
- (b) the conceptual framework of a three-compartment model in elucidating the functional polarization of transport tasks in a macro-compartmental and hence complex epithelial membrane.

The remarks addressed to the meeting focussed upon the historical development of these ideas and also on the experimental evidence which exists in the past fifteen years to support or reject them. It should be understood that while such a framework of ideation contributes to the interpretation of data which is developed, its most important impact, scientifically, may be in the design of large scientific projects and even ~~industrial~~ experiments.

The three currently controversial and unresolved questions in understanding solute-linked water transport in epithelia as perceived from prevailing theory are:

- (1) valid estimates of transepithelial salt and water permeability and flow characteristics,
- (2) the proportion of salt and water transport which is truly through the epithelial cells and that which is transcellular but via the paracellular pathway between cells, and
- (3) the ultimate validity of the need to find a tissue compartment in which ions and/or solutes are concentrated osmotically such that bulk flow

of water and small sized solutes into that compartment can occur.

The development of the three-compartment model to explain known characteristics of epithelial function from its initial and simple inception by Curran and McIntosh was presented. Subsequent modifications include the articulation of a continuous standing osmotic gradient in compartment #2 as put forward by Diamond *et al.*

More recent studies on organic solute transport mechanisms require the addition of specific steps at the mucosal or basolateral membranes. The pathways whereby solutes accumulated within the tissue actually appear in the body via vascular or lymphatic routes have been somewhat ignored. In the past two years, compelling evidence has appeared indicating that the osmotic and hydrostatic pressures in the blood and lymph as well as diffusion gradients for particular solutes must also be taken into account in explaining the final transmural step in the process.

Studies published a decade ago by this investigator suggest that the enterocyte cell compartment may modify or regulate transport of ions and solutes by virtue of volume regulatory processes. The volume of the cell compartment, the intercellular space and the submucosal space was measured by tracer biochemical techniques and also directly by quantitative morphological methods. A range of transport rates was induced by the inclusion of solutes and inhibitors in the mucosal and serosal media. A linear correlation was obtained between the volume of the intestinal cell and the transmural rate of transport of salts and water. The alteration in cell volume was ascribable to a dramatic increment in cell height, with unfolding of the lateral membranes and little or no change in the measured cell width. These studies have been recently verified by Spring, using more sophisticated optical techniques in unfixed epithelial tissues.

Other studies by Frederiksen and Leyssac, Sanborn *et al.*, and Erlij have provided data suggesting that the range of absorption rates of isosmotic fluid across epithelia represents the need for energy requiring capacities for the transfer of fluid volume units as opposed to solute units per se. In

view of these experiments, it seems appropriate to reconsider the model of a mechanical volume pump for transcellular transfer of fluid volume units encompassing a cytoplasmic component. This model should allow for a variegated and flexible specificity with regard to the actively transported solutes and obviously incorporate the presence or transport of  $\text{Na}^+$  and  $\text{Cl}^-$  ions.

## 1982 FASEB Abstract Form

DO NOT FOLD THIS FORM

Mail to:  
 Membership Services Department  
 American Physiological Society  
 9650 Rockville Pike  
 Bethesda, Maryland 20814

## MAILING ADDRESS OF FIRST AUTHOR

(Please Print or Type. Provide full name rather than initials.)

Paula T. Beall  
 Dept. of Physiology  
 Baylor College of Medicine  
 1200 Moursund  
 Houston, Texas 77030

Office 713/790-6097  
 Home 713/771-9066  
 Home/Holiday

SELECT CATEGORY NUMBERS & TITLES (SEE  
 TOPIC CATEGORY LIST): Intestinal Trans-

1st # 1048 Title: Absorption

2nd # 1047 Title: Gastrointes-

3rd # Title: Intestinal Secr.

## PRESENTATION PREFERENCE (CHECK ONE ONLY)

Poster session       Poster Discussion  
 Slide session       Indifferent  
 If your first choice is unavailable, you will  
 Accept the alternative       Withdraw the abstract

## INSTRUCTIONS

## IMPORTANT:

See sample abstracts, typing and mailing instructions on reverse side; use enclosed Check List for preparation of abstract.

In addition to Abstract Block, fill out the following items on this form:

- Mailing Address of First Author
- Topic Category Selection
- Signature Block for Member's Signature
- Check Presentation Preference Box
- Return by first class mail the original typed copy of this abstract form and the first author addressed Program Confirmation Card.

*All compounds that are designated by code or initial letters must be identified adequately in the abstract, e.g., MJ-1999: 4-(2-isopropylamino-1-hydroxyethyl) methanesulfonanilide hydrochloride.*

Each Abstract Form submitted must be signed by a member of APS, BMES, SEBM, or SMB.

Signing member, are you willing to chair a session?  
 Yes, category # 1048 Intestinal Transport

## MEMBER'S AFFILIATION (CHECK ONE ONLY):

APS       BMES       SEBM       SMB

Paula T. Beall, Ph.D.  
 Member's Name. Print or type

Paula T. Beall  
 Member's Signature

Telephone No. 713/790-6097

REMITTANCE  
 ABSTRACT HANDLING FEE \$20

Payable to FASEB

### Effect of structural perturbation by Cytochalasin B on ion and water transport in 'tight' and 'leaky' epithelia. An electrical model

By P. T. BEALL, S. P. BOWEN\*, MARIE M. CASSIDY and M. DINNO. Department of Physiology, George Washington University Medical Center, Washington D.C. 20037, and \* Department of Physics, Virginia Polytechnic Institute, Virginia 24061

The effect of serosal Cytochalasin B (CB) ( $1-5 \times 10^{-5}$  M) on  $H^+$  secretion rates and on the electrical properties of frog gastric mucosa (a 'tight' epithelium) was investigated *in vitro*.  $H^+$  secretion was monitored by mucosal NaOH titration to pH 5. Similar concentrations of CB were used to examine the effect on absorption

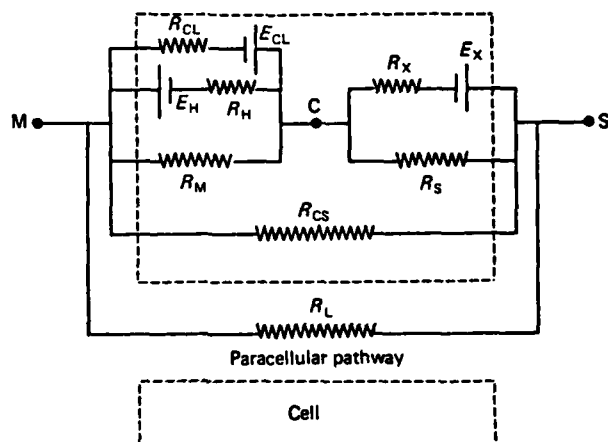


Fig. 1.  $E_H$  and  $E_{CL}$  are the electromotive forces for the secretion of  $H^+$  and  $Cl^-$  ions, respectively.  $R_H$  and  $R_{CL}$  are the intrinsic resistances of these pathways.  $E_X$  represents the electrochemical forces available for ion translocation across the basolateral membranes.  $R_X$ ,  $R_S$  and  $R_M$  are the resistances of the postulated transcellular return pathways.  $R_L$  is that of the paracellular shunt channel and  $R_{CS}$  is the resistive component offered by the structured cytoplasm.

of sodium, glucose and water in the perfused rat jejunum *in vivo* (a 'leaky' epithelium). In preparations characterized by a transepithelial resistance ( $R$ ), of  $< 150 \Omega \text{ cm}^2$  there was a significant rise in p.d. from  $16.1 \pm 2.5$  to  $19.3 \pm 1.4$  mV, an increase in  $R$  from  $120 \pm 15.5$  to  $139 \pm 12 \Omega \cdot \text{cm}^2$ , and a 25% decrease in apparent secretion rates for  $[H^+]$ . In preparations with  $R$  values  $> 170 \Omega \cdot \text{cm}^2$  the mucosal titration value fell by 48% with little or no change in the p.d. or  $R$  values. The electrical effects were completely reversible within 10 min of a CB-free wash.  $[H^+]$  secretory rates, however, continued to decline. Exposure to CB for more than 30 min caused a decline of p.d. to near zero levels although  $R$  values remained high and mucosal alkalinity increased continuously. *In vivo* absorption of Na, glucose and water by rat jejunum was inhibited by 50% during steady-state periods in which luminal CB was present.

The results can be suitably explained by an electric model (Fig. 1) where the micro-filament-disruptive action of CB is represented by changes in a cytoplasmic resistance.

This work was supported by ONR Contracts no. N0014-79-C and C0971.

SAMPLES TO SHOW STYLE

(Examples of authorship by a nonmember and a member)

Practice typing the abstract in a rectangle 5 1/4" x 4 3/4" on plain paper before using the special form.

*Note Especially:*

**Title in CAPITAL LETTERS:** Use significant words descriptive of subject content.

Author names underlined

Laboratory where research was done, city, state, and zip code

Standard abbreviations used

...3-space indentation for first line

Entire abstract in 1 paragraph typed single-spaced

No margin at top or left side

Capitalize the first letter of trade names

TEMPORARY INHIBITION OF PROTEIN SYNTHESIS INCREASES ARYL HYDROCARBON HYDROXYLASE ACTIVITY IN MAMMALIAN CELLS. James P. Whitlock, Jr.\* and Harry V. Gelboin. NIH, Bethesda, Md. 20014

Aryl hydrocarbon (benzo(a)pyrene) hydroxylase (AHH), a microsomal mixed-function oxygenase, is inducible by benz(a)-anthracene in cells cloned from Buffalo rat liver. In the absence of the polycyclic hydrocarbon inducer, inhibition of protein synthesis for 4 hrs. by cycloheximide (10  $\mu$ g/ml) or puromycin (30  $\mu$ g/ml) is followed by a 30-fold increase in AHH activity during the subsequent 4 hrs. This increase is a function of both the degree (35-97%) and the duration (0.5-4 hrs.) of inhibition of protein synthesis and is additive to the increase which follows exposure to benz(a)anthracene. The increase requires RNA synthesis during the period of inhibition of protein synthesis, but not subsequent to the removal of the block. The increase is prolonged by actinomycin D, (1  $\mu$ g/ml) when added after the release of the block of protein synthesis. Qualitatively similar results were observed in cell cultures of golden Syrian hamster embryos, DBA/2N mouse embryos, C57BL/6N mouse embryos, and the mouse cell line 3T3-4C2. The results suggest the presence of a labile protein(s) which reversibly represses AHH activity at a post-transcriptional level. (Supported in part by USPHS. NIH Grant NB #367-97)

(Example of authorship by two nonmembers with member sponsorship)

RELEASE OF PROSTAGLANDIN FOLLOWING TEMPORARY OCCLUSION OF THE CORONARY ARTERY. R.J. Kraemer\* and J.D. Folts\* (SPON: L.E. Hokin). Univ. of Wisconsin, Madison, WI 53706

(Example of authorship by two members)

LONG TERM ORGAN CULTURE OF THE RAT PANCREAS ANLAGE. A POTENTIAL MODEL FOR IN VITRO CARCINOGENESIS. Ismail Parsa and Walton H. Marsh. SUNY, Downstate Med. Ctr., Brooklyn, N.Y. 11203

1. Your abstract should be informative, containing: (a) the study's specific objectives, unless this is given by the title; (b) brief statement of methods, if pertinent; (c) a summary of the results; (d) the conclusions. It is NOT satisfactory to state: "The results will be discussed." Use short specific titles. Tables and figures are permitted within this space.

2. Use a typewriter, preferably electric, with ELITE type. Clean type before using. Use a carbon ribbon, if possible; otherwise, a reasonably new, good quality BLACK ribbon. (A new ribbon may smudge; a worn ribbon may be too faint.)

3. When using abbreviations for compounds, spell out in full the first mention, followed by the abbreviation in parentheses (see sample abstract). Do not abbreviate compounds in the title of the abstract.

4. Any special symbols, such as Greek letters, that are not on your typewriter must be drawn by hand in BLACK ink.

5. Underline names and initials of all authors. Place an asterisk (\*) after the name of each author who is not a member of a participating Society. If no author is a member, follow author(s)' name(s) by SPON: and the name of the sponsoring member. See heading of second abstract.

6. DO NOT ERASE. Remember that your abstract will appear in *Federation Proceedings* exactly as you submit it; any erasure, smudges, errors, misspellings, poor hyphenations and deviations from good usage will be glaringly apparent in the published abstract.

7. Fill in all requested information on the Abstract Form.

8. If you wish acknowledgement of receipt of your abstract also enclose a self-addressed, stamped, U.S. postal card.

# 1982 FASEB Abstract Form

DO NOT FOLD THIS FORM

Mail to:  
Membership Services Department  
American Physiological Society  
9650 Rockville Pike  
Bethesda, Maryland 20814

MAILING ADDRESS OF FIRST AUTHOR  
(Please Print or Type. Provide full name rather than initials.)

Phone: Office \_\_\_\_\_  
Home/Holiday \_\_\_\_\_

SELECT CATEGORY NUMBERS & TITLES (SEE  
TOPIC CATEGORY LIST):

1st # Title: \_\_\_\_\_

2nd # Title: \_\_\_\_\_

3rd # Title: \_\_\_\_\_

PRESENTATION PREFERENCE (CHECK ONE ONLY)

Poster session       Poster Discussion  
 Slide session       Indifferent  
If your first choice is unavailable, you will  
 Accept the alternative       Withdraw the abstract

## INSTRUCTIONS

### IMPORTANT:

See sample abstracts, typing and mailing instructions  
on reverse side; use enclosed Check List for preparation of abstract.

In addition to Abstract Block, fill out the following items on this form:

- a. Mailing Address of First Author
- b. Topic Category Selection
- c. Signature Block for Member's Signature
- d. Check Presentation Preference Box
- e. Return by first class mail the original typed copy of this abstract form and the first author addressed Program Confirmation Card.

SULFO AND SIALOMUCIN PRODUCTION BY RAT JEJUNUM FOLLOWING  
IN VIVO EXPOSURE TO LUMINAL PROSTAGLANDIN E<sub>1</sub>. Marie M.  
Cassidy, Fred G. Lightfoot\* and George V. Vahouny.  
George Washington University Medical Center, Washington, DC  
20037

Prostaglandins are known to be effective in preventing or ameliorating toxic injury to epithelial surfaces. The effect of PGE<sub>1</sub> on the protective mucus barrier in rat small intestine was tested by measuring the incorporation and secretion of Na<sup>35</sup>SO<sub>4</sub> and <sup>3</sup>H glucose labelled mucin. Groups of anaesthetised male Wistar rats were given buffered saline or saline containing PGE<sub>1</sub> (1 x 10<sup>-14</sup>-1x10<sup>-6</sup>M) by intestinal cannulation. The animals were exposed to the drug for 1 hour and the tracer substances were then injected i.v., 90 min prior to sacrifice. Perfusate contents, rinse fluids and mucosal homogenate samples were extracted for sulfo and sialo mucins, using hexadecyltrimethyl-ammonium bromide precipitation and their radioactivity expressed with reference to tissue protein and plasma levels of the isotopic tracers. Maximal stimulation of Na<sup>35</sup>SO<sub>4</sub> incorporation into mucin, a four-fold effect, was observed at 1 x 10<sup>-11</sup>M conc. of PGE<sub>1</sub> and following 60-90 min exposure to the drug. There was no significant effect on <sup>3</sup>H glucose labelled mucin, compared to paired controls. Ultrastructural studies showed enhanced mucin production, microvillar distortion and apical cell swelling. It is concluded that topical PGE<sub>1</sub> in the rat jejunum is associated with increased sulfomucin production from plasma sources. (Supported in part, by ONR Contract #N0001479-C-603)

*All compounds that are designated by code or initial letters must be identified adequately in the abstract, e.g., MJ-1999: 4-(2-isopropylamino-1-hydroxyethyl) methanesulfonanilide hydrochloride.*

Each Abstract Form submitted must be signed by a member of APS, BMES, SEBM, or SMB.

Signing member, are you willing to chair a session?  
( ) yes, category # \_\_\_\_\_

MEMBER'S AFFILIATION (CHECK ONE ONLY):

APS       BMES       SEBM       SMB

Member's Name. Print or type. \_\_\_\_\_

Member's Signature \_\_\_\_\_

Telephone No. \_\_\_\_\_

## REMITTANCE

ABSTRACT HANDLING FEE \$20

Payable to FASEB

**ABSTRACT** of poster  
or slide (oral) presentation

Type abstract in the box

**EFFECTS OF CYTOCHALASIN B ON THE ELECTROPHYSIOLOGICAL PROPERTIES OF FROG GASTRIC MUCOSA IN SULFATE MEDIA.** Mumtaz A. Dinno, Samuel P. Bowen, Paula T. Beall, and Marie M. Cassidy. VPI & SU, Blacksburg, Va., 24061 USA, Baylor Col. of Med., and George Washington Univ. Med. School.

In this investigation, the frog gastric mucosal membrane is used as a model for studying the effect of structural changes on the electrophysiological properties of biological membranes. Cytochalasin B (CB), known to cause depolymerization and disruption of microfilaments, was used as a perturbing agent to the structure. Stripped frog gastric mucosa was mounted in a modified Ussing chamber and bathed in  $\text{SO}_4^{2-}$  media. Addition of CB ( $10^{-6}$ - $10^{-4}$  mM) in the presence of histamine produced a dose-dependent response in the membrane potential (PD), resistance (R), and in the  $\text{H}^+$  rate. In the first 10 minutes the addition of  $10^{-4}$  mM CB caused a 40% reduction in the titrated amount of NaOH (used to measure  $\text{H}^+$  secretion). This was accompanied by a 50% decrease in PD and a 35% increase in R. However, at the end of 30 minutes, while the PD and the  $\text{H}^+$  rate continued to decrease to 79% and 48% respectively, R returned to values near control. These changes were irreversible. However, the effect of CB was completely reversible when removed after 2 minutes. The observed changes in PD, R, and  $\text{H}^+$  rate are clearly a reflection of the structural state of the cell layer. Furthermore, the actual inhibition of the  $\text{H}^+$  rate by CB is less than that measured. (Supported by ONR 79-C-0971.)

**DO NOT FOLD**

**FORM B/1**

**XXVIII INTERNATIONAL CONGRESS  
OF PHYSIOLOGICAL SCIENCES**

Budapest, July 13-19, 1980

Indicate below the code number of section and topics in which your abstract might be programmed (see SECTION AND TOPIC CATEGORY LIST)

1st choice No. 0108  
2nd choice No. 0106  
3rd choice No. 0105

**PRESENTATION** preference  
(check one only)

Poster presentation  
 Slide (oral) presentation  
 Either

Each Active Member may submit only one poster or slide presentation abstract.

**MAILING ADDRESS OF FIRST AUTHOR**

(please type)

last name (Dr, Mr, Mrs, Miss, Ms):

Dinno (Dr.)

first name (s):

Mumtaz A.

address:

Dept. of Physics VPI & SU

Blackburg, Virginia

24061

Postcode or Zip

USA

Country

The original typed copy of this abstract page with

- 6 copies of the whole page in original size
- one set of Author Index Cards
- two Abstract Identification Cards and
- Programme Confirmation Return Card

must reach the Congress Bureau NO LATER THAN MONDAY, DECEMBER 31, 1979 (Dec. 10 as per postmark). Return by air mail using the Reply Envelope attached.

**IMPORTANT**

Before you complete this form see the reverse side for *sample abstract, typing instructions and rules for eligibility of papers*.

Mail to:

**CONGRESS SECRETARIAT  
XXVIII INTERNATIONAL CONGRESS  
OF PHYSIOLOGICAL SCIENCES**

**BUDAPEST P.O.B. 370  
H-1445 Hungary**

## Ultrastructural Modifications of Intestinal and Colonic Mucosa Induced by Free or Bound Bile Acids<sup>1</sup>

George V. Vahouny, Marie M. Cassidy, Fred Lightfoot, Lauretta Grau, and David Kritchevsky

Departments of Biochemistry and Physiology, The George Washington University, School of Medicine and Health Sciences, Washington, D. C. 20037 [G. V. V., M. M. C., F. L., L. G.], and The Wistar Institute of Anatomy and Biology, Philadelphia, Pennsylvania 19104 [D.K.]

### Abstract

There is substantial evidence that bile acids may enhance the colon tumorigenesis induced by chemical carcinogens and that agents stimulating increased bile acid excretion may show similar promoting or enhancing activity. To test the premise that these agents might modify topographical ultrastructure of the small intestine and colon in the absence of carcinogens, rats were fed for 6 weeks on chemically defined diets containing 2% levels of three commercial bile acid sequestrants or 15% levels of wheat bran, cellulose, pectin, or alfalfa. Major qualitative and quantitative deviations from normal morphology were observed with each of the three sequestrants. Similar but less dramatic modifications occurred with diets containing alfalfa or pectin, both of which either "bind" bile acids *in vitro* or result in increased bile acid excretion. Bran and cellulose, which neither "bind" bile acids nor increase their fecal excretion, were without significant effects on intestinal or colonic morphology. The morphological deviations observed with bile acid sequestrants were shown to be a direct response to free or bound bile acids by comparing the morphological modifications resulting from daily intracolonic infusions of free bile acids, sequestrant-bound bile acids, or the sequestrant alone.

The topography and cellular proliferative activity of the intestinal mucosa are known to be influenced, both in humans and experimental animals, by the diet, by the composition of luminal contents, and by a variety of hormones. Both conjugated and unconjugated bile acids at physiological concentrations have been reported to affect intestinal ultrastructure and cause disruptive changes (10). In the colon, bile acids exert a striking influence in reversing normal salt and water absorption (8). Much of the literature on the function of dietary fibers envisions an interaction with luminal contents, whether nutrient materials, secretions, or bacterial flora. The concept that chronic ingestion of dietary fiber may drastically modify the structure of the small intestine has been reviewed in detail (6). Certain dietary fibers and fiber components interact with bile acids and result in increased fecal bile acid excretion in a manner comparable to that observed with commercial bile acid sequestrants. It is therefore conceivable that the effect of specific dietary fibers on intestinal and colonic ultrastructure might be related to bile acid-binding capacity of these materials. To test this premise, studies were conducted on the topographical ultrastructure of the small intestine and colon of rats fed for 6 weeks on chemically defined diets containing 2% levels of 3 bile acid sequestrants, cholestyramine (Questran), colestipol, or DEAE-

Sephadex (Secholex) or 15% levels of wheat bran, cellulose, pectin, or alfalfa (3).

In the small intestine, cholestyramine caused cell disruption, accompanied by cell swelling, microvillar denudation, and cell lysis predominantly in the upper third of each villus. The colonic mucosa exhibited discontinuities of the epithelial barrier, cell destruction, and hemorrhagic sites on the tissue surfaces. Similar but less severe deviations from normal morphology were observed in animals fed the 2 remaining bile acid sequestrants (4) or fed pectin or alfalfa (3). The intestinal and colonic topography of animals fed white wheat bran or cellulose was largely indistinguishable from controls, except for some evidence of increased goblet cell numbers (or activity). Coincidentally, these were the only groups demonstrating significantly reduced intestinal transit times. In general, there was a strong correlation between the bile acid-binding capacity (or effect on fecal steroid excretion) of these test materials and the morphological deviations observed, particularly in the colon (Table 1). However, we have recently shown that commercial ion-exchange resins and certain dietary fibers, notably guar gum, alfalfa, and lignin, also sequester significant amounts of phospholipid from micellar media (11). The effect of this potent detergent on intestinal and colonic morphology and function has not yet been determined.

In order to determine whether the alterations induced by cholestyramine-bound bile acids were immediate or progressive during prolonged intake of the resin, 165  $\mu$ mol of mixed bile acids bound to 100 mg cholestyramine were introduced directly into the jejunum, and the animals were sacrificed immediately. Disruptive changes in the small intestinal mucosa similar to those described above were evident.

Rats containing indwelling catheters at the junction of the caecum and colon were given twice daily for 5 days either 100 mg cholestyramine alone, 165  $\mu$ mol mixed bile acids (cholic:chenodeoxycholic:deoxycholic, 1:1:1), or cholestyramine-bound bile acids. Although there were effects of infusion of cholestyramine alone, morphological alterations of the colonic surface resulting from infusion of the free or resin-bound bile acids were comparable to those resulting from feeding 2% cholestyramine-containing diets for 6 weeks.

In studies on chemically induced colon carcinogenesis from several laboratories, it has been reported that feeding of cholestyramine to either normal (9) or germ-free rats (1), or pectin (5), and of alfalfa<sup>2</sup> appears to result in enhancement of colon tumor numbers or incidence of adenocarcinoma, irrespective of the carcinogen used. In contrast, fibers such as wheat bran and cellulose, which have little or no bile acid-binding capacity, appear to exert a protective effect on chemically induced colon carcinoma (2, 7). Our studies suggest that bile acid-sequestering materials result in disruptive changes in colonic morphol-

<sup>1</sup> Presented at the Workshop on Fat and Cancer, December 10 to 12, 1979, Bethesda, Md. Supported in part by USPHS Grant HL-02033, a grant from the USDA, and the Research and Development Fund of the Department of Biochemistry.

<sup>2</sup> B. Reddy, personal communication.

Table 1  
Correlation of bile acid-binding capacity of resins and dietary fibers with deviations in colonic morphology following feeding

Test material	% of bile acid-binding capacity	Deviations in colonic morphology (rating, 0-5)
Wheat bran	0-5	0
Cellulose	1-3	0
Pectin	(++)	+
Alfalfa	10-15	++
DEAE-Sephadex	30-40	+++
Colestipol	50-60	++++
Cholestyramine	80-100	+++++

ogy. Whether these observed changes may represent a mechanism for sensitization of the colon to chemical carcinogens is implied but remains to be tested experimentally.

## References

- Asano, T., Pollard, M., and Madsen, D. C. Effects of cholestyramine on 1,2-dimethylhydrazine-induced enteric carcinoma in germ-free rats. *Proc. Soc. Exp. Biol. Med.*, 150: 780-785, 1975.
- Barbott, T. A., and Abraham, R. The effect of bran on dimethylhydrazine-induced colon carcinogenesis in the rat. *Proc. Soc. Exp. Biol. Med.*, 157: 656-659, 1978.
- Cassidy, M., Grund, B., Lightfoot, F., Vahouny, G. V., Gallo, L., Kritchevsky, D., Story, J., and Treadwell, C. R. Alterations in topographical ultrastructure of rat jejunum and colon induced by feeding with alfalfa or cholestyramine. *Fed. Proc.*, 37: 543, 1978.
- Cassidy, M. M., Lightfoot, F., Grau, L., Kritchevsky, D., and Vahouny, G. V. The effect of feeding bile salt-binding resins on the ultrastructure of rat jejunum and colon: A transmission electron microscopy study. *Fed. Proc.*, 39: 715, 1980.
- Castledon, W. M. Prolonged survival and decrease in intestinal tumors in dimethylhydrazine treated rats fed a chemically defined diet. *Br. J. Cancer*, 35: 491-495, 1977.
- Creamer, B. Intestinal structure in relation to absorption. *Biomembranes*, 4A: 1-42, 1979.
- Freeman, H. J., Spiller, G. A., and Kim, Y. S. A double-blind study on the effect of purified cellulose dietary fiber on 1,2-dimethylhydrazine-induced rat colonic neoplasia. *Cancer Res.*, 38: 2912-2917, 1978.
- Mekhjian, H. S., Phillips, S. F., and Hofmann, A. F. Colonic secretion of water and electrolytes induced by bile acids. *J. Clin. Invest.*, 50: 1569-1577, 1971.
- Nigro, N. D., Bhadhrachari, N., and Chomchai, C. A rat model for studying colonic cancer: effect of cholestyramine on induced tumors. *Dis. Colon Rectum*, 16: 438-443, 1973.
- Saunders, D. R., Hedges, J. R., Sillery, J., Esther, L., Matsumura, K., and Rubin, E. E. Morphological and functional effects of bile salts on rat colon. *Gastroenterology*, 68: 1236-1295, 1975.
- Vahouny, G. V., Tombes, R., Cassidy, M. M., Kritchevsky, D., and Gallo, L. L. Binding of components of mixed micelles by dietary fibers. *Fed. Proc.*, 39: 715, 1980.

STRUCTURAL-FUNCTIONAL MODULATION OF MUCIN SECRETORY PATTERNS  
IN THE GASTROINTESTINAL TRACT

Marie M. Cassidy, Fred G. Lightfoot, and George  
V. Vahouny

Departments of Physiology, Anatomy, and Biochemistry,  
The George Washington University Medical Center,  
Washington, DC 20037.

INTRODUCTION

Structural-functional considerations with respect to epithelial transport mechanisms have rarely included a significant population of cells which exist in most epithelial models studied. These cells include most of the surface layer in the gastric region and 20-35% of the mucosal barrier in small and large intestine. They are actively engaged in mucin synthesis and release and it is becoming apparent that these processes are strongly modulated by an ever-growing list of neurohumoral and pharmacological agents. The mucus layer, itself once secreted is a complex physicochemical structure composed of exfoliated cells, bacteria, glycoproteins, mucopolysaccharides, electrolytes, and water. The thickness and biochemical composition of this surface layer is subject to dynamic alteration. It can, clearly, no longer be considered to be an 'inert paint' on the epithelial surface. Because of its chemical heterogeneity it does not lend itself to simple or well-defined characterization. In recent years this field has attracted growing attention, in part, because of the association of malfunction of its cytoprotective role in such diseases as gastric ulceration and cystic fibrosis. For an excellent review of mucus production in health and disease consult Forstner *et al.* (1977). This group of investigators have pioneered much of the work in this area.

Homeostatic regulation of synthesis and secretion is obviously essential to the maintenance of a surface mucus coat. The very rapid incorporation of isotopically labelled precursors was first demonstrated 25 years ago by Jennings and Florey

(1956). The resultant product, however, varies with the chemical extraction procedures employed and reproducibility is difficult from batch to batch of tissues used. Most experimentation has relied upon the incorporation of isotopic glucose and sulfur molecules into tissue fractions which almost certainly contain a component of non-mucin tissue and membrane glycoproteins (Lukie and Forstner, 1972). Autoradiographic and histochemical techniques permit estimates of mucin cell production and turnover but are not sufficiently precise to permit quantitative delineation of synthetic and secretory mechanisms (Neutra and Leblond, 1966; Gona, 1981). Glycoproteins, however, do constitute the major macromolecular moiety of the mucus secreted by vertebrate species (Reid and Clamp, 1978).

In an extensive series of experiments aimed at defining the ultrastructural histological features of the gastrointestinal mucosa evoked by aspirin ingestion, prostaglandin administration, dietary feeding of bile salt-binding resins, and the topical application of a microfilament-disruptive agent (Cytoschalasin B) morphological findings clearly pointed to modifications of normal mucus secretory patterns. These observations were followed by biochemical studies of mucus elaboration, *in vivo*, in a rat model. In almost all cases the structural and biochemical methods yielded corroborative data. The ultrastructural techniques used were light microscopy, transmission and scanning electron microscopy of the same samples. With these techniques, including blunt cryofracture of tissue specimens, correlative information concerning the detailed microarchitecture of the mucosal epithelial layer can be obtained.

#### MATERIALS AND METHODS

All of these experiments were conducted using an *in vivo* rat model. The various agents were either fed chronically or administered acutely via the luminal route. All procedures involving animals were carried out in accordance with the guidelines of the National Research Council on the care of experimental animals.

#### Bile Acid Sequestrant Feeding Studies: Animals and Diets

Male albino rats of the Wistar strain (Carsworth Farms), weighing 150-200gm were maintained in individual cages and

provided the diet and drinking water ad libitum for six weeks. They were housed in quarters maintained at 23°C and with a 12-h dark-light cycle. The isocaloric, isogravimic diets administered in these studies were comparable to those used earlier (Vahouny *et al.*, 1980) and consisted of the following ingredients in gm/100gm diet: dextrose, 55; casein, 25; corn oil, 14; sal mix, USP XIV, 5; vitamin mix, 1; in the resin-fed groups, cholestyramine, colestipol, DEAE-Sephadex was added as 2% of the diet at the expense of dextrose in the control group. Food consumption and final body weights were similar in control and treated groups.

#### Aspirin (ASA), Prostaglandin (PGE<sub>1</sub>), and Cytochalasin B (CB) Studies

Male Wistar rats weighing 200-225gm and maintained under anesthesia with sodium pentobarbital were subjected to laparotomy. The stomach, small and large intestine were identified, a cannula was inserted in the appropriate location, and 10ml of phosphate-buffered saline pH 7.2 (PBS) was infused in the control animals. In paired experiments, test infusion solutions were PBS containing either 10mg/kg body weight of ASA, PGE<sub>1</sub>, of varying concentrations or both test substances together.

In some groups of animals, the rats were lightly etherized to permit passage of a gastric tube into the stomach. Control animals were administered in this mode, either 10ml of buffered PBS (control) and the treated group received either PGE<sub>1</sub>, ASA, or mixtures of both. No morphological differences were discernible between the intubation and infusion treated animals. In the Cytochalasin B experiments, 100μM of CB dissolved in 0.1% dimethylsulfoxide (DMSO) was added to the infusion solution. In this case, control animals were infused with the DMSO, alone, contained within the PBS vehicle.

#### Biochemical Studies of Mucin Incorporation

In the feeding study, biochemical incorporation of <sup>3</sup>H glucose or Na<sub>2</sub><sup>35</sup>SO<sub>4</sub> into precipitable mucin was carried out following the overnight fasting procedure. With acute administration of ASA, PGE<sub>1</sub>, or Cytochalasin B, the abdominal cavity was closed with surgical clips and 60 minutes later, 15μc of Na<sub>2</sub><sup>35</sup>SO<sub>4</sub> and 10μc of <sup>3</sup>H glucose (New England Nuclear) was

injected intravenously. At varying times later, the contents of the entire small intestine was flushed with 10ml cold PBS and recovered as "wash fluid". 2ml blood samples were obtained by cardiac puncture and centrifuged to obtain plasma.

The intestine and colon was everted and "rinse fluid" was recovered following mild shaking of the tissue in 25ml cold PBS. The mucosal epithelium was scraped and homogenized in a further 10ml of cold PBS ("homogenate fluid"). The homogenate was centrifuged at 30,000 X g to yield a supernatant. The mucus fractions from all three fluids were obtained by two methodologies:

- a) by vacuum extraction using Buchner funnels with whatman filter paper #2. The radioactivity trapped on the filter papers was assayed by liquid scintillation spectrometry. This method was used in the preliminary studies.
- b) by precipitation, washing, and reprecipitation by 0.1% w/v  $\text{CeMe}_3\text{NBr}$  as described by Ofuso *et al.* (1978).

Mucosal protein was determined by the method of Patterson (1964). For each animal the incorporation of labelled material into the fractions collected was expressed as counts/min/mg of mucosal protein relative to the counts/min/ $\mu\text{l}$  of plasma.

Similar results between groups were obtained with both extraction procedures. In some cases, particularly in the low yield colonic experiments, wash, rinse, and homogenate fractions were combined to provide an overall index of mucin status in particular experimental groups.

#### Morphological Methods

Three rats in each group were prepared for light, transmission, and scanning electron microscopy. The alimentary tract from the pyloric sphincter to the terminal colon was removed. The fundic region of the stomach was identified: jejunal samples were taken from the middle fifth of the small intestine, and colonic samples from the mid 5cm segment of that organ. Rectangular segments of all regions were pinned flat and fixed in 3% phosphate-buffered glutaraldehyde. Efforts were made to keep the degree of tissue stretch during fixation as reproducible as possible.

During fixation the mucosal surface was brushed gently

with a sable brush to remove loose debris. For scanning electron microscopy, 1cm<sup>2</sup> tissue samples were dehydrated and critical-point dried (Samdri PVT-3) using CO<sub>2</sub>. The samples were mounted on aluminum stubs with mucosal surface uppermost and coated with approximately 10nm of gold/palladium using a Hummer I sputtering device. They were coded and observed in either an AMR 1000 or a JSB-35 scanning electron microscope using 20-25kV accelerating voltage. The microscopists were unaware of the identity of the coded samples. A preliminary assessment was made by a single viewer. Two other microscopists reassessed those samples and then analyzed the results of a repeated experiment. All of the numerical values recorded for the previously agreed upon criteria (hemorrhagic foci, number of villi, severity of damage) were pooled and examined statistically. A minimum of 300 gastric folds, jejunal villi, of colonic ridges from three animals per condition was examined, and the number of these areas with abnormal structure was recorded. The degree of deviation from normal was graded on the following scale: 1 = apical swelling of cells, disordered microvillar array; 2 = dimpling of swollen cell surface, partial denudation of microvilli; 3 = loss of most microvilli, rents or tears in apical membrane; 4 = extrusion of cell contents and loss of cells from the epithelial layer.

Light and transmission microscopy preparations were obtained by post-fixation of glutaraldehyde-fixed samples in phosphate-buffered 2% OsO<sub>4</sub>, followed by dehydration and embedment in Epon resin. Thick sections were approximately 0.5μm. Thin sections of 60nm were cut on a Sorvall MT2-B ultramicrotome, stained with toluidine blue, and examined in a Zeiss phase contrast microscope equipped with a Reichert automatic camera for photographic recording.

## RESULTS

### Normal Morphology

In these series of investigations three specific loci within the rat gastrointestinal tract were examined. They were the fundic region of the gastric mucosa, the jejunal region of the small intestine and the mid-colonic region of the large intestine. The first group of figures (Fig. 1-7) depict the ultrastructural characteristics of tissue derived from these organs as determined by scanning (SEM) and electron transmission(TEM) microscopy. In SEM, the gastric ridges appear as

curved or convoluted folds whose surfaces are occupied by mucus-containing cells. Gastric foveolae or pits lie between the folds (Fig. 1). The ridges are equivalent in width to the foveolar openings, i.e., about 3-4 cells wide. The surface cells usually present one of two distinct topographical patterns. One type possesses a smooth cobblestone appearance with adherent beads of mucus (S cells). The second type has a honeycomb structure (H cells) with shallow apical erosions. Once the mucin granules are released from the cell, the apical surface appears vacuolated. The microvilli are short and sparse on the S cells and are found mainly as projections at the edges of the H cells. In control samples, the superficial cell population can be divided generally between S and H cell types. Figure 2 is a TEM micrograph of the mucus-containing cells and quantitative morphometry shows that the granules contained within the cells are approximately 200-400nm in diameter. This figure is comparable to the measured size of the similar granules observed in SEM.



Figure 1. Control stomach fundus, SEM: S points to cells with smooth surface covering while H denotes the cells with a honeycomb vacuolated appearance.  
X = 900

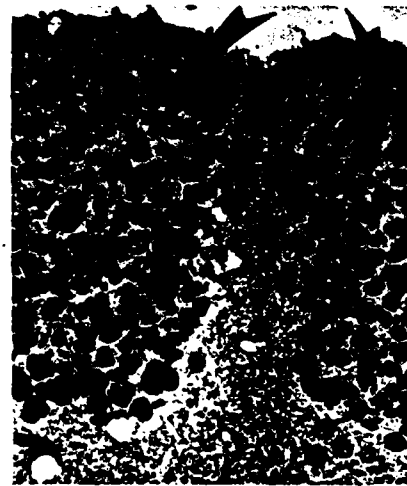


Figure 2. Control stomach fundus, TEM: Appearance of mucin-containing cells on the surface of the gastric ridges in the rat.  
X = 8,800

The architectural configuration of the mucosal surface of the small intestine is arranged as leaf-shaped villi. The surface is relatively smooth, interrupted occasionally by indentation of goblet cells and lateral folds on the surface of the villi (Fig. 3).

In transmission electron microscopy (Fig. 4), the goblet cells are clearly distinguishable from the contiguous absorptive epithelial cells. The mucin granules are of varying electron density and can be observed existing within the cell type. The microvilli are usually sparse when compared to the dense brush-border covering of the epithelial cells. The brush-border usually shows a fuzzy coat or electron dense amorphous material identified as the glycocalyx.

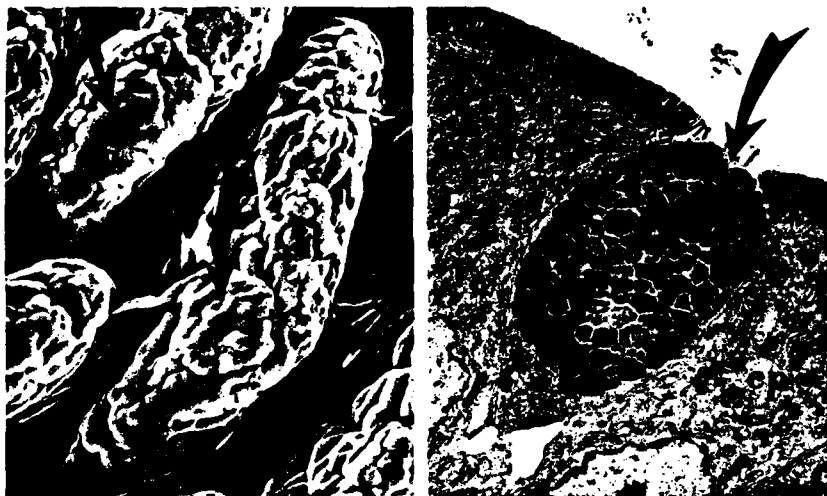


Figure 3. SEM of control samples of rat jejunum: Leaf-shaped villi with lateral ridges are evident. Arrows point to the location of goblet cells containing mucin.  $X = 280$

Figure 4. Control rat jejunum, TEM: A goblet cell containing mucinogen granules is seen (gc) with two adjacent epithelial cells (ep). In this organ, goblet cells are interspersed among the predominant enterocytes in the ratio of  $\sim 1:7$ .  $X = 3,600$

The surface of the colonic tissue is arranged in shallow whorled-shaped folds as distinct from the vertical villi in the small intestine and the deep convoluted folds of the gastric mucosa. The circular or hexagonal form of the colonic folds

have central and peripheral crypt regions. The mucin-containing goblet cells appear at regular spacing intervals within the epithelial cell population (Fig. 5). They possess few microvilli on their apical surface and the luminal orifice of these cells is considerably larger in surface area than that of the narrow-mouthed goblet cells in the jejunum. In multiple random samples, exocytosis of amorphous, non-granular secretory material is observed frequently.

In thin sections of colon, the goblet cells have an appearance very similar to their counterparts in the small intestine (Fig. 6). When secretion of cell contents is observed, the apical surface of the cell lacks apparent microvilli. In quiescent mucin cells such as that shown in figure 6, the microvillar appendages of adjacent epithelial cells overlap with those of the goblet cell itself and their specific cell origin is not clear.

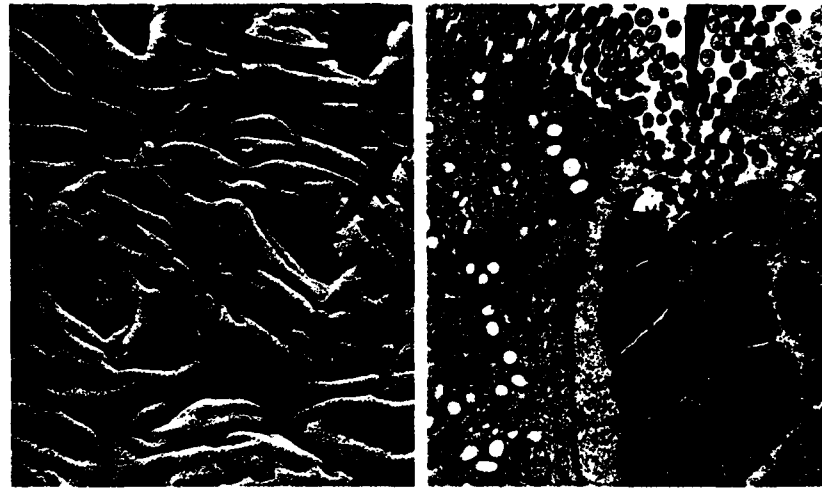


Figure 5. Control rat colon, SEM: The mucosal topography is arranged in circular or whorl-like configurations. Goblet cells (gc) with wide lumens are seen at regular intervals among the epithelial cells (ep). Crypt regions (arrows) are at the base or center of the folds.  
X = 660

Figure 6. Control rat colon, TEM: A goblet cell (gc) containing mucin droplets lies between two epithelial cells. Microvilli appear in longitudinal and cross-sectional view (arrows).  
X = 12,000

Blunt cryofracture of fixed tissue offers another visual perspective on the relationship of mucin cells to the epithelial cell population. The epithelial cells are uniform in appearance, but goblet cells, containing mucin, possess a unique sub-structure. The information obtained from this preparation correlates well with the cytological information obtained from SEM and TEM procedures.



Figure 7. Control colon, SEM: This image is obtained by SEM preparation of tissue sample fixed *in situ*. Goblet cell (gc) and mucus (m) of two adjacent luminal surfaces are shown. Epithelial cells (ep) are identified as the neighboring cells which have less distinct morphological features in this type of preparation. X = 3,600

#### Effect of Aspirin and Prostaglandin E<sub>1</sub>

With the administration of aspirin (ASA), both gastric and jejunal regions showed distinct structural abnormalities. Hemorrhagic lesions were discernible by eye on the luminal surfaces of both areas and were never observed in control animals. Ultrastructural examination of the lesions present a picture of blood clots and tissue debris and convey no useful information concerning alterations in the structure of the underlying cells. Hence electron microscopy was performed on tissue samples not directly associated with hemorrhagic foci.

Table 1 summarizes the findings with respect to the effect of ASA on gastrointestinal morphology. Less mucin was visible on the surface of both stomach and jejunum of rats administered ASA. In the small intestine, severe cell injury was limited to the uppermost third of the villi. The nature of the necrotic damage is delineated in figure 8.



Figure 8. ASA-treated rat jejunum, SEM: Microvilli (mv) are clumped and are actually missing from some areas of the cells. Tears in the apical membrane occur (arrows) leading to cell destruction.  
X = 4,000



Figure 9. ASA-treated rat jejunum, TEM: Microvilli (mv) are missing from a portion of an epithelial cell (ep). The tips of the microvilli have an unusual affinity for lead during the staining procedures (arrow).  
X = 3,600

Individual cells are greatly swollen, denuded of microvilli and frequently show rents or tears in the membrane covering. In light and transmission microscopy, abnormal histological features were found at the base of the mucosal layer. Normally the epithelial cells adhere quite closely to the underlying basement membrane, but with ASA treatment, the basal epithelial membranes detach from the submucosal structures and intercellular spaces are grossly distended compared to control morphology. Damaged cells, however, are frequently surrounded by epithelial cells possessing normal

structure. Sequential stages of cell necrosis were identified in both fundic and jejunal regions of all 18 rats treated with aspirin and quantitative morphometry from this study is included in Table 1.

Table 1  
Effects of Ingestion of ASA on Rat Gastrointestinal Morphology

	Stomach	Jejunum
Number of animals treated with ASA	18	18
Number of animals exhibiting gross hemorrhagic lesions (a)	15	12
% of gastric ridges or villi exhibiting deviation from normal structure (b)	$42.6 \pm 8.1$	$66.5 \pm 13.0$
Degree of cellular damage	$1.55 \pm 0.4$	$3.12 \pm 0.7$

Control number of animals in this study was 9.

- a) Stomach lesions were found predominantly in fundus and ranged from 1-2mm wide and from 3-7mm long. Some were punctate in character. Jejunal lesions were fewer and smaller in size ( $\sim 0.5$ mm wide and 0.5-2mm long).
- b) A total of 300 gastric ridges and 300 intestinal villi were examined in both control and treated tissues.
- c) Damage criteria are outlined in Methods.

(Reprinted with permission from J Submicr Cytol (Cassidy and Lightfoot, 1979)

In  $7 \times 10^{-7}$  PGE<sub>1</sub> animals intraluminally perfused or intubated with mucin accumulation in the lumen and adhering to the surface was evident to the naked eye and in all modes of microscopy. Individual cells were dimpled and distorted in shape with a considerable degree of plasticity in the arrangement of the apical membrane into microvilli (Fig. 10 & 11). In addition to the visual evidence of stimulated mucin production and distortion of the normal tightly packed microvilli, one other phenomenon was observed in the PGE<sub>1</sub> treated animals. Normal cell exfoliation is difficult to detect in random control



Figure 10.  $\text{PGE}_1$ -treated rat jejunum, TEM: Mucus secreted in  $\text{PGE}_1$  condition develops a web-like structure, with occasional bead formation overlaying the surface cells.  $\text{X} = 4,000$



Figure 11.  $\text{PGE}_1$ -treated jejunum, TEM: Cells show apical swelling with pleitropic microvilli (arrow) and some denudation.  $\text{X} = 1,300$

micrographs, but in the presence of  $\text{PGE}_1$ , there was a stimulation of cell extrusion into the lumen of the gut. This enhanced cell extrusion was found in both scanning and transmission electron microscopy (Fig. 12) and clumps of intact cells were routinely seen in the lumen entrapped in the secreted mucus.

Figure 13 relates the effect of  $\text{PGE}_1$  concentration administered to the percentage of jejunal villi affected by this agent. There is clearly a bimodal dose-response on the ultrastructural topography of the small intestine. Only the first peak ( $10^{-6} - 10^{-5} \text{ M}$ ) is strongly associated with visual evidence of increased surface mucin availability. The amount of  $^{35}\text{SO}_4$  labelled mucus secreted into the luminal fluid, found by rinsing the mucosal surface or recovered from the mucosal homogenate, is shown in figure 14.



Figure 12.  $\text{PGE}_1$ -treated rat jejunum, TEM: Exfoliation of an intact cell with microvilli still attached (arrow).  $\times = 2160$

EFFECT OF  $\text{PGE}_1$  ON CELLS AT VILLAR APICES

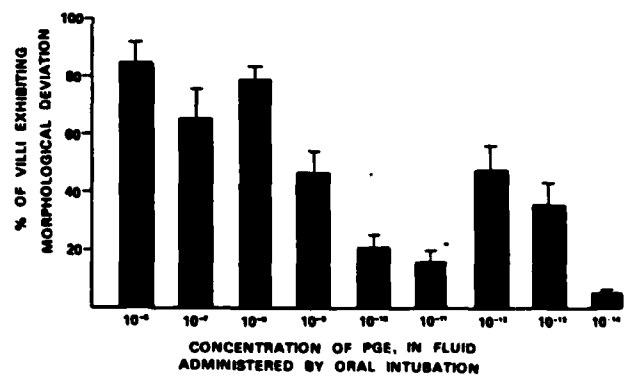


Figure 13. Dose-response curve relating the magnitude of the observed morphologic effect of  $\text{PGE}_1$  (cell swelling, microvillar disarray, cell exfoliation) at a range of concentrations from  $1 \times 10^{-12} \text{ M}$  to  $1 \times 10^{-1} \text{ M}$ .

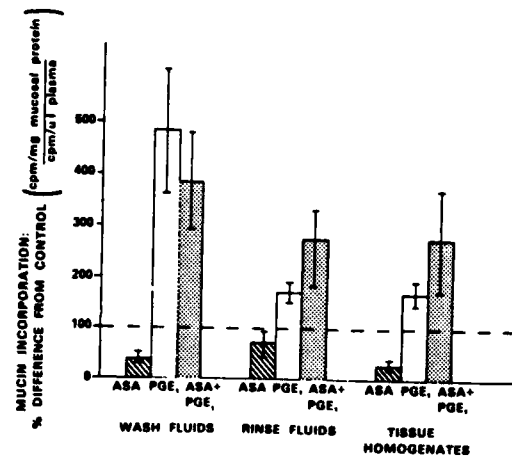


Figure 14. The average % difference from control + (standard error) for wash, rinse, and homogenate fluids obtained from the small intestine of ASA, PGE<sub>1</sub>, and ASA + PGE<sub>1</sub>-treated rats. Each treatment was compared to a control experiment (----) performed at the same time. In all 3 fluids, <sup>35</sup>S mucin is significantly greater with PGE<sub>1</sub> compared to ASA ( $P < 0.01$ ). Both rinse and homogenate fluids of intestine exposed to ASA alone were different at the  $P < 0.05$  probability level.

Instillation of ASA into the alimentary tract for 90 minutes reduced the release of isotopically labelled mucus while instillation of PGE<sub>1</sub> for the same time period stimulated secretion when compared to the effect of buffered saline alone. When the results are expressed as the cumulative incorporation of the blood tracer into mucus for each animal, i.e., cpm/mg protein of total recovered extract (wash, rinse, homogenate) / cpm/ul of plasma, the difference between ASA and PGE<sub>1</sub> treatment was statistically more significant (Table II).

Table 2

Incorporation and Release of  $^{35}\text{S}$  Labelled Mucin

Control	ASA	PGE <sub>1</sub>	ASA + PGE <sub>1</sub>
4.6 $\pm$ 2.0	0.4 $\pm$ 0.2	41.9 $\pm$ 12.0	7.3 $\pm$ 0.1

Means  $\pm$  SE of Cumulative counts/min/mg protein  
Counts/min/ $\mu\text{l}$  of plasma

Values for ASA and PGE<sub>1</sub> are significantly different from control and from each other ( $P < 0.05$ )

## Effects of Bile Salt Sequestrant Feeding

With all three resins fed for a period of six weeks at a 2% concentration, damage to the mucosa of the small and large intestine was evident. The colons of the cholestyramine-treated rats showed a whorled configuration with visual evidence that a large number of the goblet cells were engaged in the process of secretion (Fig. 15). Sheets of mucus were present, overlying the mucosal surface. Many of the surface cells were swollen, had disrupted microvilli, or were eroded at higher magnification (Fig. 16). Similar, but quantitatively less cell injury was observed with the other two resins, Colestipol and DEAE-Sephadex.

Table 3 summarizes the ability of the different resins to bind the more commonly available bile salts *in vitro* and attempts to relate this parameter to the effect of chronic feeding of these resins on the morphology of the colon in the rat. There appears to be at least a qualitative correlation between these two parameters. Cholestyramine-feeding was associated with significantly greater ultrastructural damage compared to the lesser bile salt sequestrant, Sephadex. The effects of these agents are, in general, more severe in the colon than they are in the jejunum. Mucin production by the colon was tested in these animals by measuring the 90-minute incorporation of tagged tracer molecules in the blood into sulfo and sialomucin glycoproteins. Cholestyramine and DEAE-Sephadex significantly enhanced the production of the sialomucin material, while Colestipol feeding was associated with a stimulation of sulfomucin (Table 4). These results are preliminary and do require much more study in terms of time and concentration dependence of the effects observed.



Figure 15. Colon of chole-tyramine-fed rats, SEM: Surface cells are distorted in shape with a greater degree of mucin (m) secretion compared to control chow-fed animals.  $X = 408$



Figure 16. Colon of chole-tyramine-fed rat, SEM: Surface cells are apically swollen with partial loss of microvilli (arrows).  $X = 3,040$

Table 3  
Effect of Anion-Exchange Resins on Bile Salt-Binding In Vitro  
and Colonic Morphology In Vivo

Resin addition or feeding	Bile salt-binding <u>in vitro</u> %	% of colonic ridges with abnormal structure	Extent of deviation from normal (1.0 - 4.0)
	Taurocholate	Glycocholate	
DEAE-Sephadex	35.0	35.2	40.6 $\pm$ 9.1 2.5 $\pm$ 0.6
Colestipol	57.0	56.0	55.0 $\pm$ 10.1 2.9 $\pm$ 0.4
Cholestyramine	81.5 $\pm$ 0.2	69.3 $\pm$ 0.3	39.5 $\pm$ 10.5 3.2 $\pm$ 0.6

Table 4  
 Incorporation of  $^3\text{H}$  Glucose and  $\text{Na}_2^{35}\text{SO}_4$   
 into Rat Colonic Glycoprotein  
 with Feeding of Bile Acid Sequestrants for 5 weeks

	$^3\text{H}$ Glucose	$\text{Na}_2^{35}\text{SO}_4$
Control	140.1 $\pm$ 3.0	192.2 $\pm$ 1.0
Cholestyramine (Questran)	339.5 $\pm$ 7.0*	279.8 $\pm$ 3.0
Colestipol	169.4 $\pm$ 5.0	458.4 $\pm$ 2.0**
DEAE-Sephadex	331 $\pm$ 8.0*	93.4 $\pm$ 1.0**

Numbers given are expressed as cpm/mg protein  $\pm$  cpm/ $\mu\text{l}$  plasma

\* Significantly different from control  $P < 0.01$

\*\* Significantly different from control  $P < 0.05$

#### Effects of Cytochalasin B

The presence of Cytochalasin B (at a concentration of 50 $\mu\text{M}$  in 0.1% DMSO in the physiological saline bathing the luminal surface of the small intestine for one hour) resulted in some distinct alterations in ultrastructural topography. Normally, individual epithelial boundaries are only faintly delineated and the junctional regions of the cells are tightly apposed at the apices. With Cytochalasin B, microfilamentous fragments appear on the surfaces of the cells (arrow) and goblet cells have larger orifices than in control perfused tissue (Fig. 17). There is a widening of the intercellular junctions at the luminal surface with a consequent cell separation width of one micron. Morphological structures also appear in the 'opened' intercellular areas which are similar in size to microfilaments (Fig. 18). Sialomucin formation is significantly reduced by the presence of Cytochalasin B to the luminal perfusion fluid (Table 5) with no effect on the measured sulfomucin component.



Figure 17. Rat jejunum treated with  $50\mu\text{M}$  Cytochalasin B, SEM: (gc) = goblet cell. Arrow points to microfilament-type material.  
 $X = 1,440$



Figure 18. Rat jejunum treated with Cytochalasin B, SEM: Note widening of apices of intercellular junctions (arrows).  
 $X = 4,230$

Table 5

Incorporation of  $^3\text{H}$  Glucose and  $\text{Na}_2^{35}\text{SO}_4$   
into Rat Jejunal Glycoprotein

	$^3\text{H}$ Glucose	$\text{Na}_2^{35}\text{SO}_4$
Control	$201.4 \pm 3.5$	$159.6 \pm 5.0$
Cytochalasin B (50 $\mu\text{M}$ )	$92.3 \pm 4.0^*$	$155.5 \pm 6.0$

Values expressed as means  $\pm$  SE: cpm/mg protein  $\div$  cpm/ $\mu\text{l}$  plasma\* Significantly different from control  $P < 0.1$ 

## DISCUSSION

## Distribution of Mucus-Secreting Cells in the Gastrointestinal Tract

At this point in time, mucus secreted by the cells of the gastrointestinal mucosa cannot be characterized as an adequately defined moiety. The viscous fluids found in the lumen or adhering to the surface contain the other usual components of gastric or intestinal juice secretions, e.g., bacteria, enzymes, ions, etc. The major organic constituent of these fluids is glycoproteins which are synthesized and secreted by morphologically identifiable cells in the mucosa. Information concerning the biochemical pathways involved and the physiological homeostasis of synthesis and secretion of mucin is still fragmentary in nature and phenomenological from an experimental point of view. Some general principles are, however, beginning to emerge from investigations of malfunction in the gastrointestinal tract and in other organ systems such as the respiratory, salivary, and reproductive epithelia.

In the acid-secreting fundic region of the stomach, the mucin cells are found predominantly occupying the surface of the gastric ridges (Lambert *et al.*, 1968; Lev *et al.*, 1972).

The cells which are active in  $H^+$  secretion lie at the lower portions of the foveolae or gastric pits. In control animals, intubated or perfused with physiologically buffered saline, the population of surface cells could be divided into two distinct populations based on morphological observations with the scanning electron microscope. One group possesses a smooth, unbroken surface (S cells) while the second group demonstrates a vacuolated, apical appearance reminiscent of a honeycomb structure (H cells). Similar shallow apical erosions on the surface cells have been interpreted by Pfeiffer and Weibel (1973) as representing the normal mode of cell loss and turnover in the stomach. Both S and H cells are topographically polygonal in outline and individual cells can be faintly discerned. The approximate diameter of both types of cells is in the range of 4.5 to 7.0  $\mu$ m in the rat. Small circular and ovoid granules  $\sim$ 200nm in diameter appear on the surface of the H cells and correspond to the dimensions of the intracellular granules in TEM (Fig. 2). Cells on the lateral sides of the gastric ridges are mostly of the S type. We believe that the H cells are not reflective of normal exfoliation and repair, but instead represent a phase of normal mucin secretion processes as proposed by Riddle *et al.* (1974) and Harding and Morris (1977). From an extensive series of studies in this laboratory we consider that the most likely interpretation of the S and H conformation is as follows: The smooth cells (S) are in a mucin synthetic phase coated with a thin layer of mucus, which is derived from the coalescence of secreted mucin granules. The honeycomb configuration (H cells) which have also been observed in biopsied human tissue (Riddle *et al.*, 1979) are believed to be in the actual process of mucus secretion. Gastric mucus appears to be released, at least initially, in a granular form rather than as a soluble amorphous material.

Jejunal tissue from control animals exhibited an ultra-structural topographical picture which agrees closely with information derived from transmission electron microscopy. The indentations in SEM represent the narrow openings of intestinal mucus-secreting goblet cells which are surrounded by absorptive epithelial cells. Individual cell outlines are faintly distinguishable in SEM as has been reported by other investigators (Riddle *et al.*, 1974; Harding and Morris, 1977). The release of the mucin droplets is seen occasionally as an amorphous substance when viewed in the SEM. Goblet cells on the villi occur every 4-5th epithelial cell.

Rat colonic tissue is arranged in low ridges which sometimes have a topographical whorled configuration. The goblet cells are seen at regular distances from each other and with respect to the number of intervening columnar epithelial cells. On the basis of light microscopy it has been pointed out that the goblet cell distribution around the circumference is significantly non-random and that the architectural pattern is such that they are situated around the crypt circumference as far from each other as possible (Góralski *et al.*, 1975). The most likely pattern of distribution favored is in the form of a spiral with a variable pitch from crypt to surface.

Both goblet and columnar cells are formed in the crypts and migrate upwards in similar fashion and with identical life spans. It is, therefore, likely that the goblet cell and the columnar enterocytes have the same progenitor (Freeman, 1965). The secretory process is apocrine in type. Formation of mucus has been shown to be constant from the time of formation in the crypts throughout the migration of the cell up the villus (Moe, 1955). It is not yet established whether the secretory process is a one-time or recurrent event during the 2-5 day life span of the cell. With respect to the putative functions of mucin in the alimentary tract (Table 6), it would also be of interest to determine whether the mucus cell is fixed, as such, at the time of formation or whether in fact there is a degree of plasticity in development between enterocytes and mucin-containing cells during villar or fold migration. A continuation of morphological techniques, e.g., SEM, TEM, histochemistry, and autoradiography can be of considerable utility in answering these questions.

Table 6

## Putative Functions of Alimentary Mucins

1. Buffering capacity
2. Lubrication, transit of alimentary materials
3. Cytoprotection of mucosal cells from injury
4. 'Waterproofing' of mucosa
5. Locus of antibacterial, antiviral reactions
6. Locus of antigenic response to orally ingested materials
7. Retardation of ion and water fluxes across the mucosa

Aspirin, PGE<sub>1</sub> in a Jejunal Ulceration Model

These studies confirm that normal cell turnover involves the shedding of intact cells into the lumen. The apex of each villus in control tissue appears to be covered with a fairly smooth and unbroken layer of cells with a very occasional cell being seen to project upwards from the surface. In ASA-treated jejunum, a clear line of cell injury traverses to the tips of many villi. Such damage is not observed on the sides of the villi. It would seem that the more sevescent cells are most susceptible to this stress agent and also to other such agents as certain dietary fibers, bile salts, and bile salt sequestrants (Cassidy *et al.*, 1981). A similar finding holds true for the gastric ulceration model (Cassidy and Lightfoot, 1979). Gross evidence of tissue damage is more apparent in the stomach of the ASA-fed rats compared to the jejunal region (Table 1). Ultrastructural injury was significantly more extensive, however, in the small intestine, both in terms of the degree of surface area affected and the degree of cellular disruption. The discrete sequential cytotoxic alterations in cell structure from apical swelling to cell destruction are interpreted as the initial steps in the pathway leading to the development of ulcerative lesions in both loci.

Prostaglandin E<sub>1</sub> (PGE<sub>1</sub>) has been shown to inhibit gastric secretion (Classen *et al.*, 1971; Robert *et al.*, 1968) and mucosal blood flow (Jacobson, 1970) while preventing ulcer formation (Robert *et al.*, 1971). Intestinal lesions induced by aspirin and indomethacin have been shown to be associated with prostaglandin deficiency presumably by an inhibition of prostaglandin synthesis (Whittle, 1976). The cytoprotective effect of prostaglandins in the jejunum where H<sup>+</sup> secretion is not a factor may be due to alterations in tissue blood flow, mucosal permeability, mucin secretion, or a combination of these effects. We have examined the mucin secretion hypothesis using both ultrastructural and biochemical techniques (Lightfoot and Cassidy, 1978; Cassidy and Lightfoot, 1980). While PGE<sub>1</sub> administration is associated with usual evidence of mucin production, overt cell injury is not apparent. There is distortion of cell shape and microvilli and an apparent enhancement of cell extrusion into the lumen of the gut. The increased cell loss is observable by both SEM and TEM, but such a cytokinetic effect has not yet been verified by autoradiographic techniques. The topographical effects are bimodal with respect to PGE<sub>1</sub> concentration. Prostaglandins are known to significantly alter the absorptive

function of the enterocytes: in general by promoting secretion of fluids and electrolytes instead of the normal uptake of these nutrients (Binder, 1979). The apical cell membrane of these cells exhibits a degree of unfolding of the microvilli which could be interpreted as a cellular response to dramatic changes in epithelial cell volume such as has been proposed for volume regulation in villated cultured cells (Knutton *et al.*, 1976).

Aspirin has a marked effect in diminishing the rate of <sup>35</sup>S incorporation into mucin in the jejunum while a significant stimulation is observed with  $1 \times 10^{-6}$  M PGE<sub>1</sub> (Table 2). Aspirin has previously been observed to inhibit the synthesis (Kent and Allan, 1968) and the availability of intracellular gastric mucin (Lev *et al.*, 1972). Carbenoxolone, a drug which accelerates the healing of gastric ulcers, significantly enhances the formation of glycoproteins (Shillingford *et al.*, 1974). The ameliorative effect of prostaglandins on gastrointestinal ulceration by topical aspirin appears to be due in part to the ability of PGE<sub>1</sub> to reconstruct a protective mucus barrier, thereby preventing access of toxic materials to the absorptive surface. It remains to be determined whether the increase in mucin production with PGE<sub>1</sub> and the corresponding decrease with ASA is due to opposite effects at a simple step in the synthetic/secretory process. (A) Both PGE<sub>1</sub> and Carbenoxolone markedly enhance the gastric gel mucus thickness *in vivo* (Bickel and Kaufman, 1981). (B) Mucus glycoproteins can, in fact, inhibit the diffusion of H<sup>+</sup> ions in an *in vitro* chamber (Pfeiffer, 1981), a finding which has been interpreted as being due to the steric hindrance offered by this unstirred layer rather than the buffering properties of the mucus, *per se*.

#### Effects of Bile-Sequestrant Feeding on the Colon

A pattern of erosive damage of the surface cells in the colon is observed with chronic feeding of the bile salt-binding resins (Table 3). The stages in individual cell destruction are very similar to those seen in gastric or jejunal ulceration. Damage to the mucosa of the intestine is known to occur with oral administration of several agents, such as laxatives (Gaginella and Phillips, 1976; Saunders *et al.*, 1975), cholera enterotoxin (Asakura *et al.*, 1974), and bile salts themselves (Low-Bear *et al.*, 1970). In 5-day colonic perfusion studies designed to test whether the necrotic agent

in this case was bile salts, the resin, or the bile salt-resin complex per se, it was found that both bile salt mixtures or the resin evoked equal injury which was equivalent to that found in the feeding studies. When the bile salt-resin complex was infused, there was, again, significant loss of mucosal integrity, but the individual effects were not potentiated (Cassidy *et al.*, 1981). Many of the injury-provoking agents such as bile salts and cathartic agents markedly enhance the permeability of the intestine and the colon. With the mucosal irritation and disruption caused by the feeding of the resin materials there was also the morphological evidence of stimulated mucin secretion. This perception was borne out by a higher rate of precursor incorporation into glycoproteins in these animals (Table 4). Many factors associated with the type of cell degeneration seen with aspirin or bile salt sequestrant treatment are believed to stimulate cytokinetic proliferation in both the small and large intestine by a postulated tip-to-crypt feedback mechanism. If the administration of these agents is linked to altered rates of cell repair and renewal it may be that enhanced mucin synthesis and secretion is a necessary consequence since the cell replacement process is temporally and spatially similar for both columnar and mucus cells. Sulfomucin production has been correlated with gastric and colonic carcinomas (Sipponen *et al.*, 1980).

#### Effects of Cytochalasin B

Cytokinins, such as Cytochalasin B, disrupt the macromolecular organization of the epithelial cell cytoplasm (Pratley and McQuillen, 1973), modify cell-to-cell junctional coupling (Bentzel and Hainau, 1979), and inhibit ion and water transport processes (Beall *et al.*, 1980). We have found 50% inhibition of normal fluid and sodium absorption by rat jejunum perfused *in vivo* (Beall *et al.*, 1980). Tissue samples from the perfused jejunum consistently exhibit several morphological peculiarities. In transmission micrographs, there is disarray of the microfilaments normally seen in the microvilli. There is a widening or 'gap' appearance in the junctional regions between adjacent epithelial cells, and short threads are present on the surface of the cells, although these have not been positively identified as microfilamentous material. It has been suggested by Bentzel and Hainau (1979) that the cytoskeletal framework of the epithelial cell is responsible for the assembly of the junctional

components. In 'leaky epithelia', such as rat jejunum, rapid and reversible restructuring of the junctions could regulate net transport efficiency without necessarily incurring the energy cost required for the mediation of active transport. Clearly, Cytochalasin B induces abnormal architecture in both intracellular and intercellular morphology and may be of use in the experimental exploration of the relationship between the cytoskeletal system and transport mechanisms. This agent also diminishes the incorporation of glycoprotein by the jejunal mucosa, as has previously been noted for the microtubular disruptive factor, colchicine. The implication of these preliminary studies is that the microfilament/microtubular sub-structure of the mucosal cell plays a role in the functional vectorial conveyance of materials across the mucosal layer whether the moieties involved be absorbed electrolytes and water or a secreted organic component, e.g., mucin. The growing list of agents which have been found to modulate the latter function, mucus secretion, is summarized in Table 7.

#### SUMMARY

1. Mucus-producing cells are clearly identifiable sub-populations of cells in many of the epithelial transport model systems studied, i.e., gastric, jejunal, and colonic epithelia of the rat.
2. The distribution of these cells varies from a predominant location on the mucosal surface of the stomach to a regular degree of interspersion among the dominant columnar epithelial cell population in the small and large intestine.
3. The functional state of these cells can be assessed by a variety of morphological techniques and their biochemical synthetic and secretory capacity estimated by isotopic tracer procedures.
4. In the gastric or jejunal acute ulceration model, sulfo-mucin production is decreased by aspirin and markedly enhanced by Prostaglandin E<sub>1</sub>, providing additional evidence for the cytoprotective role of the mucin blanket.
5. With chronic feeding of the bile salt sequestrants which provoke colonic mucosal irritation and injury, there is also a stimulated mucin output.
6. Disruption of the cytoskeletal framework of the mucosal cells by Cytochalasin B or colchicine depresses mucin production.

Table 7  
Agents which Alter Synthesis or Secretion  
of Gastrointestinal Mucin Substances

Agents	Effect
1. General irritants	Stimulate discharge
2. Aspirin	Inhibits discharge
3. Prostaglandins	Stimulates discharge
4. Bacterial toxins	Stimulates discharge
5. Hormones	Stimulates discharge
	Stimulates discharge
	Stimulates discharge
	Inhibits discharge
	Stimulates discharge
	Stimulates discharge
	Inhibits discharge
	Stimulates discharge
	Inhibits discharge
	Stimulates discharge
	Inhibits discharge
	Stimulates discharge
	Inhibits discharge
	Stimulates discharge
	Inhibits discharge
	Stimulates discharge
	Inhibits discharge
	Stimulates discharge
	Inhibits discharge
	Stimulates synthesis
	Stimulates discharge
	Inhibits synthesis
	Inhibits synthesis
	Stimulates synthesis & discharge
	Stimulates synthesis & discharge

7. Many of the compounds currently known to phenomenologically perturb mucus synthesis and/or secretion (Table 7) are utilized as probes in the delineation of electrolyte and water transport processes in these epithelial models. It is of interest to note in this volume that renal epithelial tissues do not appear to possess a significant mucin cell population. The developing concept of an association between mucus secretion and antigenic or immune responses may account for this fact. In several epithelial systems, however, modulation of mucin cell function should be taken into consideration in the construction of transport models.

#### ACKNOWLEDGEMENTS

This work was supported in part by an ONR contract #N00014-79-C-603 (MMC) and by a grant from the Department of Agriculture #5901-0410 (GVV & MMC). We also thank Ms. Beth Dillinger for her excellent typing skills.

#### REFERENCES

Asakura H, Tsuchiya M, Watanabe Y, Enomoto Y, Morita A, Morishita T, Fukumi H, Ohashi M, Castro A, Uylanoge C (1974). Electron microscopic study on jejunal mucosa in human cholera. *Gut* 15:531.

Beall PT, Bowen SP, Cassidy MM, Dinno M (1980). Effect of structural perturbation by Cytochalasin B on ion and water transport in 'tight' and 'leaky' epithelia: an electrical model. *J Physiol* 308:90.

Bentzel KJ, Hainau B (1979). Cellular regulation of tight junctions in a resorptive epithelium. In Binder HJ (ed): "Mechanisms of Intestinal Secretion," New York: Alan R. Liss, p 275.

Bickel M, Kauffman GL (1981). Gastric gel mucus thickness: effect of distention, 1b, 1b dimethyl prostaglandin E<sub>2</sub> and carbenoxolone. *Gastroenterology* 80:770.

Binder HJ (1979). Net fluid and electrolyte secretion: the pathological basis for diarrhea. In Binder HJ (ed): "Mechanisms of Intestinal Secretion," New York: Alan R. Liss, p 1.

Black JW, Bradbury JE, Wyllie JH (1979). Stimulation of colonic mucus output in the rat. *Proc of the Brit Pharm Soc* 456p.

Cassidy MM, Lightfoot FG (1980). Effects of Prostaglandin E<sub>1</sub>

administered by gastric intubation on mucus secretory patterns in the small intestine. In Samuelson B, Ramwell PW, Paoletti R (eds): "Advances in Prostaglandin and Thromboxane Research," New York: Raven Press, p 1589.

Cassidy MM, Lightfoot FG (1979). Electron microscope study of gastrointestinal response to acetylsalicyclic acid. *J Submicr Cytol* 11:449.

Cassidy MM, Lightfoot FG, Grau LE, Roy T, Astory J, Kutchesky D, Vahouny GV (1980). Effect of bile salt-binding resins on the morphology of rat jejunum and colon. A scanning electron microscope study. *Dig Dis and Sci* 25:505.

Cassidy MM, Vahouny GV, Lightfoot FG (1981). Dietary fiber, bile acids and intestinal morphology. In Vahouny GV, Kritchesky DK (eds): "Dietary Fiber in Health and Disease," New York: Plenum Press.

Classen M, Koch H, Birkhardt J, Topf G, Demling F (1971). The effect of prostaglandin E, on the pentagastrin stimulated gastric secretion in man. *Digestion* 4:333.

Forstner JF, Tabbal I, Forstner G (1973a). Goblet cell mucin of rat small intestine: chemical and physical characterization. *Can J Biochem* 51:1154.

Forstner G, Shen M, Lukie B (1973b). Cyclic AMP and intestinal glycoprotein synthesis: the effect of B-adrenergic agents, theophylline and dibutyryl cyclic AMP. *Can J Physiol Pharmacol* 51:122.

Forstner G, Sturgess J, Forstner J (1977). Malfunction of intestinal mucus and mucus production. *Adv in Exp Med & Biol* 89:349.

Freeman JA (1963). Goblet cell fine structure. *Anat Rec* 154:121.

Gaginella TS, Phillips SF (1976). Ricinoleic acid (Castor oil) alters intestinal surface structure. A scanning electron microscopic study. *Mayo Clin Proc* 51:5.

Gona O (1981). Prolactin and ergocryptine effects on mucus glycoproteins of the rat ileum. *Histochemical Journal* 13:101.

Goralski A, Sawicki W, Blaton O (1975). Non-random distribution of goblet cells around the circumference. *Cell Tiss Res* 160:551.

Harding RK, Morris GP (1977). Feedback control by functional villus cells on cell proliferation and maturation in intestinal epithelium. *Exp Cell Res* 73:197.

Jacobson EC (1970). Comparison of prostaglandin E, and nor-epinephrine on the gastric mucosal circulation. *Proc Soc Exp Biol Med* 133:516.

Jennings MA, Florey MW (1956). Autoradiographic observations

on the mucous cells of the stomach and intestine. *Q J Exp Physiol* 41:131.

Kent PW, Allen A (1968). The biosynthesis of intestinal mucins: The effect of salicylate on glycoprotein biosynthesis by sheep colonic and human gastric mucosal tissues *in vitro*. *Biochem J* 106:645.

Knutton S, Jackson D, Graham JM, Micklem KJ, Pasternak CA (1976). Microvilli and cell swelling. *Nature* 262:52.

Lev R, Siegel H, Jerzy Glass GB (1972). Effects of salicylates on the canine stomach. A morphological and histochemical study. *Gastroenterology* 62:970.

Lightfoot FG, Cassidy MM (1978). The effect of aspirin and prostaglandin E<sub>1</sub> on intestinal mucus secretory pattern. In O'Hare AMF (ed): "Scanning Electron Microscopy," Illinois: SEM Inc.

Low-Berger TS, Schneider RE, Dobbins WO III (1970). Morphological changes of the small intestinal mucosa of guinea pig and hamster following incubation *in vitro* and perfusion *in vivo* with unconjugated bile salts. *Gut* 11:486.

Lukie B, Forstner G (1972). Synthesis of intestinal glycoprotein incorporation of [<sup>1-14</sup>C] Glucosamine *in vitro*. *Biochim Biophys Acta* 261:353.

Moe H (1955). On goblet cells, especially of the intestine of some mammalian species. *Internal Rev Cytol* 4:299.

Mukherjee A, Patnaik R, Bhagavan BS, Nair PP (1981). Glycoprotein synthesis in colonic epithelial cells from rats. *Cell Biol International Reports* 5:409.

Neutra M, Leblond CP (1966). Synthesis of the carbohydrate of mucus in the Golgi complex as shown by electron microscopic radioautography of goblet cells from rats injected with glucose-H<sub>3</sub>. *J Cell Biol* 30:119.

Nimmerfall F, Rosenblaler J (1980). Significance of the goblet cell mucin layer, the outermost luminal barrier to passage through the gut wall. *Biochem and Biophys Res Comm* 94:960.

Ofuso F, Forstner J, Forstner G (1978). Mucin degradation in the intestine. *BBA* 543:476.

Patterson DSP (1964). Apparent protein spectra (200-210m $\mu$ ) determined in a double-beam ultraviolet spectrophotometer and the estimation of the protein content of crude tissue-enzyme preparations. *BBA* 86:405.

Pfeiffer CJ (1981). Experimental analysis of hydrogen ion diffusion in gastrointestinal mucus glycoprotein. *Am J Physiol* 240:G176.

Pratley JN, McQuillen NK (1973). The role of microfilaments in frog skin ion transport. *J Cell Biol* 56:850.

Reid L, Clamp JR (1978). The biochemical and histochemical

nomenclature of mucus. *Br Med Bull* 34:5.

Riddle JM, Rosenburg BF, Lucas CE, Sugawa C (1974). The surface topography of acute erosive gastritis. In Tohari O, Corvin I (eds): "SEM 11JRI Proceedings, Part III," Chicago: Institute of Technical Research, p 769.

Robert A, Nezamis JE, Phillips JP (1968). Effect of prostaglandin E, on gastric secretion and ulcer formation in the rat. *Gastroenterology* 55:481.

Robert A, Stöwe DF, Nezamis JE (1971). Prevention of duodenal ulcers in the rat by administration of prostaglandin E<sub>2</sub> (PGE<sub>2</sub>). *Scand J Gastroenterol* 6:303.

Saunders DR, Sillery J, Rachmilewitz D (1975). Effect of dioctyl sodium sulfosuccinate on structure and function of rodent and human intestine. *Gastroenterology* 69:380.

Shillingford JS, Lindup WE, Parks DV (1974). The effects of carbenoxolone on the biosynthesis of gastric glycoproteins in the rat and ferret. *Biochem Soc Transactions* 1104.

Sipponen P, Seppala K, Varis K, Hjelt L, Ihamaki T, Kekki M, Siurala M (1980). Intestinal metaplasia with colonic-type sulphomucins in the gastric mucosa; its association with gastric carcinoma.

Vahouny GV, Tombes R, Cassidy MM, Kritchevsky D, Gallo L (1980). Dietary Fibers: V binding of bile salts, phospholipids and cholesterol from mixed micelles by bile acid sequestrants and dietary fibers. *Lipids* 15:1012.

Whittle BJ (1976). Relationship between the prevention of rat gastric erosions and the inhibition of acid secretion by prostaglandins. *European Journal of Pharmacology* 40:233.

Williams SE, Turnberg LA (1981). Demonstration of a pH gradient across mucus adherent to rabbit gastric mucosa: evidence for a 'mucus-bicarbonate' barrier. *Gut* 22:94.

From: DIETARY FIBER IN HEALTH AND DISEASE  
Edited by Vahouny and Kritchevsky  
(Plenum Publishing Corporation, 1982)

## Dietary Fiber, Bile Acids, and Intestinal Morphology

MARIE M. CASSIDY, FRED G. LIGHTFOOT, and GEORGE V. VAHOUNY

### 1. INTRODUCTION

The rates of occurrence and mortality from colorectal cancer have been positively correlated with total fat intake in several populations (Carroll and Khor, 1975; Correa and Haenszel, 1978; Wynder, 1979). The possible relationships between fat ingestion and the subsequent steps in lipid metabolism have been explored in studies aimed at determining the link between bowel cancer risk, dietary fats, products of fat metabolism, and their appearance in the stool composition. Of the populations with higher incidences of bowel cancer there is also evidence of higher fecal steroids, bile acids, and 7-dehydroxylase activity (Hill *et al.*, 1975, Reddy *et al.*, 1975a) compared to control studies. Subjects with higher levels of fat consumption also demonstrate a high fecal concentration of important lipid metabolites (Reddy *et al.*, 1976).

Studies with animal models have evinced additional evidence supporting a relationship between bile acids, luminal lipid metabolites, and intestinal carcinogenesis (Nigro *et al.*, 1976; Reddy, 1975b). In several studies a low incidence of bowel cancer is observed in conjunction with a diet moderately high in fats.

---

MARIE M. CASSIDY • Department of Physiology, The George Washington University, School of Medicine and Health Sciences, Washington, D.C. 20037. FRED G. LIGHTFOOT • Department of Anatomy, The George Washington University, School of Medicine and Health Sciences, Washington, D.C. 20037. GEORGE V. VAHOUNY • Department of Biochemistry, The George Washington University, School of Medicine and Health Sciences, Washington, D.C. 20037.

This difference has been attributed to a protective effect of dietary fibers as a component of the diet (Burkitt *et al.*, 1972). The mechanisms postulated to account for this amelioration in effect include transit time of fecal material, alterations in gut floral metabolism, alterations in stool composition, particularly with respect to bile acid metabolites, binding of carcinogenic or precarcinogenic materials to luminal materials such as nondigested fibers, and alterations in lipid absorption leading to hypcholesterolemia. The mechanism of action of dietary fibers has generally been considered as being limited to their interactions with some component of the gut contents, whether such contents be ingested food substances, physiological secretions, or bacterial flora. However, it is also possible that fiber per se or bile salt derivatives interact directly by some mechanism with the mucosa to evoke a fundamental change in the intrinsic absorptive capacity of the intestinal tract. Long-term effects of dietary patterns may be associated with biochemical and morphological alterations in the absorptive barriers.

Fatty acids and bile acid administration both evoke intestinal salt and water secretion and cause substantial and reversible alterations in the ultrastructural histology of the mucosal surface (Philips and Gaginella, 1979). The secondary bile acids have been demonstrated to be tumor promoters in experimental animals (Barisawa *et al.*, 1974), as is pancreaticobiliary diversion to the mid small bowel (Williamson *et al.*, 1979). Bile acid accumulation has been proposed to be responsible for the diarrhea states associated with colonic cancer. In an extensive series of studies designed to probe the mechanisms underlying the putative antiatherogenic and anticarcinogenic effects of a semipurified chronic dietary fiber intake and that of bile salt sequestrants, we have studied the ultrastructure of the small and large bowel in considerable detail.

## 2. MATERIALS AND METHODS

### 2.1. Animals and Diets in the Chronic Feeding Studies

Male albino rats of the Wistar strain (Carsworth Farms), weighing 150–200 g, were maintained in individual cages and provided the diet and drinking water *ad libitum* for 6 weeks. They were housed in quarters maintained at 23°C and with a 12-hr dark-light cycle. The isocaloric, isogravie diets administered in these studies were comparable to those used earlier (Vahouny *et al.*, 1980) and consisted of the following ingredients in g/100 g diet: dextrose, 55; casein, 25; corn oil, 14; salt mix, USP XIV, 5; vitamin mix. The ability of these various materials to bind cholesterol, phospholipids, and bile salts *in vitro* was also

determined and compared to the quantitative morphological observations derived from scanning electron microscopy.

## 2.2. Methods

### 2.2.1. Chronic Feeding Studies

The dietary fiber materials, which were fed for a period of 6 weeks at a level of 15 g/100 g diet, included alfalfa (Bio-Serv, Frenchtown, N.J.), white wheat bran (Bio-Serv, Frenchtown, N.J.), cellulose (Solka floc, Brown and Co., Berlin, N.H.), and pectin (Bio-Serv, Frenchtown, N.J.). In the resin-fed groups cholestyramine (Questran, from Dr. H. P. Garrett, Mead Johnson, Evansville, Ind.), colestipol, or DEAE-Sephadex (Secholex, a gift from Dr. A. Howard, Cambridge, England) was added as 2% of the diet at the expense of dextrose in the control group. Control animals were maintained on Purina Rat Chow. Food consumption and final body weight were similar in control and treated groups.

### 2.2.2. Colonic Infusion Studies of Bile Acids and Bile Salt Sequestrants

Wistar rats weighing 200 g were fasted for 2 days, with water *ad libitum*. A polytechnic catheter (PE #200) was implanted lumenally at the junction of the cecum and the colon. It was threaded under the skin and externalized at the dorsal surface behind the neck. The animals were allowed to recover in individual cages and had free access to chow and water for the remainder of the study. Twice daily at 9:00 a.m. and 3:00 p.m. for 5 days, 1.0 ml of the appropriate test substances in 0.9% saline was introduced into the colon via the indwelling catheter. The test substances included: (1) Saline control (0.9% NaCl). (2) Cholestyramine: 100 mg given twice daily, which corresponds to the amount ingested per diem by rats fed a purified diet containing 2% cholestyramine. (3) Mixed bile acids: 164  $\mu$ mol mixture of cholate, chenodeoxycholate, and deoxycholate in the proportions of 1.1 : 1.3 : 1.0 in 1 ml saline. This is equivalent to the amount of total and mixed bile acids sequestered by the dose of cholestyramine employed. (4) Cholestyramine-bile acid mixture: 100 mg of cholestyramine and 164  $\mu$ mol of the mixed bile acids. This mixture was prepared by incubation of the resin and bile acids and reisolation of the resin containing bound bile acids as described previously (Vahouny *et al.*, 1980). A total of five animals were used for each group in two sets of experiments. All animal procedures were in accordance with the National Research Council's guide for the care and use of laboratory animals.

AD-A167 878

A MORPHOFUNCTIONAL STUDY ON THE EFFECT OF CYTOCHALASIN

2/2

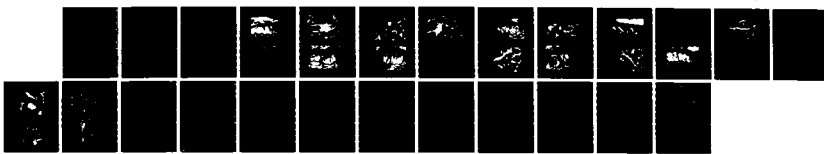
B ON INTESTINAL WATER TRANSPORT (U) GEORGE WASHINGTON

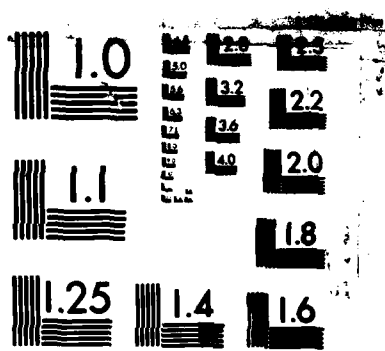
UNIV WASHINGTON DC M M CASSIDY 10 MAY 86

UNCLASSIFIED N00014-79-C-0603

F/G 6/15

NL





MICROCOPY RESOLUTION TEST CHART  
NATIONAL BUREAU OF STANDARDS 1963 A

### 2.2.3. Morphological Methods

Three rats in each dietary group and three in the control group were prepared for both light and scanning electron microscopic (SEM) examination. At the end of the 6-week feeding period the rats were anesthetized with sodium pentobarbital and subjected to laparotomy. The alimentary tract from the pyloric sphincter to the terminal colon was removed and the jejunum was identified as the middle fifth of the small intestine. Colon samples were derived from the middle 5-cm segment of that organ. Rectangular segments of both regions were pinned flat as mucosal surface uppermost and fixed in 3% phosphate-buffered glutaraldehyde. Efforts were made to keep the degree of tissue stretch during fixation comparable in all conditions.

During fixation the mucosal surface was brushed gently with a sable brush to remove loose debris. For SEM 1-cm<sup>2</sup> tissue samples were dehydrated and critical-point-dried (Samdri PVT-3) using CO<sub>2</sub>. The samples were mounted on aluminum stubs with mucosal surface uppermost and coated with approximately 10 nm of gold/palladium using a Hummer I sputtering device. They were coded and observed in either an ARM 1000 or a JSM-35 scanning electron microscope using 20–25 kV accelerating voltage. The microscopists were unaware of the identity of the coded samples. A preliminary assessment was made by a single viewer. Two other microscopists reassessed those samples and then analyzed the results of a repeated experiment. All of the numerical values recorded for the previously agreed upon criteria (number of villi, severity of damage) were pooled and examined statistically (cf. Table I). A minimum of 300 jejunal villi and 300 colonic ridges from three animals per condition were examined, and the number of villi or ridges with abnormal structure was recorded.

The degree of deviation from normal was graded on the following scale: 1, apical swelling of cells, disordered microvillar array; 2, dimpling of swollen cell surface, partial denudation of microvilli; 3, loss of most microvilli, tears in apical membrane; 4, extrusion of cell contents and loss of cells from the epithelial layer. The extent of agreement between the viewers was  $\pm 3.5\%$ .

Light and transmission electron microscopy (TEM) preparations were obtained by postfixation of glutaraldehyde-fixed samples in phosphate-buffered 2% OsO<sub>4</sub> followed by dehydration and embedment in Epon resin. Sections approximately 0.5  $\mu\text{m}$  thick were cut on a Sorvall MT2-B ultramicrotome, stained with toluidine blue, and examined in a Zeiss phase contrast microscope equipped with a Reichert automatic camera for photographic recording.

Thin sections for TEM were stained with uranyl acetate and lead citrate and examined in a JEOL 100B transmission electron microscope. Quantitative morphology of lipid density in the epithelial cell layer was determined by volume measurements of lipid : cell ratios using the MOP III Digitizing Systems (Baltimore Instrument Co., Baltimore, Md.).

### 2.2.4. Bile Acid and Lipid Binding by Fibers and Resins

Binding of bile salts and lipids was determined as previously described by this laboratory (Vahouny *et al.*, 1980). Forty milligrams of the appropriate resin or fiber source was added to 5 ml of each micellar solution in a stoppered tube and the mixture was shaken in a Dubnoff incubator at 37°C for 1 hr. The tubes were centrifuged at 30,000g for 10 min and the entire supernatant was unified by mechanical agitation on a Vortex mixer prior to assay. Aliquots (0.1 ml) of the supernatant were added to 10 ml liquid scintillant (Scintiverse, Yorktown Research, Elmhurst, Pa.), and radioactivity was determined in a Beckman LS 250 liquid scintillation spectrometer using external standardization. Controls of the appropriate micellar media without added binding substances were carried through the same procedure. Binding was determined as the difference between the radioactivity of each micellar component added and that recovered in the supernatant after incubation. All studies were carried out at least three times and all isotope analyses were carried out in duplicate. Figures represent the mean  $\pm$  standard error of the mean by statistical analysis.

## 3. RESULTS

SEM of jejunal tissue from animals fed the control chow diet is exemplified by Fig. 1. The villi are leaf-shaped, with some folds along the lateral sides. Individual epithelial cells are faintly demarcated as hexagonal shapes. Focal indentations in the smooth contour (arrow) have been identified as mucin-secreting goblet cells by cross-correlation with TEM studies. Figure 2 is a TEM of a goblet cell with contiguous enterocytes on either side. The goblet cells (GC) contain mucin granules of varying electron density and usually show some degree of secretory activity. The epithelial microvilli constitute a tightly packed brush border (BB) with a fuzzy coat or glycocalyx on the outer tips. The ultrastructural topography of control rat colon is similar in many respects to that of the small intestine (Fig. 3). The microvilli are, however, somewhat less densely packed and the ratio of goblet cells to epithelial cells is greater than in the jejunum (arrows). The ingestion of 15% alfalfa for 6 weeks was associated with disruption of the uppermost mucosal cells in both small intestine (Fig. 4) and large bowel (Fig. 5). Swollen, distorted epithelial cells and loss of apical membrane integrity were more obvious in the colonic samples.

Figure 6 is representative of jejunal samples from the bran-fed rats. These were essentially comparable to control samples. Occasional exfoliation of intact cells was seen and with the standard preparative procedures more mucin was associated with the surface of the tissue. The colons of the same animals were normal in appearance (Fig. 7), but as in the small intestine, there was evidence





FIGURE 1. Rat jejunum, control sample. Individual villi are leaf-shaped with a smooth topographical appearance. Arrow points to apical indentation which is a goblet cell orifice.



FIGURE 2. Rat jejunum, control TEM showing the typical intracellular structure of a goblet cell (GC) with adjacent brush border (BB) and glycocalyx material on the surface of the microvilli.



FIGURE 3. Rat colon, control SEM. The epithelial surface has whorled or folded appearance and the interspersed goblet cells show a wider orifice at the luminal surface than do those of the jejunum.



FIGURE 4. Rat jejunum from alfalfa-fed animals. The more apical cells exhibit cell swelling, loss of microvilli, and cell injury (arrows).



FIGURE 5. SEM of a colonic sample from affa-fa fed rats. There is extensive loss of microvilli, and breaks in the apical membrane integrity of the epithelial cells (arrows). Many cells are swollen and distorted.



FIGURE 6. SEM of bran-fed animals. The appearance is essentially similar to normal control tissue. Visually, these animals seemed to have more mucin material associated with the tissue surface.



FIGURE 7. SEM of colonic surface in bran-fed rats. The epithelial cells are normal in shape and microvillar density. A larger proportion of the surface cells are goblet cells compared to controls and mucus secretion is apparent from many of these cells.

of enhanced goblet cell secretory activity (arrows). Cellulose feeding for 6 weeks had little apparent effect on the surface mucosal integrity of either small (Fig. 8) or large intestine (Fig. 9). More mucin was visually apparent on these samples, as with the bran-feeding regimen. There was some clumping and mild disarray of the microvillar processes in the colonic epithelial cells in this condition.

In the animals fed 2% cholestyramine, tissue damage at the villar apices was always observed (Fig. 10). Injured cells were frequently surrounded by normal cells and in several cases hemorrhagic debris was found on the tissue surface of both jejunum and colon. Complete loss of the microvillar covering was frequently found (Fig. 11) and a substantial portion of the colonic surface was thus affected by cholestyramine ingestion. Figure 12 is a micrograph from colestipol-treated animals and milder degrees of cell disruption were observed in this condition. Swollen, partially denuded jejunal cells surrounded by normal cells were apparent. The colonic samples were less smooth topographically than controls and showed evidence of cell necrosis, with several of the surface cells being completely stripped of microvilli (Fig. 13). Individual cell boundaries were sharply defined.

Chronic ingestion of 2% DEAE-Sephadex appeared to be associated with more convoluted jejunal villi than those characteristic of animals maintained on control chow. The jejunal surface was fairly normal, but some minor degree of



FIGURE 8. SEM of jejunum from cellulose-treated animals. Arrow points to goblet cell secreting a strand of mucus.



FIGURE 9. SEM of colonic surface from cellulose-fed rats. The microvilli are less densely packed than in control tissue and goblet cell activity is evident.



FIGURE 10. Jejunal villus from cholestyramine-treated animals. Cells at the villar apices exhibit swelling, microvillar denudation, and membrane damage.

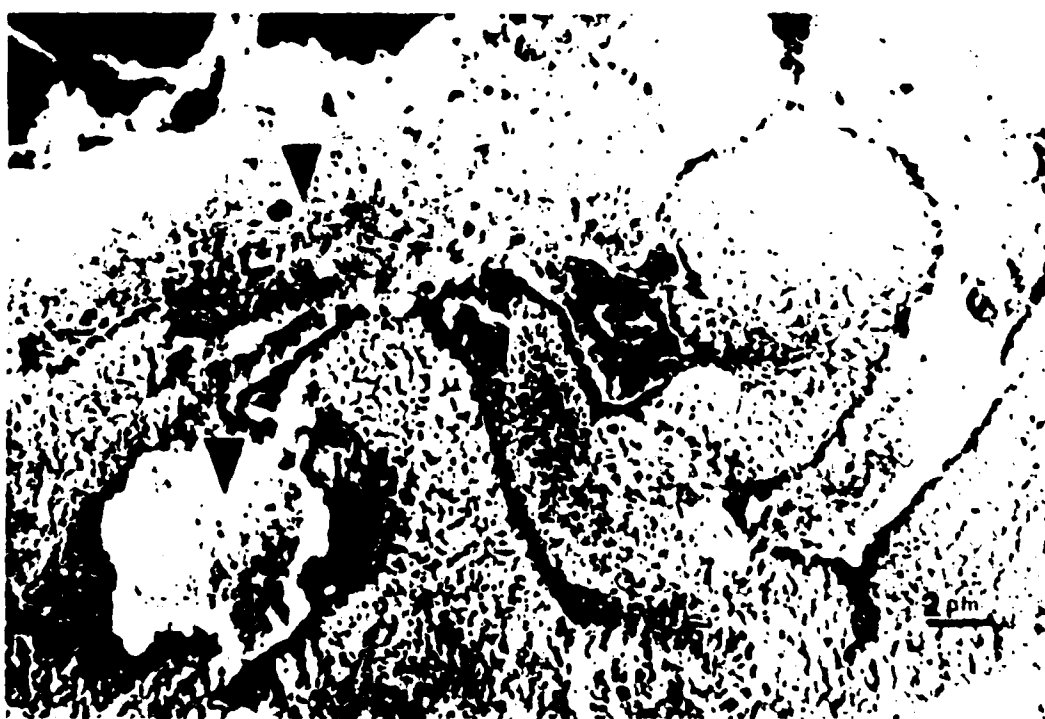


FIGURE 11. Colonic surface of cholestyramine-treated animals. Arrows point to areas of cell damage, apical membrane disruption, and epitheliolysis.



FIGURE 12. Jejunal villus from colestipol-treated rats. Occasional patches of microvillar denudation were observed.

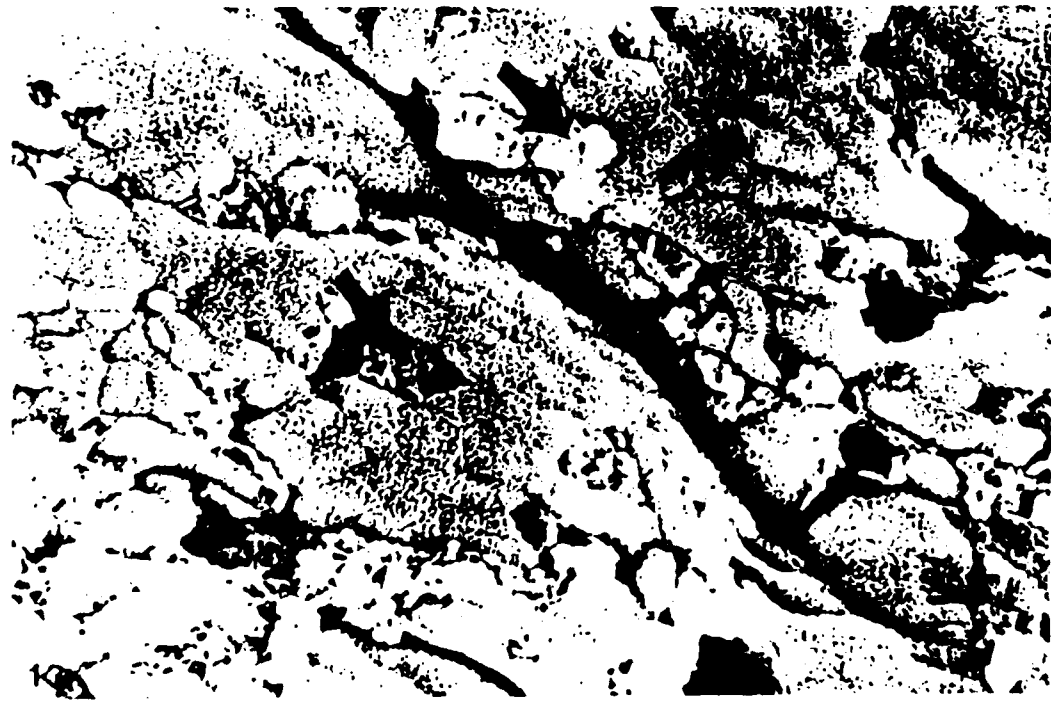


FIGURE 13. SEM of colonic surface in colestipol-fed animals. Many cells are devoid of the microvillar covering and others show progressive signs of cell injury.

cell swelling occurred (Fig. 14). Instead of the smooth ridges usually seen in control colonic tissue, the cells were arranged in deep whorls (Fig. 15) with random patches of cells devoid of microvilli. The alterations in ultrastructural intestinal morphology with chronic feeding semipurified fiber or bile-salt binding resins, as depicted in the preceding micrographs, have been quantitatively estimated. This was achieved by a blind-coding system of examination by three microscopists and the results are shown in Table I. Also included in this table is the *in vitro* bile salt-binding capability of the four fibers and the three resin substances used. It is apparent that a relationship does exist between the degree of bile salt binding *in vitro* of a specific dietary agent and the effect of chronic feeding of this agent on intestinal mucosal topography. The ingestion of 15% pectin or alfalfa or 2% cholestyramine or colestipol is associated with significant morphological deviations in both small and large intestine compared to control animals maintained on regular chow, bran, or cellulose. Figure 16 is a transmission electron micrograph of cholestyramine-treated jejunum showing intracellular accumulation of lipid droplets.

In a series of experiments designed to test whether the resin per se or the resin-bile salt complex was the necrotic agent the effect of bile salt resin or resin-bile salt complex was probed by twice daily colonic infusion of these



FIGURE 14. SEM of jejunal villi from animals treated with DEAE-Sephadex. Individual cell outlines are more clearly demarcated compared to controls and some loss of microvilli was apparent.



FIGURE 15. Colonic surface of Sephadex-treated rats. There is a mild disarray or clumping of the microvilli with occasional patches of denudation.



FIGURE 16. TEM of epithelial cells from cholestyramine-fed animals. In this condition the cells exhibit a high density of lipid droplets (arrows) compared to controls. The lipid globules are particularly prominent in the apical half of the enterocytes.

TABLE I. Effect of Fiber and Resin Feeding on Bile-Salt Binding and Morphology<sup>a</sup>

Dietary regimen	Average bile acid binding capacity <i>in vitro</i> (0-100%)	Percentage of intestinal villi with structural abnormality		Extent of deviation from control	
		Jejunum	Colon	Jejunum	Colon
Control chow	0	7.1 ± 2.3 <sup>d</sup>	5.0 ± 0.8 <sup>d</sup>	0.2 ± 0.1	0.1 ± 0.05
Bran	5 <sup>a</sup>	5.0 ± 1.1 <sup>d</sup>	15.0 ± 4.9 <sup>a</sup>	0.12 ± 0.08	0.5 ± 0.03
Cellulose	0 <sup>c</sup>	7.5 ± 2.1 <sup>d</sup>	22.1 ± 4.1 <sup>a</sup>	0.23 ± 0.07	0.7 ± 0.10
Pectin	7 <sup>b</sup>	30.7 ± 4.7 <sup>a</sup>	29.4 ± 8.0 <sup>a</sup>	1.18 ± 0.1	1.32 ± 0.1
Alfalfa	15 <sup>a</sup>	32.8 ± 7.2 <sup>a</sup>	58.6 ± 4.3 <sup>a</sup>	0.9 ± 0.2	3.2 ± 0.2
DEAE-Sephadex	30-40	13.0 ± 3.6 <sup>b</sup>	40.6 ± 9.1 <sup>a</sup>	1.6 ± 0.7	2.5 ± 0.06
Colestipol	50-60	35.9 ± 12.6 <sup>a</sup>	55.0 ± 10.1 <sup>a</sup>	11.5 ± 0.4	2.9 ± 0.4
Cholestyramine	80-100 <sup>a,c</sup>	64.2 ± 4.7	39.5 ± 10.5 <sup>a</sup>	3.7 ± 0.2	3.2 ± 0.6

<sup>a</sup> Reprinted with permission from Cassidy *et al.* (1980, 1981). Values shown are means ± SE for a minimum of 300 intestinal villi or colonic folds.

<sup>b</sup> After Kricheldorf and Story (1975).

<sup>c</sup> After Vahouny *et al.* (1981).

<sup>d</sup> After Cassidy *et al.* (1981).

<sup>e</sup> Significantly different from control ( $p < 0.01$ ).

<sup>f</sup> Significantly different from control and DEAE-Sephadex.



FIGURE 17. SEM of colonic surface from animals perfused twice daily for 5 days with the control colonic catheterization fluid. The tissue is normal in appearance.



FIGURE 18. SEM of colonic surface in animals administered cholestyramine by colonic infusion for 5 days. Loss of microvilli, cell swelling, and membrane destruction are evident.

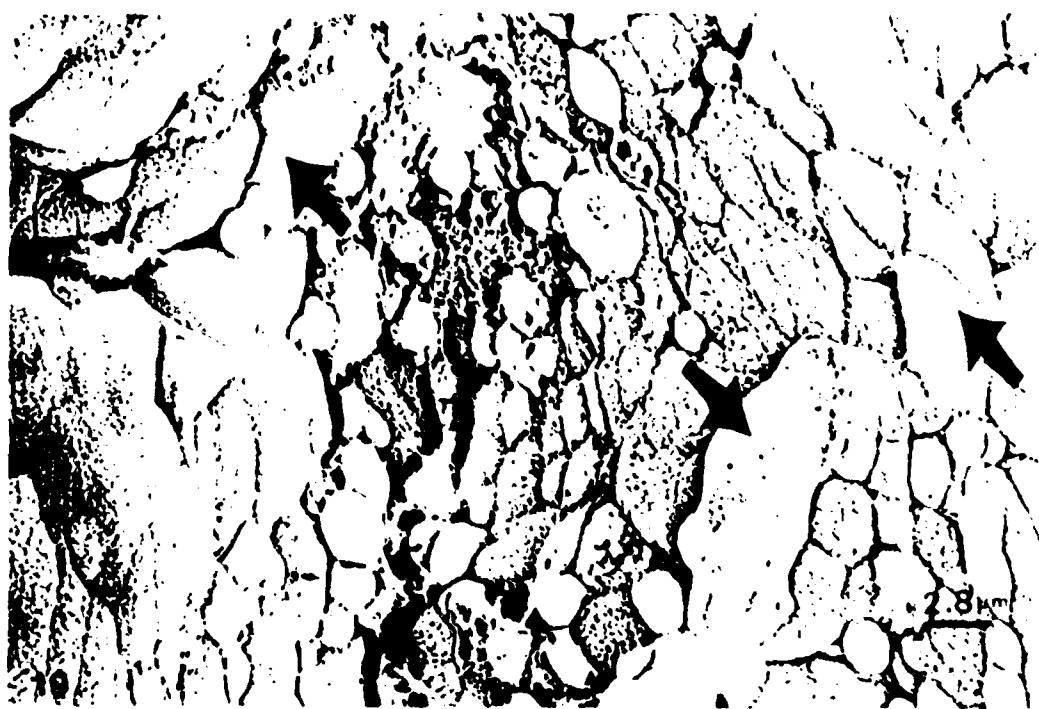


FIGURE 19. SEM of colonic tissue from rats exposed to the mixed bile salt mixture via colonic infusion. The sequence of cell swelling, denudation of microvilli, membrane destruction, and cell lysis is apparent.



FIGURE 20. Colonic surface from rats infused with the bile salt-cholestyramine mixture for 5 days. There is a distortion of cell architecture (arrows), some loss of microvilli, and patches of cell injury.

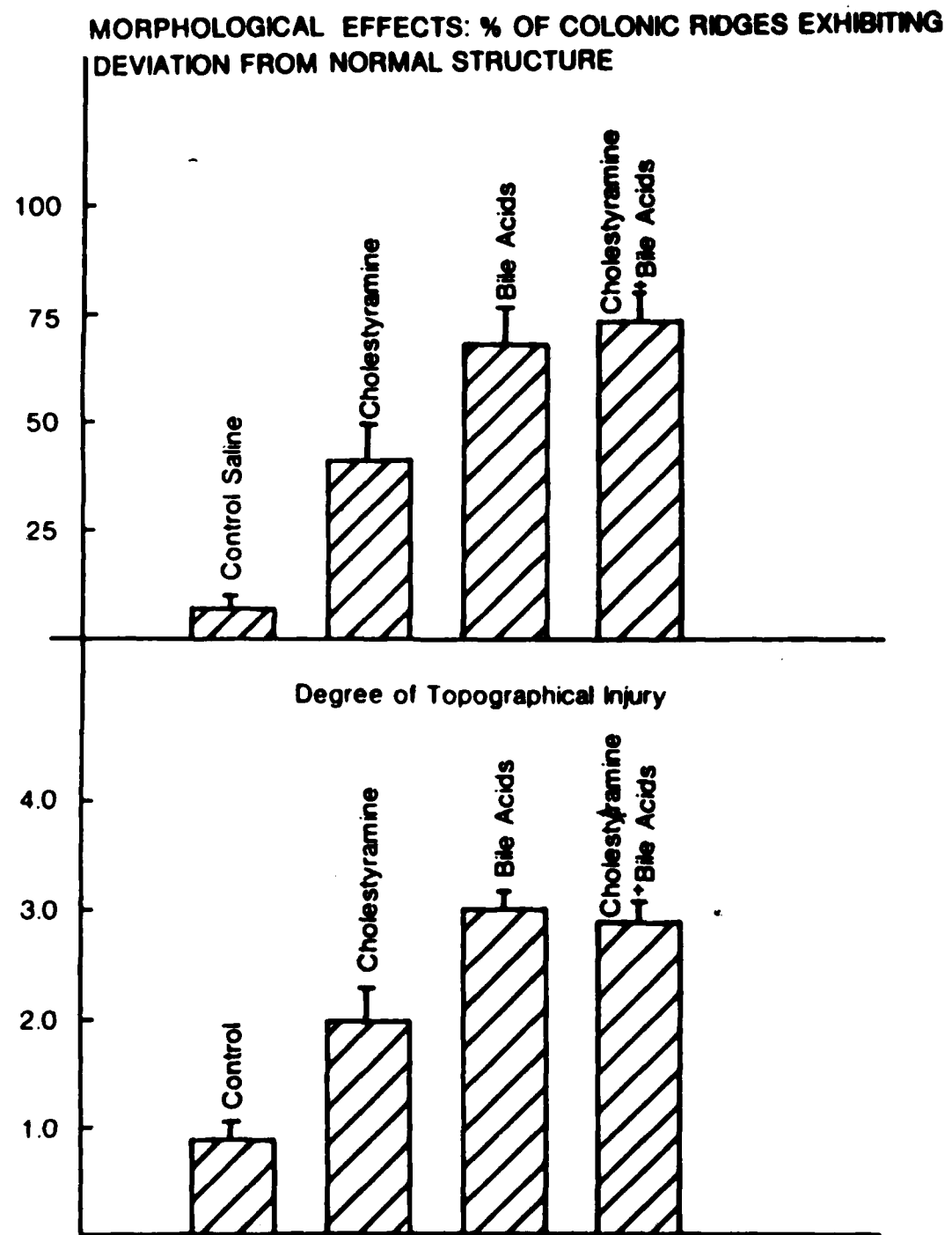


FIGURE 21. Histogram of frequency and degree of morphological damage in the colonic infusin studies. Both cholestyramine and the bile salt solutions evoked similiar deviations from normal histology, but the infusion of both materials together does not potentiate the individual effects.

mixtures. With administration of standard physiological saline the colonic topography did not differ from that of the animals fed the control diet (Fig. 17). With the addition of cholestyramine to the control medium the sequence of cell damage and epitheliolysis was clearly evident (Fig. 18). The mixed bile salt mixture without cholestyramine showed a very similar pattern of injury (Fig. 19). When cholestyramine bound to the bile salts was infused a similar pattern of tissue damage was evident (Fig. 20), although distortion of cellular architecture was more obvious (arrows). The extent and degree of morphological effect of these agents was quantitated and the results are expressed in Fig. 21 as a histogram. Both cholestyramine and the mixed bile salt mixture caused similar effects on colonic topography. Surprisingly, perhaps, the infusion of both ma-

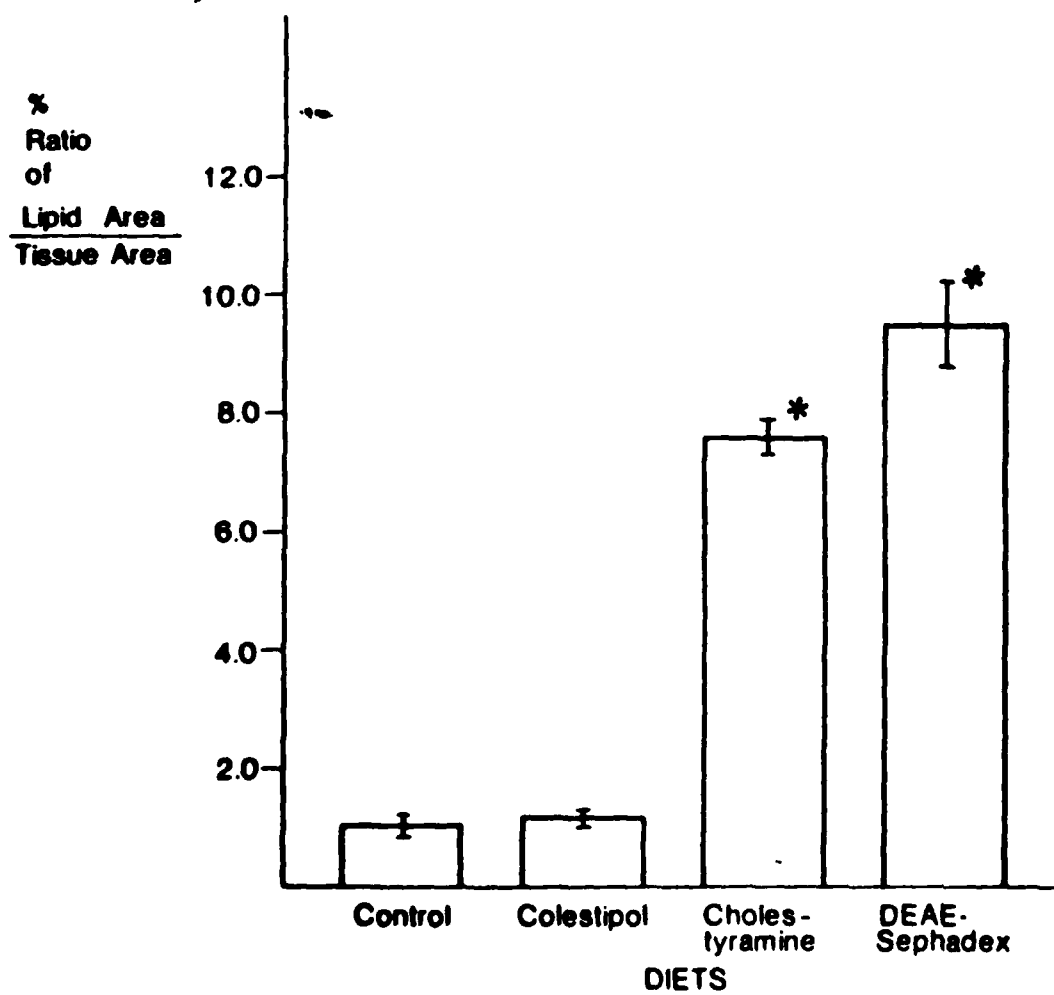


FIGURE 22. The morphometric lipid density of jejunal epithelial cells in groups of rats fed the control diet, DEAE-Sephadex, colestipol, or cholestyramine. Both cholestyramine and DEAE-Sephadex show significantly greater mucosal lipid accumulation when compared to control-fed animals and colestipol-treated rats. \*, Significantly different from control ( $p < 0.01$ ).

TABLE II. Binding of Components of Taurochenodeoxycholate-Phospholipid Micelles by Bile Acid Sequestrants and Dietary Fibers\*

Test substance <sup>b</sup>	Binding, %		
	Bile salt	Phospholipid	Cholesterol
Cholestyramine	91.9 ± 0.6	99.0 ± 0.2	86.2 ± 4.8
DEAE-Sephadex	84.2 ± 0.3	99.4 ± 0.2	99.6 ± 0.1
Guar gum <sup>c</sup>	31.1 ± 2.7	21.7 ± 4.6	23.4 ± 0.7
Guar gum <sup>d</sup>	37.6 ± 3.0	33.6 ± 1.6	27.2 ± 0.5
Lignin	38.7 ± 1.4	1.6 ± 1.5	14.5 ± 0.7
Alfalfa	14.4 ± 1.1	1.5 ± 1.3	83.6 ± 0.6
Wheat bran	12.1 ± 0.7	0 ± 0	9.5 ± 0.8
Cellulose	3.5 ± 1.0	1.3 ± 1.0	4.7 ± 1.7

\* Reprinted with permission from Vahouny *et al.* (1981).

<sup>b</sup> Micellar mixtures contained 5 mM taurochenodeoxycholate, 625 µM lecithin, 250 µM monolein, 500 µM oleic acid, and 250 µM cholesterol. Triplicate incubations were carried out with 40 mg of each test substance and contained various combinations of [7α-<sup>3</sup>H]taurochenodeoxycholate, [1-<sup>14</sup>C]dioleylphosphatidylcholine, and either [1,2-<sup>3</sup>H]cholesterol or [4-<sup>14</sup>C]cholesterol.

<sup>c</sup> Figures represent means from 6-12 incubations ± SEM.

<sup>d</sup> Low viscosity, food grade.

<sup>e</sup> High viscosity.

terials together did not appear to evoke a potentiation of their individual effects. These cells are apically swollen and separated from the neighboring cells. Several of the cells are partially or completely denuded of their microvilli.

The lipid accumulation phenomenon was derived only from morphological visualization of the material. In the chronic feeding studies the post hoc observation of this effect precluded identification of the lipid material by virtue of the necessary fixation and preparative methodology. An attempt was made to quantify the observations by morphometric analyses of large numbers of representative tissue sections. The results are presented in Fig. 22. Both the cholestyramine- and DEAE-Sephadex-treated animals showed a significantly greater degree of lipid density in the epithelial layer compared to control-fed or colestipol-treated rats. A partial piece of evidence which may explain this finding is shown in Table II. When these resins are incubated *in vitro* with micelles of varying composition cholestyramine and DEAE-Sephadex are capable of binding up to 98-99% of available phospholipid in addition to their sequestration effects on cholesterol and bile salts.

#### 4. DISCUSSION

SEM of the alimentary epithelial surface possesses certain advantages as a morphological technique. It avoids the tedious thin-sectioning and stereological reconstruction associated with transmission or light microscopy procedures. Rapid

assessment of surface mucosal integrity, even in human biopsy material, is possible, and is a factor of considerable importance in utilizing this methodology in the determination of the etiologic factors and their progressive identification in a wide variety of gastrointestinal disease states. A disadvantage lies in the fact that only the upper third of the intestinal surface, by virtue of its architectural configuration, is accessed by this technique. It is generally considered, however, that the epithelial cells in this region constitute the more differentiated and hence functionally competent cells in the mucosal layer. The transport of important solutes, e.g., inorganic ions, water, glucose, and amino acids, has been ascribed to the cells in this particular region of the villi and hence their morphological characteristics deserve serious study.

In the studies outlined in this paper we have attempted to characterize the morphological consequences of certain dietary regimens in a rat model. The data thus far obtained would seem to indicate that there is a morphological component which should be added to the expanding list of intestinal mechanisms associated with modification of dietary patterns by fiber ingestion or the administration of bile salt sequestrant materials. A complete and detailed appraisal of normal variations ascribable to species, diet, developmental status, or of the normal ultrastructural topography of small and large intestine is still lacking. Hence, it must be emphasized that the information presented here represents an attempt to quantify readily observable morphological characteristics in groups of animals subjected to feeding regimens in which lipid absorption and metabolic characteristics are fairly well defined. Two primary questions arising from these findings are: (1) Are the differences which have been noted attributable to a degree of deviation which might be expected to be within the normal range? (2) Can such deviations in mucosal structure be interpreted in light of other known and relevant physiological and biochemical observations derived from these or other similar feeding studies?

In regard to the first question, it would seem reasonably well established that normal mucosal cell production, exfoliation, and replacement in the gastrointestinal tract is an unobvious phenomenon when viewed by ultrastructural techniques (Cassidy and Lightfoot, 1979; Creamer *et al.*, 1961). The kinetics of the phenomenon and its regulation have been documented by biochemical and autoradiographic techniques. Currently it seems as if cell expulsion at the villus tips occurs via loss of intact cells (Harding and Morris, 1977; Lightfoot and Cassidy, 1978) without any overt disruption of apical membrane integrity. The cell swelling, loss of microvilli, distortion, and injury seen with certain fibers and resins have not been reported in any control population of rats either by us or others (Gaginella *et al.*, 1977; Ivey *et al.*, 1978). The cell damage phenomenon appears to be limited to those cells of the small intestine or colon that are closest to the lumen. We have, therefore, concluded that the ultrastructural differences induced by the perturbant feeding patterns are mainly limited to the mature, senescent enterocytes in both small and large intestine.

It is accepted that various types of irritant agents that evoke similar stages of cell necrosis can stimulate crypt cell production, migration, and villar repair rates via a tip to crypt feedback mechanism (Sprinz, 1971). Specific experimental examples include the effect of aspirin in an ulceration model (Yeomans *et al.*, 1973) and bile salt influences on epithelial cell dynamics (Roy *et al.*, 1975). It is true that particular dietary regimens and hormonal agents stimulate jejunal and colonic hypertrophy (Dworkin *et al.*, 1976; Hageman and Stragand, 1977; Maudsley *et al.*, 1976; Mak and Chang, 1976).

These results would suggest that one possible intestinal adaptation to chronic feeding patterns or bile salt sequestrations may involve altered rates of cytokinetic loss and renewal. The limited focal lesions found in our studies may represent early mucosal irritation and injury which could lead to later hyperplastic and perhaps neoplastic responses. Further studies are necessary to demonstrate such a continuum between mild epithelial cell damage and longitudinal development of carcinomatous lesions. The type of *in situ* cell degeneration noted here causes breaks in the continuity of the mucosal barrier allowing penetration of luminal materials to subepithelial layers. In the *normal* mature rat, 1.7% of intact antigenic protein is absorbed by the small intestine and 0.13% by the colon (Nigro *et al.*, 1973; Asano *et al.*, 1973; Warshaw *et al.*, 1977). The mechanism of necrosis may relate to membrane damage by lysolecithin or to extraction of membrane phospholipids, leading to epitheliolysis.

With respect to a putative association between other documented effects of these dietary materials and the observed structural changes, we have probed several other possible mechanisms implicated in the antiatherogenic and anti-carcinogenic sequelae of high-fiber feeding. Particular studies carried out with the same groups of rats included intestinal transit times, the direct measurement of cholesterol absorption into the lymphatic system, certain parameters of hepatic lipid metabolism, and the bile salt-binding capabilities of these agents *in vitro*.

Only cellulose and bran significantly reduced intestinal transit time (Vahouny *et al.*, 1980). There was qualitative evidence of more goblet cell activity and mucin secretion in both of these conditions, although these preliminary observations have not been quantitatively documented. It is not yet established whether cells in the crypt region are predetermined to remain as such or whether some lability between columnar and goblet cells occurs during the villar maturation process. Cellulose feeding induced a significant depression of cholesterol absorption, while the bran diet mildly lowered lipid uptake. Neither of these semipurified diets bind bile acids *in vitro* and their effect on mucosal surface structure is indistinguishable from controls.

Feeding of pectin and alfaalfa and the three resins, on the other hand, is associated with lowered cholesterol absorption, binding of bile salts from mixed micelles, and the microscopic appearance of distinctly abnormal mucosal ultrastructure. It would seem that the most clearly discernible correlation between

the morphological and biochemical findings lies in the *in vitro* bile salt sequestration phenomenon. There is some evidence that bran and cellulose exert a protective effect against the induction of tumorigenesis with 1,2-dimethylhydrazine in the colon (Barbott and Abraham, 1978; Fleiszer *et al.*, 1978; Freeman *et al.*, 1978). By contrast, bile acids, fed as such, enhance the mutagenic activity of several carcinogens, even in germ-free animals (Reddy *et al.*, 1978). A similar type of stimulation is observed with cholestyramine (Nigro *et al.*, 1973; Asano *et al.*, 1970). In the colonic perfusion studies we found similar damage to the colonic surface when either bile acids or cholestyramine or the bile acid-resin complex was presented twice per diem for 5 days. There was no evidence of an additive histological effect when bile salts and cholestyramine were used together. Chadwick *et al.* (1979) have recently emphasized the specific bile salt molecular structure required to cause various effects in the intestinal tract, including salt and water secretion and epitheliolysis. Ammon (1979) has concluded that biliary lecithin is critical for the protection of mucosal gallbladder from the potentially damaging effects of bile salts. The finding by Levine *et al.* (1980) that antral instillation of bile salts significantly elevates serum gastrin levels in man suggests that gastrin secretion may be modulated by these dietary regimens and, in consequence, trophic effects on intestinal epithelium could be predicted.

One other observation from our morphological appraisals is the significant accumulation of lipid droplets within the jejunal enterocytes with cholestyramine or DEAE-Sephadex administration. The nature of this material has not yet been identified, but was apparent in three out of four separate feeding studies. An explanation for such lipid-laden cells rests on the assumption of a greater blockage of lipid exit mechanisms at the basolateral membranes of the mucosa than that initially presumed to occur at the micellar entry step, when bile sequestrants are present in the lumen. An obligatory requirement for luminal phospholipid in the exit step via chylomicron packaging and exit has been postulated (O'Doherty *et al.*, 1973). Our observations on the capacity of the sequestrants to bind, not only cholesterol and bile acids, but also 98-99% of available phospholipids in mixed micelles is pertinent. With the feeding of cholestyramine or DEAE-Sephadex there may be a lack of intracellular phospholipid for this essential step. An analogous finding of intracellular lipid deposition has been reported with the use of hydrophobic detergents. Detergent and resin agents may prove to be useful probes of lipid serosal transfer mechanisms in the intestinal tract. It should be mentioned that alternatively (1) permeation of resin into the cell could conceivably bind intracellular phospholipid essential to chylomicron formation, or (2) the resin could also bind other essential luminal components of the lipid transfer process, e.g., pancreatic cholinesterase (Gallo *et al.*, 1980).

In summary, we have sought to investigate structural alterations in the alimentary organs in response to chronically ingested dietary materials. Whether the relationships we have consistently observed are causative or merely correl-

ative epiphenomena remains to be determined in studies designed to test possible underlying mechanisms. Ultimately, any mechanism involved in the explanation of health status relating to diet must originate from some signals which are perceived by this organ and relayed to a host of other homeostatic systems, whether these be morphological, biochemical, physiological, or pathological in nature. Scanning electron microscopy offers a relatively easy and rapid approach to the assessment of morphological modifications and also provides novel clues in the pursuit of other important adaptive responses which may lie in the molecular or biochemical realm.

**ACKNOWLEDGMENTS.** This work was supported in part by USPHS grant HL-02033 (GVV), USDA grant 7900497 (GVV), Office of Naval Research Contract #N0014-79-C-603 (MMC), and the ITT Continental Baking Co. Research and Development Fund of the Biochemistry Department, George Washington University.

## REFERENCES

Ammon, H. V., 1979. Effect of taurine conjugated bile salts with and without lecithin on water and electrolyte transport in the canine gallbladder *in vivo*, *Gastroenterology* **76**:778-783.

Asano, T. M., Pollard, M., and Madsen, D., 1970. Effect of cholestyramine on 1,2-dimethylhydrazine induced enteric carcinoma in germfree rats, *Proc. Soc. Exp. Biol. Med.* **150**:780-785.

Barbott, T. A., and Abraham, R., 1978. The effect of bran on dimethylhydrazine-induced colon carcinogenesis in the rat, *Proc. Soc. Exp. Biol. Med.* **157**:656-659.

Barisawa, I., Magadia, N. E., Weisburger, J. H., and Wynder, E. L., 1974. Promoting effect of bile acids on colon carcinogenesis after intrarectal installation of *N*-methyl-*N*-nitrosoguanidine in rats, *J. Natl. Cancer Inst.* **55**:1093-1097.

Burkitt, D. P., Walker, A. R. P., and Painter, N. S., 1972. Effect of dietary fiber on stools and transit times and its role in the causation of disease, *Lancet* **2**:1408-1412.

Carroll, K. K., and Khor, H. T., 1975. Dietary fat in relation to tumorigenesis, *Prog. Biochem. Pharmacol.* **1975**:308-353.

Cassidy, M. M., and Lightfoot, F. G., 1979. Electron microscopic study of gastrointestinal response to acetylsalicylic acid, *J. Submicrosc. Cytol.* **11**:449-462.

Cassidy, M. M., Lightfoot, F. G., Grau, L. E., Roy, T., Kritchevsky, D., and Vahouny, G. V., 1980. Effect of bile salt-binding resins on the morphology of rat jejunum and colon: A scanning electron microscopy study, *Dig. Dis. Sci.* **25**:504-512.

Cassidy, M. M., Lightfoot, F. G., Grau, L., Story, J., Kritchevsky, D., and Vahouny, G. V., 1981. Effect of chronic intake of dietary fibers on the ultrastructural topography of rat jejunum and colon: A scanning electron microscopy study, *Am. J. Clin. Nutr.* **34**:218-228.

Chadwick, V. S., Gaginella, T. S., Carlson, G. L., and Delongnie, J. C., 1979. Effects on molecular structure of bile-acid induced alterations in absorptive function, permeability and morphology, *J. Lab. Clin. Med.* **94**:661-664.

Correa, P., and Haenszel, W., 1978. The epidemiology of large bowel cancer, *Adv. Canc. Res.* **26**(2):141.

Creamer, B., Shorter, R. J., and Banforth, J., 1961. The turnover and shedding of epithelial cells, *Gut* **196**(2):110-120.

Dworkin, L. D., Levine, G. M., Farber, M. J., and Spector, M. H., 1976. Small intestinal mass of the rat is partially determined by indirect effects on ultraluminal nutrition. *Gastroenterology* 71:626-630.

Fleiszer, D., Murray, D., MacFarlane, J., and Brown, R. A., 1978. Protective effects of dietary fiber against chemically induced bowel tumors in rats. *Lancet* 2:552-553.

Freeman, J. J., Spiller, G. A., and Kinn, Y. S., 1978. A double-blind study on the effects of purified cellulose dietary fiber on 1,2-dimethylhydrazine-induced rat colonic neoplasia. *Cancer Res.* 38:2912-2917.

Gagnella, T. S., Lewis, J. C., and Phillips, S. F., 1977. Rabbit ileal mucosa exposed to fatty acids, bile acids and other secretagogues. Scanning electron microscopic appearances. *Dig. Dis. Sci.* 22:781-789.

Gallo, L., Chiang, Y., Vahouny, G. V., and Treadwell, C. R., 1980. Localization and origin of rat intestinal cholesterol esterase determined by immunocytochemistry. *J. Lipid Res.* 21:537-545.

Hageman, R. F., and Stragand, J., 1977. Fasting and refeeding cell kinetic response of jejunum ileum and colon. *Cell Tissue Kinet.* 10:3-14.

Harding, R. K., and Morris, G. P., 1977. Cell loss from normal and stressed gastric mucosae of the rat. An ultrastructural analysis. *Gastroenterology* 72:857-863.

Hill, M. J., Drasar, B. S., Williams, R. E. O., Meade, T. W., Cox, A. G., Simson, J. E. P., and Morson, B. C., 1975. Fecal bile acids and clostridia in patients with cancer of the large bowel. *Lancet* 1:535-539.

Ivey, K. J., Baskin, W. M., Krause, W. J., and Terry, B., 1978. Effect of aspirin and acid on human jejunal mucosa: An ultrastructural study. *Gastroenterology* 76:50-75.

Kritchevsky, D., and Story, J., 1975. *In vitro* binding of bile acids and bile salts. *Am. J. Clin. Nutr.* 28:305-306.

Levine, J. S., Connan, J. E., and Kern, M., 1980. Effect of antral instillation of bile salts on fasting serum gastrin levels. *Dig. Dis. Sci.* 25:449-452.

Lightfoot, F. G., and Cassidy, M. M., 1978. The effect of aspirin and prostaglandin E<sub>1</sub> on intestinal mucus secretory patterns. *Scanning Electron Microscopy* 2:719-729.

Mak, K. M., and Chang, W. W. L., 1976. Pentagastrin stimulates epithelial cell proliferation in duodenal and colonic crypts in fasted rats. *Gastroenterology* 71:1117-1120.

Maudsley, D. V., Lief, J., and Kobayashi, Y., 1976. Ornithine decarboxylase in rat small intestine. Stimulation with food or insulin. *Am. J. Physiol.* 231:1557-1561.

Nigro, N. E., Bhadrachari, N., and Chomachi, C., 1973. A rat model for studying colonic cancer. Effect of cholestyramine on induced tumors. *Dis. Colon Rectum* 16:438-443.

Nigro, N. D., Campbell, R. L., Singh, D. V., and Lin, Y. N., 1976. Effect of diet high in beef fat on the composition of fecal bile acids during intestinal carcinogenesis in the rat. *J. Natl. Cancer Inst.* 57:883-888.

O'Doherty, P. J. A., Kakis, G., and Kuksis, A., 1973. Role of luminal lecithin in intestinal fat absorption. *Lipids* 8:249-255.

Philips, S. F., and Gagnella, T. S., 1979. Effects of fatty acids and bile acids on intestinal water and electrolyte transport. In: *Mechanisms of Intestinal Secretion* (H. Binder, ed.), Alan R. Liss, New York, pp. 287-294.

Reddy, B. S., Weisburger, J. H., and Wynder, E. L., 1975a. Effect of high risk and low risk diets for colon carcinogenesis of fecal microflora and steroid in man. *J. Nutr.* 105:878-884.

Reddy, B. S., Mastromarino, A., and Wynder, E. L., 1975b. Further leads on metabolic bowel cancer. *Cancer Res.* 35:3421-3426.

Reddy, B. S., Narisawa, T., Vukusich, D., Weisburger, J. H., and Wynder, E. L., 1976. Effect of quality and quantity of dietary fat and dimethylhydrazine in colon carcinogenesis in rats. *Proc. Soc. Exp. Biol. Med.* 151:237-239.

Reddy, B. S., Weisburger, J. H., and Wynder, E. L., 1978, Colon cancer: Bile salts as tumor promoters, in: *Carcinogenesis*, Vol. 2 (T. J. Slaga, A. Swak, and R. K. Boutwell, eds.), Raven Press, New York, pp. 453-464.

Roy, C. C., Laurendeau, G., Doyon, G., Chartrand, L., and Rivest, M. R., 1975, The effect of bile and sodium taurocholate on the epithelial dynamics of the rat small intestine, *Proc. Soc. Exp. Biol. Med.* 149:1000-1004.

Sprinz, H., 1971, Factors influencing intestinal cell renewal cell, *Cancer* 28:71-74.

Vahouny, G. V., Roy, T., Gallo, L., Story, J., Kritchevsky, D., and Cassidy, M. M., 1980, Dietary fibers. III. Effects of chronic intake on cholesterol absorption and metabolism in the rat, *Am. J. Clin. Nutr.* 33:2182-2191.

Vahouny, G. V., Tombes, R., Cassidy, M. M., Kritchevsky, D., and Gallo, L. L., 1981, Dietary fibers. V. Binding of bile salts, phospholipids and cholesterol from mixed micelles by bile acid sequestrants and dietary fibers, *Lipids* 15:1012-1018.

Warshaw, A. L., Bellini, G. A., and Walker, W. A., 1977, The intestinal mucosal barrier to intact antigenic protein. Differences between colon and small intestine, *Am. J. Surg.* 133:55-58.

Williamson, R. C., Bauer, F. L. R., Ross, J. S., Watkins, J. B., and Malt, R. A., 1979, Enhanced colonic carcinogenesis with azoxymethane in rats after pancreaticobiliary diversion to mid small bowel, *Gastroenterology* 76:1386-1392.

Wynder, E. L., 1979, Dietary habits and cancer epidemiology, *Cancer* 43:1955-1961.

Yeomans, N. D., St. John, D. J. B., and du Boer, W. G. R. M., 1973, Regeneration of the gastric mucosa after aspirin-induced injury in the rat, *Am. J. Dig. Dis.* 18:773-780.

END

DTIC

6- 86